TWO PHASE FLOW INDUCED VIBRATIONS FOR TUBE BANKS IN CROSS FLOW:

Creating an Experimental Facility

TWO PHASE FLOW INDUCED VIBRATIONS FOR TUBE BANKS IN CROSS FLOW: Creating an Experimental Facility

by
Richard Dam
B. Eng. & Management (Mechanical Engineering)

A Thesis
Submitted to the School of Graduate Studies
in Partial Fulfillment of the Requirements
for the Degree of
Master of Engineering

McMaster University
April 1991

Master of Engineering (1991) McMaster University
(Mechanical Engineering) Hamilton, Ontario

Title: Two Phase Flow Induced Vibrations for Tube Banks in Cross Flow: Creating an Experimental Facility

Author: Richard F. Dam, B. Eng. & Mgmt (Mechanical)
(McMaster University, Hamilton Ontario)

Supervisors: Dr. R.L. Judd
Dr. D.S. Weaver

Number of Pages: 198

Abstract

Two phase flow induced vibrations is a field that has many inherent modelling difficulties, making research in the area challenging. In order to study the problem more closely, a two phase flow loop using Freon 11 had been designed and commissioned at McMaster University. The initial design required some modifications to make the loop as "user friendly" as possible. The final result meets this desired capability.

The loop was designed so that research into vibrations in tube bundles could be carried out. A test section had been designed to facilitate this task. However, this design also required modifications. Additionally, new vibration monitoring instrumentation making use of light was developed to avoid the detrimental effects of Freon 11. The introduction of these items has resulted in a complete facility for the purpose of studying two phase flow induced vibrations. Preliminary experiments revealed a problem relating to tube tuning. Generally, the results are promising and some interesting new phenomena were observed as well.

Acknowledgements

The author wishes to acknowledge the following persons for their contributions to work presented in this thesis:

Supervisor: Dr. D.S. Weaver

Technicians: F. Drieman
R. Lodewyks
D. Schick
J. Verhaeghe

Research Assistants: A. Chopra
P. Feenstra
F. Kneppert

A special acknowledgement is given to my other supervisor Dr. R.L. Judd for the confidence he has shown in me, helping me to gain the most I could from work on this project.

Most of all, I want to thank my wife, Marianne, for the constant support she has given and the endurance she has shown throughout the past few years. I would also like to thank my son, Justin, who without knowing it has made completing this thesis a little easier.

Table of Contents

Appendices

Table of Figures

List of Tables

Nomenclature

A_x	- surface area of loop section x
C_L, C_R	- effective random excitation coefficient
C_m	- added mass coefficient
d	- tube diameter
E	- energy
f	- tube frequency
	- subscripts - n - natural
	s - structural
	a - air
	g - gas or vapour
G	- mass flux
	- subscripts - p - pitch
	r - critical pitch mass flux
h	- enthalpy
	- subscripts - test - test section
	f2 - section prior to heater
	ft - saturation (liquid)
	fg - latent
h_T	- heat transfer coefficient
H	- reading from DP cell
J	- joint acceptance
k	- tube stiffness
K	- constant in Conner's equation

L	- tube length
m	- mass
	- subscripts - eq - equivalent
	s,T - tube mass
	a,added - added mass
m_d	- mass damping parameter
$\dot{m}$	- mass flowrate
P	- tube pitch (without subscripts)
P	- power (with subscripts)
	- subscripts - h - heater
	L - heat loss
	net - net power
Q	- flowrate
S	- power spectral density
S_l	- slip ratio
ΔT_x	- temperature difference of loop section x
U	- velocity
V	- velocity
	- subscripts - r - reduced
	p - pitch
	u - upstream
W	- velocity
	- subscripts - v - vapour
	l - liquid
x	- quality

Y	- amplitude
α	- added mass coefficient components
δ	- damping
ζ	- critical damping
ϵ	- tube frequency constant
Θ	- tube eigenfunction of first mode
ϕ	- void fraction
ρ	- density

Chapter 1

Introduction

Flow induced vibrations of tube arrays is a subject of considerable interest to many persons involved in the design of heat exchangers and nuclear steam generators. However, the theoretical development of this phenomenon is in the preliminary stages for single phase flow and is practically nonexistent for two phase flow. Consequently, there is a considerable amount of research to be carried out, particularly with respect to two phase flow.

The interest in the problem of flow induced vibrations in tube banks stems largely from the destructive effects that such vibrations have on an affected system. The vibrations are known to cause problems in two ways. First, there is the possibility of large amplitude vibrations that can result in tube clashing and the subsequent failure from fretting or fatigue. Additionally, small amplitude vibrations are present at all times, which tend to cause tube wear at the supports.

The history of research into this phenomenon spans approximately three decades, although greater progress has been made in the last two decades. In papers by Paidoussis (1981)(1982), and Weaver & Fitzpatrick (1987), an outline of this research is given, from which the review discussion is summarized. In addition, this information has been augmented with details of developments that have occurred since 1980.

The review ends with the discussion of two phase flow vibrations research and the concerns at present. The topic project for this thesis is primarily concerned with addressing some of these concerns. To provide continuity between this work and that of Westermann (1987), section 1.1 will deal with the goals of the project. A summary of the physical modelling will also be included.

For the work presented in this thesis, the first concern was the completion of the commissioning work. This involved the construction of a two phase flow loop that would not only meet the physical design requirements, but would also be easily operated by anyone with the appropriate background without detailed instructions. Although the loop already existed, several modifications were necessary to improve the operating characteristics. Once operational, the next step involved the determination of the capabilities of the loop.

The determination of the loop capabilities relied on pressure and temperature measurements, and observations of loop behaviour. Although encouraging results were obtained, visible results would be obviously more reliable. The test section incorporated large windows, which would make visual observations possible. However, the structural integrity of the original test section design was questionable. Consequently, the second goal of this project was the redesign, construction, testing, and installation of the test section. The successful conclusion of this phase of the

project, signalled the beginning of the testing phase, where the loop's capabilities could be quantitatively tested.

The third aspect of the project dealt with the development of instrumentation for the measurement of vibrations, one of the main requirements of the facility. Conventional techniques were rendered less reliable because of the physical scale used and the destructive nature of the working fluid. Therefore, a new method, using light as the medium to transmit displacement information from the tubes to a measuring device, was developed. This required considerable time and effort to ensure that the resulting instrumentation would be practical.

The final objective of the project brings all the previous efforts to a conclusion by beginning the work of establishing benchmark results for use as points of reference for future experiments. Furthermore, these results serve to verify that the culmination of the efforts described in this thesis, is an experimental facility capable of providing useful information in the measurement of two phase flow vibrations.

1.1 Prior Work on the Two Phase Flow Loop

1.1.1 General Goals

The initiating goals of this project relate to the study of two phase flow induced vibrations in the U-bend region of a nuclear steam generator. Past studies have provided

inconclusive results as to the complete nature of the mechanisms unique to two phase flow. Additionally, there is considerable interest in studying the effects of using a single component two phase flow as opposed to a two component two phase flow.

When comparing air-water tests to steam-water tests, there are both similarities and differences observed. Although fluidelastic instability appears to occur predictably in two phase flow, there are differences in the actual response. For instance, a significant difference has been observed in the effective damping of the tubes in air-water as compared to steam-water. Therefore, this project is intended to gain insight into the mechanisms of two phase flow and to address modelling concerns in this type of experiment.

1.1.2 Physical Modelling

Since the cost of a full scale steam-water experiment is high to both build and operate, the tube bundle was scaled in size and an alternative fluid was chosen. Freon 11 provided the best match to the needs of the experiment by allowing the generation of high void fraction with only a relatively small amount of power. Moreover, the fluid would behave in a manner similar to water.

Table 1.1 is taken from the thesis of Westermann (1987) and it summarizes the physical scaling parameters for the experiment. From the table the pitch ratio, mass ratio,

reduced velocity, and Cauchy Number are seen to be modelled well in relation to a steam generator. Although the remaining parameters are not as well modelled, the experiments are still expected to provide useful information about the phenomenon of cross flow induced vibrations in two phase flow.

The tube bank itself is composed of cantilever tubes made of yellow brass mounted in a parallel triangular pattern. This does not duplicate the more complicated boundary conditions of the U-bend region of the steam generator. To compensate, the physical scaling parameters, as seen in table 1.1, must be properly accounted for. This technique has been used in past studies to provide design information for the building of heat exchangers and particularly steam generators. Chapter 2 will discuss the results from past studies in greater detail.

Table 1.1

Scaling Parameter Comparison:

U-bend Region of Typical Steam Generator vs Test Section

PARAMETER	DEFINITION	STEAM GENERATOR	TEST SECTION*
Pitch Ratio	p/d	1.3 - 1.5	1.443
Mass Ratio	$m/\rho_H d^2$	21 - 35	20
Reduced Velocity	V_P/fd	13 - 24	15
Fluid Damping	δ	0.45 - 1.6	0.24
Cauchy Number	$E/\rho_H V_P^2$	50 - 150 x 10^6	40 x 10^6
Reynolds Number	Gd/μ_L	40,000 - 100,000	14,000
Density Ratio	ρ_L/ρ_V	33	100
Viscosity Ratio	μ_L/μ_V	5.5	30
Void Fraction	B	0.82 - 0.90	0.85

*Test section at design conditions

Chapter 2

A Review of Cross Flow Induced Vibrations

2.1 Historical Development

A review of the papers presented up to 1959 leads to the conclusion that the dominant thinking of the time attributed the vibrations observed to the occurrence of vortex shedding within the tube bundle. However, Owen in 1964 disputed the possibility of any vortex shedding within tube bundles, claiming that there simply was not room enough for this to happen. This argument fell on deaf ears in North America, and the phenomenon of vortex shedding was not seriously questioned until the 70's.

In 1966, Roberts proposed the idea of fluidelastic instability causing large amplitude vibrations. The source of these vibrations was attributed to the forces developed as 'jet switching' occurred in response to tube movement. Although further theoretical explanations were not provided, interest developed in the prediction of the onset of fluidelastic instability. In 1970, Conners presented the following equation:

$$U/(f*d)=9.9*m_d^{.5}$$

Throughout the 70's, research concentrated on the

evaluation of K in Conners' equation as presented in the following form:

$$V_r = K * m_d^{.5}$$

where V_r= reduced velocity and m_d= mass damping parameter.

Towards the end of the 70's, attention was given to the question of vortex shedding. The argument concerned the source of vibrations in the turbulence[1] region prior to fluidelastic instability. The existence of various peaks in the response did not confirm their existence, which meant that some visualization studies were required.

Furthermore, the 80's brought scepticism concerning the validity of Conners' equation. The constant K tended to obscure the mechanisms involved, and the exponent on the mass damping parameter was questionable. These criticisms were, in part, a result of efforts to better understand the underlying cause of the fluidelastic instability, whereas in the past, the emphasis had been on developing design criteria. Consequently, the analysis of the experimental data took a more fundamental approach, and the results obtained have provided the basis for some theoretical modelling.

Finally, the effects of two phase flow became a topic of interest, with the research undertaken being primarily in support of the nuclear industry. However, the vibration

---

[1]Turbulence is a general term to describe the chaotic nature of the flow.

mechanisms appear much more complicated then those corresponding to single phase. Moreover, modelling two phase flow is in itself a problem. Therefore, information is more difficult to obtain, and this frustrates the learning process. As a result, there is little understanding of two phase cross flow induced vibrations at the time of this writing.

2.2 The Nature of the Problem

Axisa et al. (1987) wrote a paper on the numerical techniques available to solve the various problems associated with flow induced vibrations. Although there is value in the actual equations for design purposes, the paper, in this context, is more useful in providing insight into the complexity of the problem. The discussion can be divided into two main areas of concern. First, there is the vibration theory which predicts the vibration of the tube, and second, there is the amplitude response theory to predict the vibration amplitudes due to fluid forces.

If a single tube is considered, as it vibrates in air, the easiest thing that can be determined is the equation of motion. Furthermore, the solution of the relevant equation allows the determination of the mode shapes and natural frequencies of the tube. However, to properly pose the problem, the boundary conditions of the tube must be considered. That is, the type of tube support must be specified, in conjunction with the number of supports along the tube length.

As explained, the tube is relatively easily modelled in air, and based on this analysis the motion of the tube can be predicted for a given forcing function. The results of this analysis would then be used to determine the wear rate of the tube at its supports. However, if the tube is loosely supported, the tube can move within its support, resulting in

impact and sliding problems in addition to the nonlinear response that these variable boundary conditions impose.

If it is assumed that the analysis discussed so far is successful, there still remains the question of several input parameters. For instance, the forcing function that results from the turbulence buffeting is neither constant nor sinusoidal in nature. Moreover, as the response of the tube changes, and the fluid conditions change, the fluid motion around the tube will vary, making the forcing function even more difficult to predict.

Furthermore, the fluid interaction with the tube tends to change the damping and the effective mass of the vibrating tube. Hydrodynamic coupling then complicates the problem by providing the means for one tube to influence the other tubes within the tube bank. The result is that the prediction of single tube vibration is a considerably simpler task then that of a tube array.

The summary of the preceding discussion is that the vibration aspects and fluid mechanics aspects are complicated by the interaction of the two together. In addition, the physical constraints of the system, such as those provided by the supports, pose an added dimension to the problem. Therefore, the problem is not straight forward even in single phase flow. The inclusion of the effects of two phase flow tends to complicate the problem even further. However, as the remainder of the discussion will show, efforts are being made

to understand this phenomenon.

2.3 The Response of Tube Arrays in Single Phase Flow

The idealized response of a tube array to single phase flow can be seen in figure 2.1 taken from Paidoussis (1982). There are generally four mechanisms associated with this response curve, which are:

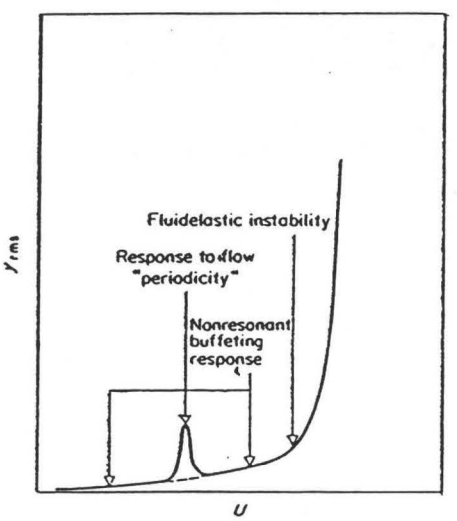

Figure 2.1 Paidoussis(1982)
Typical Amplitude Response

i) turbulence buffeting

ii) vortex shedding (peak on diagram)

iii) fluidelastic instability

iv) acoustic resonance (not shown)

From these four mechanisms, only the first three will be considered, since acoustic resonance is a special case that occurs when the acoustic frequency of the flow matches the surrounding system. However, each of the other mechanisms will be discussed in turn.

2.3.1 Vortex Shedding

The first question to be answered concerning vortex shedding deals with the dispute over whether the phenomenon occurs within tube bundles. Paidoussis (1982) gave guidelines for the possibility of Strouhal resonance to occur. (Strouhal resonance is another name for vortex shedding resonance. The Strouhal number is usually used to predict the occurrence of resonance for this mechanism.) These guidelines were as follows:

i) Gas in tightly spaced arrays

ii) Liquid in tightly spaced arrays

iii) Widely spaced arrays

iv) Coincidence of f_s, f_a, f_n

The first two criterion are valid only if the upstream flow has a low turbulence level, which is especially critical for gas flows, as vortices are highly unlikely for this case.

Moreover, the vortex shedding was only observed to occur within the first few rows of the bundle, although wider spacing may allow periodicity further into the array. Finally, the fourth condition describes the coincident resonance of the acoustic, tube, and flow frequencies. It is generally expected that such an occurrence would result in the destruction of the system in a short period of time.

These guidelines are not given in an exact form, and leave some room for speculation. For instance, how wide is widely spaced, or how low is low turbulence. However, in general, some indication of the expected response of the system can be obtained by consideration of these guidelines.

Additionally, there have been reports that describe the occurrence of vortex shedding in more concrete terms. Yeung and Weaver(1981) found that for their array, if Re were greater than 4400, then there was no evidence of vortex shedding. This finding corresponds to those given by Paidoussis, since at the Reynolds number involved the flow would be expected to be turbulent. However, Weaver and Fitzpatrick (1987) discuss some evidence of vortex shedding in the turbulent region for some geometries.

For the purposes of design, knowledge of Strouhal resonance occurrence is useful. Yeung and Weaver also provided a representative Strouhal number on which design could be based. According to their research St=0.57, which is specific to their geometry. However, other reports of Strouhal number

give values of this magnitude and therefore this figure is representative of the values one might expect. The basic design criterion is to avoid designing a system that might operate at or near a Strouhal number of this value. Using this design criterion, conservative solutions are obtained, and the design can be limited if avoidance of Strouhal resonance is an additional constraint. From the research side, large peaks in the turbulence response were generally attributed to vortex shedding, but now it is known that vortex shedding occurs at discrete frequencies and tends to have a thin peak, whereas turbulence effects tend to be broad band.

Subsequently, it should be noted that the determination of the existence of such a peak is not as simple as figure 2.1 might indicate. First, the peak may appear much broader, depending on the flow conditions. The peak may also occur closer to the instability region (e.g. water), which can obscure the onset of instability and consequently confuse the issue as to the mechanism occurring.

2.3.2 Turbulence Buffeting

Previously, it was mentioned that Owen (1964) had disputed the existence of vortices in tube bundles. In support of this claim, he presented a turbulence based form of the Strouhal number to predict the peak values that would otherwise be attributed to vortex shedding. The principal behind this technique was that the dominating frequency of the

turbulence was coincident with the natural frequency of the tubes. However, as discussed under vortex shedding, this physical interpretation has been proven incorrect in general. Turbulence buffeting does produce peak responses, but these peaks are broad and move with increasing Re, as compared to the discrete and stationary Strouhal resonance.

The effects of turbulence buffeting are not, however, something to be ignored as they are the main source of continual vibrations resulting in tube wear in the long term. Paidoussis (1982) describes two methods for amplitude prediction by Pettigrew and Gorman, and Blevins. The root mean square response of the tube is predicted through spectral response theory, with the assumptions made that the excitation is broad band and occurs mainly over the natural frequency of the tube. The final equations take the following form:

Pettigrew- $y_{rms}=S^{.5}*f_n/(4*\pi^5*f_n^3*m^2*\zeta)^{.5}$

$S^{.5}=.5*\rho*d*U^2*C_R$

Blevins- $y_{rms}=S_F^{.5}*f_n*J*\Theta/(64*\pi^3*f_n^3*m^2*\zeta)^{.5}$

$(U/d*S_F)^{.5}=.5*\rho*d*U^2*C_L$

These two equations are basically the same, with Pettigrew's being a special case of Blevins'. Pettigrew assumes further that the forces are perfectly correlated along the tube length, and that the tube under consideration is a simply supported single span case.

To use these equations, values for C_L and C_R are

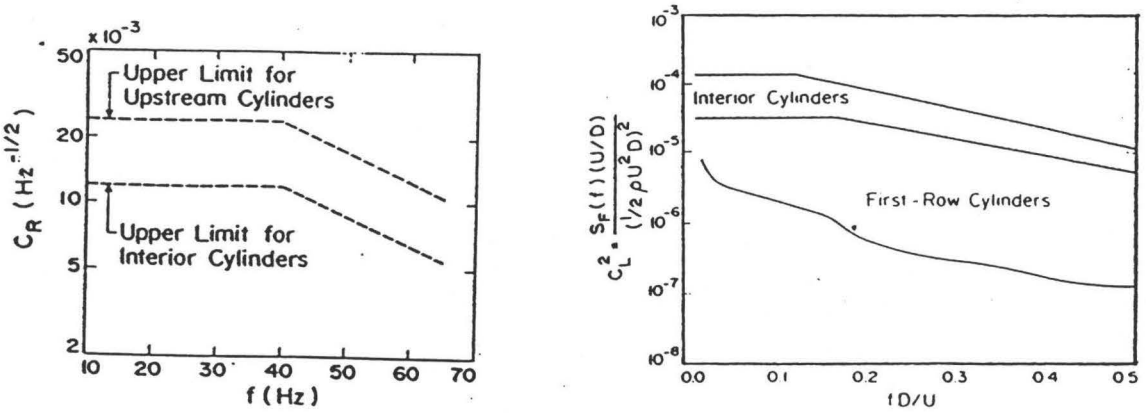

Figure 2.2 Paidoussis(1982)
Experimental Coefficients

required. Graphs of these values are provided in figure 2.2. There are two interesting comments that can be made concerning these equations. First, sample calculations using these two equations yield two very different results. Pettigrew's equation predicts amplitudes an order of magnitude higher. This may be attributable to the definition of vortex response used, where Pettigrew may have included some Strouhal peaks. Regardless, Pettigrew's equation is conservative at worst, which can only lead to overdesign.

Moreover, looking at the graphs of figure 2.2, it is evident that there is a discrepancy as to the behavior of the first row of tubes. Since Blevins' results are from air, and Pettigrew's from water, it can be surmised that the nature of the experiments led to this result. For instance, the upstream turbulence, type of liquid, and relative tube spacing can affect the response of the first row tubes. In this respect,

the air experiments are less likely to develop Strouhal response, whereas the water experiments are extremely susceptible to this phenomenon.

2.3.3 Fluidelastic Instability

In 1970, Conners presented what has come to be known as Conners' equation.

$$V_r=K*m_d^{.5}$$

Included in the mass damping term is the equivalent mass of the tube in the form:

$$m=m_s+m_a$$

The added mass term leads to hydrodynamic coupling, the first topic concerning the fluid tube interaction .

2.3.3.1 Hydrodynamic Coupling

The natural frequency of the tube is dependent on the effective damping of the tube, which in turn is a function of the mass of the tube. Moreover, the natural frequency is also a function of the tube stiffness. Hydrodynamic coupling has an effect on both of these parameters. The fluid that moves as if it were part of the tube, tends to act as if mass were added to the tube. Moreover, the fluid tube interaction can also affect the tube's apparent stiffness.

However, the most easily seen example of hydrodynamic

coupling is the comparison of tube response to that of a bundle. A tube will vibrate at its first natural frequency for the first mode, whereas, a tube bundle vibrates in a band of natural frequencies for the first mode. The tighter the array, the wider the band of frequencies observed. Therefore, it is concluded that the effect of the fluid is to transmit information from one tube to the other and the system modelling is further complicated as a result.

Lever and Weaver (1982), used the assumption that the onset of fluidelastic instability can be predicted by considering a particular tube to be essentially independent of the other tubes. The surrounding tubes are merely assumed to define the boundaries of the flow around the tube. This was experimentally verified by showing that a single flexible tube in an otherwise rigid array would go unstable at essentially the same conditions as an entirely flexible array. However, upon refinement of the model, Yetisir and Weaver (1988) have since found that for higher mass damping values in the flow, this is not the case, and upstream tubes can affect those in downstream, and transverse directions.

2.3.3.2 K Value

In the study of fluidelastic instability, the evaluation of the K in Conners' equation has received the most attention. One reason for wanting to evaluate this parameter is to avoid criteria that result in overly conservative designs. However,

the form of the equation has been subject to criticism as Weaver and El-Kashlan (Paidoussis (1982)) proposed the following form:

$$V_r = C(m/\rho D^2)^{0.29}\delta^{0.21}$$

Intuitively, the relationship seems to be overly simplified, which leads to speculation that the equation should take another form. In particular, the damping value exponent has been shown to be less than 0.5 for other equations. For instance, Tanaka and Takahara presented the following form:

$V_r \propto (m/(\rho * d^2)^{.5}\delta^{.5}$ low density flow

$V_r \propto (m/(\rho * d^2)^{.5}\delta^{.2}$ higher density flow

while Chen proposed:

$0.01 < m_d^{.5} < 0.5$ $V_r = 3.4(m_d)^{0.18}$

$0.5 < m_d^{.5} < 3.5$ $V_r = 4.0(m_d)^{0.41}$

$3.5 < m_d^{.5}$ $V_r = 7.6(m_d)^{0.42}$

There have been other proposals for predicting the onset of instability, with emphasis in the 1980's on trying to physically and theoretically explain the behavior of tubes in cross flow. As mentioned previously, Lever and Weaver presented a model not requiring lift coefficients for the tubes. Yetisir and Weaver have now extended the model and it would appear to be the most useful and the most promising model developed to date. Other attempts using potential theory, such as Paidoussis(1984), have not only had poor results, but also did not lend themselves to easy evaluation,

since they require inputs which are difficult to obtain. It is interesting that a totally theoretical model should predict with better results than the semi-empirical models.

The efforts to establish theoretically based models will help in the development of the theory for this area of study. In the meantime, plots, such as those seen in figure 2.3, will continue to provide the basis for design. From this figure, the problem of over design can be seen. For different geometries and flow conditions, there appear to be different results. Moreover, there is the problem of determining if the

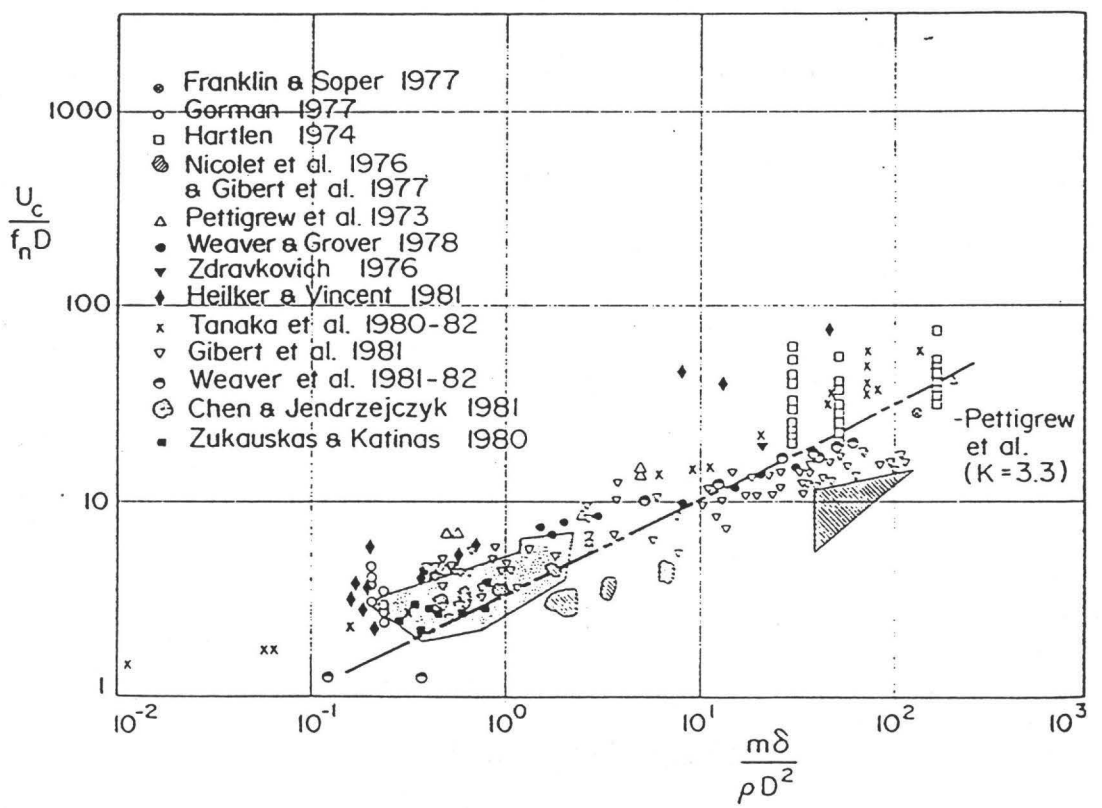

Figure 2.3 (Paidoussis 1981)
Traditional Plot for the Threshold
of Fluidelastic Instability

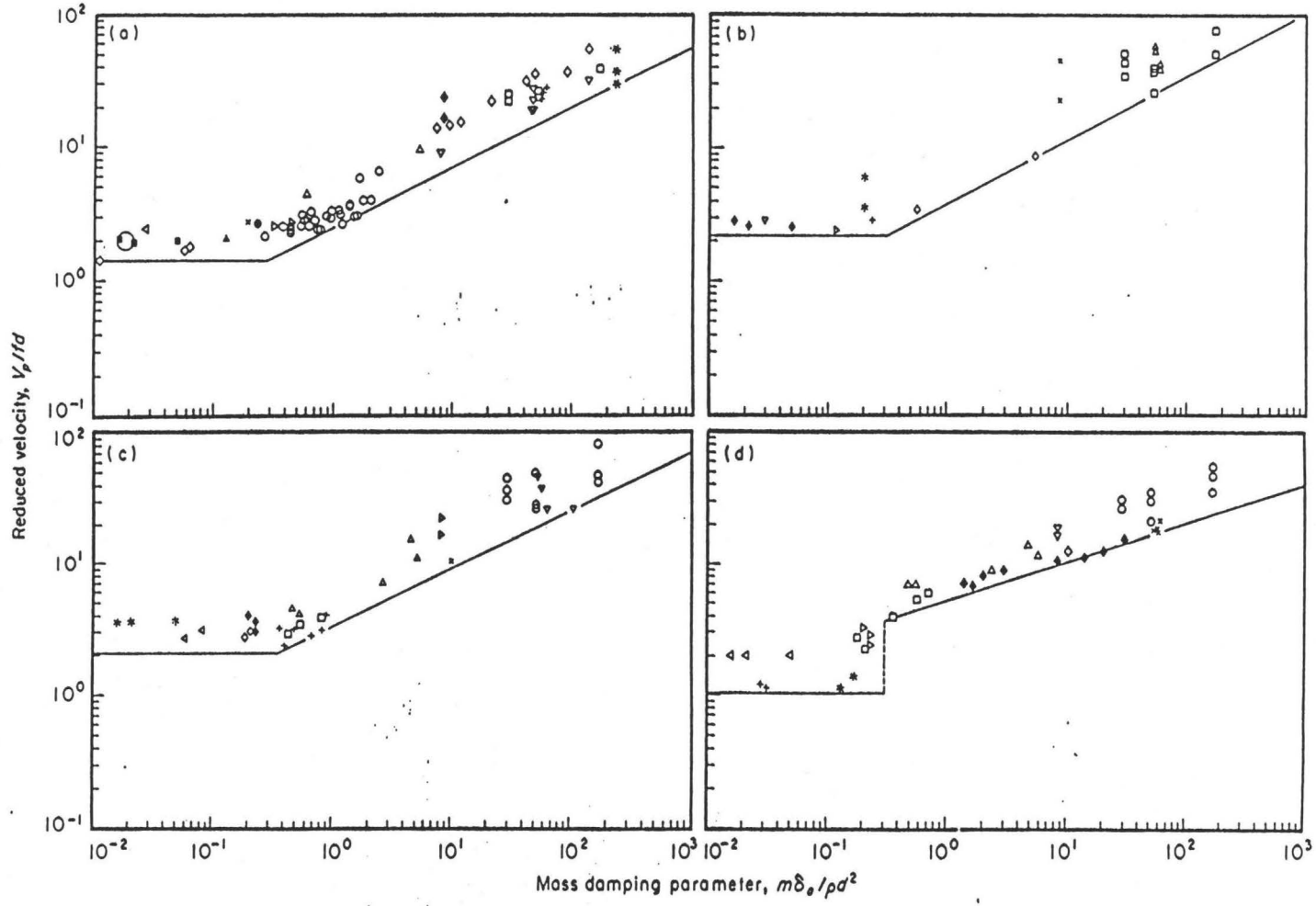

Critical flow velocities for fluidelastic instability for various array geometries (a) Square arrays. (b) Rotated square arrays. (c) Normal triangular arrays. (d) Parallel triangular arrays.

Figure 2.4 (Weaver and Fitzpatrick 1987)

Critical Flow Velocities

scatter is physically dependent since there are going to be differences in the definition of instability. Therefore, analysis with respect to geometry should prove useful for providing an indication as to the mechanisms involved and the effects of geometry.

Some of the scatter in figure 2.3 can be attributed to the geometries used. Chen first presented plots for different geometries, and Weaver and Fitzpatrick (1987) replotted the curves and added some data, as seen in figure 2.4. These plots show some notable differences, such as jumps and slope discontinuities. In general, each plot consists of a mass damping independent region for low m_d, followed by a linear relationship, after a critical value, between V_r and m_d.

2.3.4 What Is Known

The motion of the tube can be described by using the two axes, drag or streamwise direction, and lift or transverse direction. Experiments indicate that the motion of the tube can be considered to act in each direction, each independent of the other. That is, the transverse motion does not influence the streamwise motion. This is exemplified by the observation that the transverse direction tends to become unstable first. Using these two bits of information, Lever and Weaver(1982) formulated their model development for tube motion by considering the transverse direction only.

Furthermore, the above results were obtained for tubes

with symmetric stiffness. Alternatively, Weaver and Koroyannakis(1981) obtained results for tubes with asymmetric stiffness. It was found that fluidelastic instability was delayed in the asymmetric tubes, although it was also found that the ratio of the stiffness values does not affect the amount of the delay. Moreover, the tube motion is also independent of the instability, since the tube motion had several different patterns, including a figure eight, when the instability ensued.

Weaver and Yeung (1983) studied the effects of flow direction on the instability threshold by considering various angles of approach of the flow for several geometries. The results showed that the effects are dependent on the geometry used. Instability occurred earlier for the normal triangular array, whereas there was a slight delay for the same change in flow approach angle for the parallel triangular array. Moreover, the original onset of instability was also dependent on the configuration used.

These types of studies help to determine the important variables for the problem. Consideration of damping has also contributed to the understanding of the problem. Paidoussis (1987) discussed the mechanisms behind fluidelastic instability, and identified two underlying mechanisms that occur, depending upon the mass damping of the system. These are:

i) damping controlled mechanism- The effective damping of

the system is affected by 'negative fluid damping', which sets up the situation where the fluid can easily put more energy in than the tube can damp out. This occurs for lower m_d.

ii) stiffness controlled mechanism- The motion of the tube is amplified by the motion of the fluid, which adjusts quickly. The effects of hydrodynamic coupling are more prominent. This generally occurs at higher m_d.

These mechanisms were originally disputed by Lever and Weaver (1982) during the development of a theoretical model, but the continued development of this model by Yetisir and Weaver (1988) has confirmed that these are the mechanisms involved, although, the transition between mechanisms is continuous. That is, as the mass damping parameter approaches high values, the fluid response is such that it appears to act something like the stiffness controlled mechanism. Therefore, as the mass damping parameter increases, the fluid reaction changes and as a result the interaction is eventually more stiffness-like than damping. The implication is that any generalized theory must not include specific terms for either damping or stiffness, but should predict behavior similar to these two mechanisms implicitly.

2.3.5 Summary of Single Phase Response

The understanding of the mechanisms behind the phenomenon is slowly developing. Although a large base of data exists,

this has been primarily used for design correlations. It is acknowledged that the equation proposed by Conners is useful, but the underlying mechanisms are not explicitly accounted for. Therefore, the model development underway may contribute to the development of theory by looking at the problem from first principles. At this time, the theory development is in its early stages.

2.4 Two Phase Flow

The previous discussion inherently indicated that the level of understanding of the single phase phenomenon is now becoming significant. However this level of knowledge is still only a beginning. The situation in two phase flow is, understandably, at a lower level of comprehension. The understanding of two phase flow induced vibrations does have a foundation to build on in the single phase work, although this provides only guidelines for attacking the problem. The complications in the two phase region stem largely from the two phase flow itself. The theory for two phase flow is extremely detailed and comprehensive, owing to the complicated nature of this phenomenon. Therefore, superimposing the two phase problem on the single phase discussion already presented, we can see the difficult nature of the overall problem. Paidoussis (1982) claimed that two phase flow induced vibrations are not understood, and as of yet, they can not be modelled properly.

This introduction may appear somewhat discouraging. However the studies in single phase flow give a good indication of where to look. Studies in two phase flow have shown that all the response modes of single phase can be found in two phase, with the exception of vortex shedding. The inherent turbulence induced by the two phase flow has the effect of suppressing the formation of periodic vortices. The vortex action reappears for low void fractions where the

conditions for single phase vortices are coincidently met. Therefore, the studies can concentrate on the remaining mechanisms, and for this discussion, the acoustic resonance problem will also be ignored.

2.4.1 Preliminary Problems

As indicated, there are several additional problems introduced in two phase flow, some of which will be addressed here. The areas of concern can be categorized as follows:

i)Two Phase Flow Modelling- Assumptions must be made in the modelling of the two phase flow. The most common assumption is that the flow is homogeneous, and that there is no slip between the phases. This assumption will clearly be more applicable in some cases than in others. Axisa et al. (1984) did a study in which the homogeneous assumption was verified. Figure 2.5 gives plots of volume averaged void fraction and homogeneous void fraction versus the flow velocity. Using ten gamma densitometers across the test section, a void fraction profile was determined for the two positions plotted, namely upstream and downstream of the tube bundle. From these plots an area averaged void fraction could be obtained.

The spatial distribution tended to be more uniform in the downstream results. Therefore, for the downstream position the homogeneous assumption is more appropriate. Furthermore, the validity of the assumption is seen to be a function of void

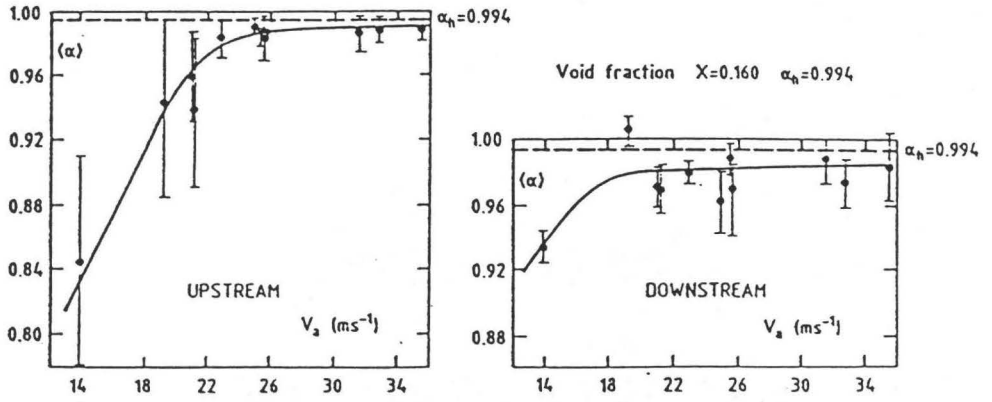

Figure 2.5 Air- Water tests- Void fraction vs Flow velocity Axisa et al. 1984

fraction, which can be interpreted as meaning that the homogeneous assumption is valid for particular flow regimes. For this specific case, the flow becomes more homogeneous as the flow rate increases. This is expected, since higher turbulence will occur at the higher flow velocity and tend to mix the two phases in a uniform fashion.

One conclusion from these results is that for experimental design, having several rows of tubes prior to the monitored tubes aids in justifying the homogeneous assumption by generating a uniform flow.

ii) Two Phase Simulation- The cost of performing steam-water experiments is prohibitive in most cases. Therefore, the two phases are simulated using fluids that can duplicate the density ratio and the general two phase behavior of the flow.

The most common liquid combination is air and water. Recently, some doubt has arisen concerning the validity of the results in air-water. This question is predominantly a consequence of the phase state changes that can occur in single component two phase flows. Moreover, the resulting pressure distribution around the vibrating tube may result in phase changes. The basis for doubt is increased when looking at the two phase flow equations, where the need of interfacial equations to complement the standard continuity, momentum, and energy equations, indicates the importance of the phase interactions.

Some work has been done to compare the air-water approximation to steam-water. Axisa et al. (1988) claimed that the forces from turbulence excitation are of the same magnitude in either flow. However, the turbulence level was shown higher for air-water than Freon-water by Gay et al. (1988), which indicates that there is some dependence on the nature of the two phase flow. Pettigrew et al. (1988) also noted that the collapsing of the turbulence force spectra required the inclusion of Reynolds number and void fraction. These results showed that flow regime is an important parameter. Therefore, there is some conflict concerning the effects of the two phase simulation on force levels. However the entire behavior of the system is definitely flow regime dependent.

Furthermore, Pettigrew et al. (1988), in a supplementary paper, showed that damping is influenced by the two phase

fluid used. Here, the air-water combination tended to provide greater damping than the steam-water results. This is significant, since damping has been found to be important in determining the amplitude of vibration and the onset of fluidelastic instability in single phase flow. The interesting contrast is that the fluidelastic instability does not appear to be greatly affected by two phase flow, which is supported by both Pettigrew and Gay. It may be concluded that the mechanism behind fluidelastic instability must still be investigated.

iii) Data Analysis- The influence of two phase flow on data analysis is partially a result of the effects discussed in the previous two sections. That is, the assumption of the two phase model (i.e. homogeneous etc.) determines the evaluation of the velocities and other fluid properties. Furthermore, the response obtained by the two phase flow is somewhat dependent on the fluids used and the flow regime that is created. Therefore, there is some difficulty in generalizing results for application to all flows.

These problems are enhanced by the tendency for the flow turbulence to be higher than that observed in single phase flow, which makes interpretation of data more difficult. For example, the onset of fluidelastic instability is obscured and therefore definitions are required to indicate when fluidelastic behavior is being observed. Some definitions include:

1) y_{rms}= 2% of tube diameter

2) tube clashing

Variations in definition result in a wide scatter in the data, which makes comparison difficult.

2.4.2 Two Phase Flow Continued...

The previous discussion has hinted at some results which will now be expounded upon. These include the areas of hydrodynamic coupling, damping, fluidelastic instability, turbulence excitation, and the way in which flow regime tends to affect many of these problems.

2.4.2.1 Hydrodynamic Coupling

The only thing that has been addressed in this area is the assumption of the added mass associated with the two phase flow. Axisa et al. (1984) used

$$m_a = \rho * \pi * d^2/4 \quad ,$$

which is a function of the two phase flow distribution. Therefore, if the flow conditions are not well known (eg. slip), then this value will be incorrect. In contrast, Pettigrew used

$$m_a = m_s * ((f_g/f)^2 - 1) \quad ,$$

which requires knowledge of the natural frequency in two phase flow. This is experimentally difficult to obtain since the two phase flow can not be captured with its flow distribution intact. Therefore, the evaluation is done in flowing liquid,

which is then used in conjunction with vibration theory to back out the natural frequency.

The latter of these two methods is somewhat involved, and as Axisa points out, $m_a << m_s$. Therefore, there is not much error in the final result regardless of the assumptions involved.

2.4.2.2 Damping

Damping results in two phase flow can be somewhat misleading. Axisa et al. (1984) found no difference in damping in the drag and lift directions as a function of quality or void fraction. However, Pettigrew et al. (1988) looked at damping as a function of mass flux, which shows no dependence when overall damping is considered, but shows significant dependence when lift and drag directions are considered independently. Figure 2.6 shows the dependence for various void fractions.

There are two things that can be taken from figure 2.6. First, the drag direction damping tends to be higher than the lift direction damping in all cases. Second, for higher mass flux, the lift direction damping decreases rapidly, while the drag direction damping increases or decreases at a slower rate. This is most evident for the 50% void case. The significance of this observation is that it supports what is observed experimentally. As the velocity of the flow increases, the lift direction tends to become unstable first.

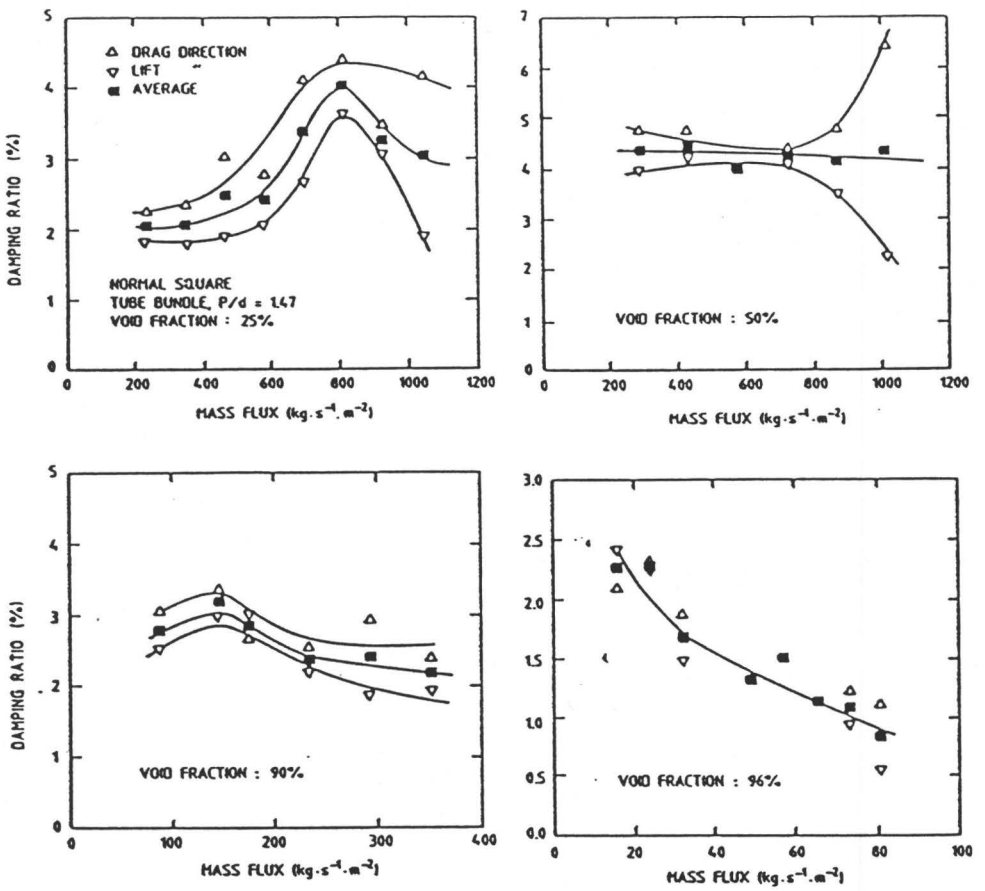

Effect of Mass Flux on Tube Damping in Lift and Drag Directions for Normal Square Bundle of p/d=1.47

Figure 2.6 Pettigrew et al. 1988

Effect of Mass Flux on Tube Damping

The reduction of the damping parameter in the lift direction corresponds to the negative damping phenomenon observed in experiments.

In comparison to Axisa's work, Pettigrew also obtained results that showed the damping coefficient to be consistently higher in the drag direction when plotting damping vs void fraction, as seen in figure 2.7. The slight skewing of the curves between geometries would seem to indicate some dependence of damping on geometry, and consequently on the resulting flow patterns. This comparison does not consider the flow regime dependency of the results. Pettigrew found the results to be affected by flow regime.

2.4.2.3 Fluidelastic Instability

The evidence discussed above demonstrated that the onset of fluidelastic instability was not dependent on the two phase medium used. However, when compared to single phase response, there are differences in two phase response. First, in general, it is expected that the fluidelastic instability will occur at a higher velocity than that for single phase, although, the amount of delay can be subject to the definition used for the occurrence of the phenomenon. Second, the presence of bubbles has been shown to result in different effects for different conditions.

Hara (1988) did a study on the effects of bubbles on a single row of tubes. Experiments were done for single phase

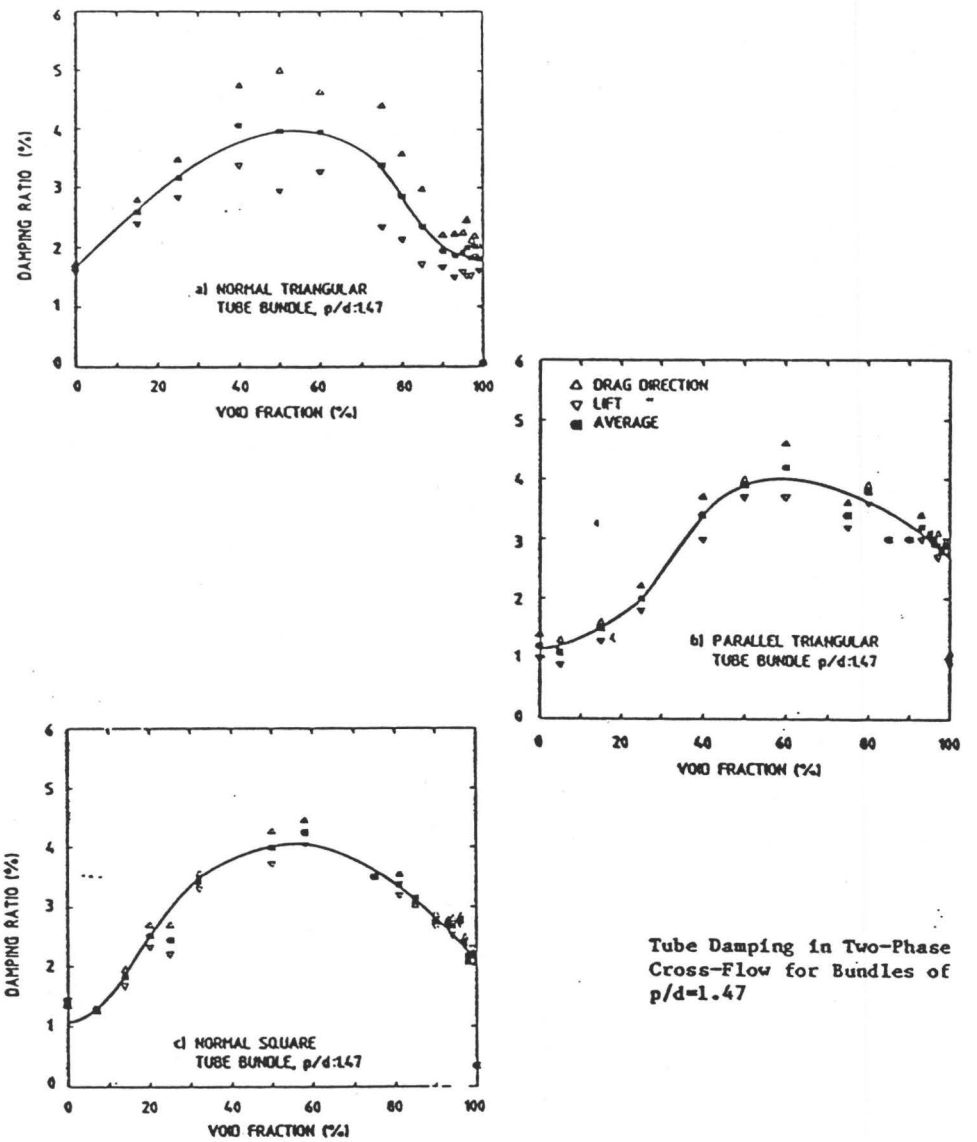

Tube Damping in Two-Phase Cross-Flow for Bundles of p/d=1.47

Figure 2.7 Pettigrew et al (1988)

Tube Damping in Two Phase Cross Flow

flow and then for various qualities and flow rates using air-water flow. The definition of tube clashing was used for the onset of fluidelastic instability. The results were presented in terms of the void and reduced velocity, with an attempt to demonstrate the changes between the single phase case and the two phase case.

The effects of the bubbles were simplified as follows. At low reduced velocity and for void fractions less than or equal to 30%, the tube vibrations increased in magnitude, where no instability had been observed before. For voids greater than 30% the vibrations became violent at these reduced velocities. For V_r=2.9 the vibrations were suppressed for voids up to approximately 20%. In contrast, at V_r=10.2, where strong vibrations had been observed in single phase, a 5% void suppressed the vibrations, which were again evident at 10% void. Finally, for the range of reduced velocity of 13.0 to 20.4, almost nonexistent vibrations in single phase were gradually increased to the point of instability by increasing the void fraction.

These results appear to differ somewhat from those found in other studies. However, it is evident that the two phase flow can appear to enhance or suppress vibrations. The effects described appear typical of results in turbulence buffeting region, but these results also indicate that the mechanism involved in fluidelastic instability must include the distribution of the two phases and their interaction.

Consequently, the void fraction is also an important parameter in determining the nature of the excitation mechanism. This conclusion is intuitive in that the behavior of the system must be flow regime dependent. The most obvious case is found in intermittent flows, where the impact of the phases would significantly affect the forcing function.

The effects of flow regime are seen in results by Pettigrew et al. (1988), where conditions from both the bubbly and intermittent regimes were used. From figure 2.8 it is seen that the slope changes for the points indicating the onset of fluidelastic instability. This change of slope can be shown to result from the flow regime changes. Pettigrew et al also presented the results in a form independent of the damping in two phase flow. This is done since two phase damping values are difficult to obtain, and are not generally known. Therefore, for use in design, the data were presented in the form of figure 2.9.

2.4.2.4 Turbulence Buffeting

The effects of bubbles on the vibration amplitudes has already been discussed in the previous section. The overall response of the tubes in the turbulence buffeting region can be characterized as being proportional to the velocity, whereas, the single phase response is proportional to the square of the velocity. Moreover, the forces measured in two phase flow are approximately ten times those of the single

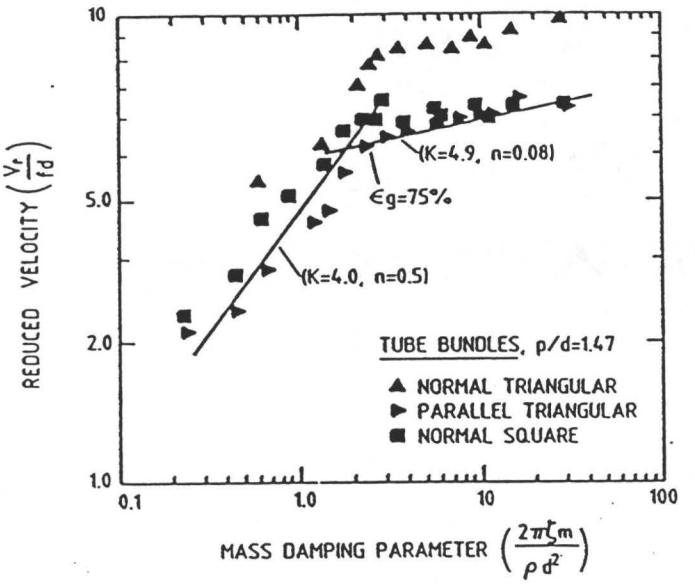

Fluidelastic Instability of Tube Bundles of p/d=1.47

Figure 2.8 Pettigrew et al. (1988)

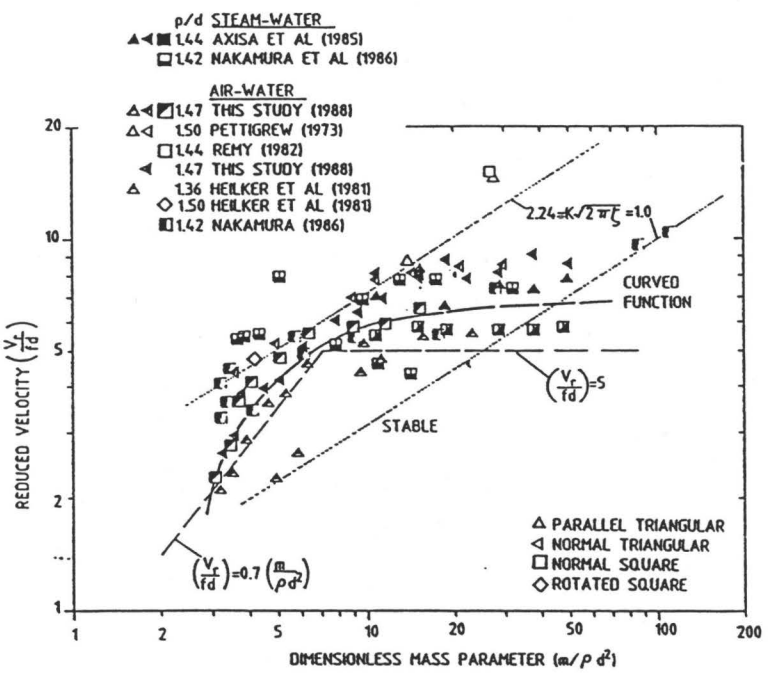

Figure 2.9 Pettigrew et al. (1988)

phase. Additionally, collapsing the force data required the inclusion of void and an inverse Reynolds number dependence, these plots again showed the effects of flow regime.

2.4.3 Numerical Methods and Modelling

Chen (1988) doesn't acknowledge the existence of any analytical or numerical methods for general applications. However there have been some efforts made. Earlier, Axisa et al. (1988) was cited as a source of numerical methods for a wide range of cross flow induced vibrations problem components. Moreover, Goyder (1988) developed an analytical model for fluidelastic instability, where the void and slip conditions were included using time and space averages. The final equation uses multipliers that are obtained from charts to account for the slip and void conditions. The results of this work have not been experimentally verified, but provide the framework for future efforts.

The use of finite elements is a popular solution technique in today's technical environment. The application to the problem of flow induced vibrations is not straight forward since the problem involves the interaction of fluid and mechanical forces. Rao (1988) performed a finite element study, where the fluid flow was replaced by empirically determined forces on the tubes. The results were favourable for air data, which indicates that the results are only as good as the modelling done, as expected. However, this

approach has the potential for accurately modelling the tube for various supports and materials. Therefore, once definitive knowledge is obtained concerning the fluid forces, some good results may be obtained.

2.5 Some Conclusions

The single phase aspect of the problem is now evolving into a more theoretically based understanding, but much work has yet to be done. Two phase flow has apparent differences and, as such, requires more fundamental experimentation. The mechanisms involved in two phase flow are more complicated than single phase, as are the experimental interpretations of data. Therefore much more effort will be needed to fully understand the phenomenon in two phase flow.

There are some glimpses of the important parameters coming to light. The flow regime is a dominating factor in determining the system behavior. Moreover, there are indications that the effects of two phase flow are void fraction and Reynolds number dependent. These are results particular to the two phase case. However, there are some similarities to single phase, such as the apparent damping reducing as instability becomes imminent. This leads to some speculation as to the similarity of the single and two phase mechanisms.

From the design point of view, there is little concern over present practice not being conservative. All indications are that design for fluidelastic instability is conservative based on air-water results or single phase results. The only problem is that the equipment will be over designed. To accommodate the design side of the problem, some researchers have plotted their results without the damping parameter,

since two phase damping values are largely unknown. However, the usual Conners' equation has been recommended with the use of K=3.3 as determined by Pettigrew et al. (1988).

The future requires much time and effort in the experimental determination of the important aspects of the problem. Some areas of concern are the validity of air-water results, particularly in the turbulence region, and the two phase damping. Moreover, there may be some interest on the effects of boiling on the tubes, since this represents a deliberate change of state occurring in the fluid next to the tube. These effects could be insignificant for high voids, but become increasingly important as the void fraction decreases.

Generally, the results to date indicate different modes of forced excitation in two phase flow. These mechanisms are still hidden within the empirical constants of the analysis done and further study is required to determine what is happening. From these experiments, the question of what is different about two phase flow can be answered.

Chapter 3

Commissioning of a Two Phase Flow Loop

From the review presented in the previous chapter areas of concern can be noted. The two phase flow loop, which is the primary concern of this thesis, is intended to address some of these concerns. Specifically, the loop must be able to provide information on the various problems associated with modelling the two phase flow induced vibrations. Therefore, the test section has large windows for viewing the flow, and the homogenizing bundles can be altered to create different flow circumstances. Moreover, the loop is able to generate a wide range of conditions to provide information on the effects of different fluid properties. That is, the loop provides the capability to study many of the concerns researchers may have for single component two phase flow induced vibrations.

This chapter describes the fundamental operation of the two phase flow loop constructed for the study of two phase cross flow induced vibrations and the modifications incorporated for this thesis. The original design and thermodynamic analysis of the loop can be found in the thesis by Gerry Westermann entitled "The Design and Construction of a Flow Loop for the Study of Two Phase Crossflow-Induced Vibration of Heat Exchanger Tubes". Although several modifications have been made to the original design, a second

thermodynamic analysis was not warranted. Moreover, the discussion provided in the following pages is taken in part from the operating manual written for the loop, a copy of which is included in the appendices. Therefore, to obtain further details concerning various components and the general operation of the loop, refer to the operating manual.

3.1 The Loop

The loop, as shown in Figure 3.1, consists of two parallel subloops, which are both supplied by a 2 HP gear pump. In addition, there are also two more components referred to as the service loop and the water line. The former is used in charging and discharging the Freon 11 from the main loop, while the latter provides the cooling water for the coolers. The first two subloops interact to provide the necessary conditions to generate and regulate the two phase flow.

3.1.1 Main Flow Subloop

The first of the two parallel subloops is the main flow subloop. The fluid that is to pass through the test section flows through this portion of the loop. The path consists of eight components, some of which are common with the second subloop.

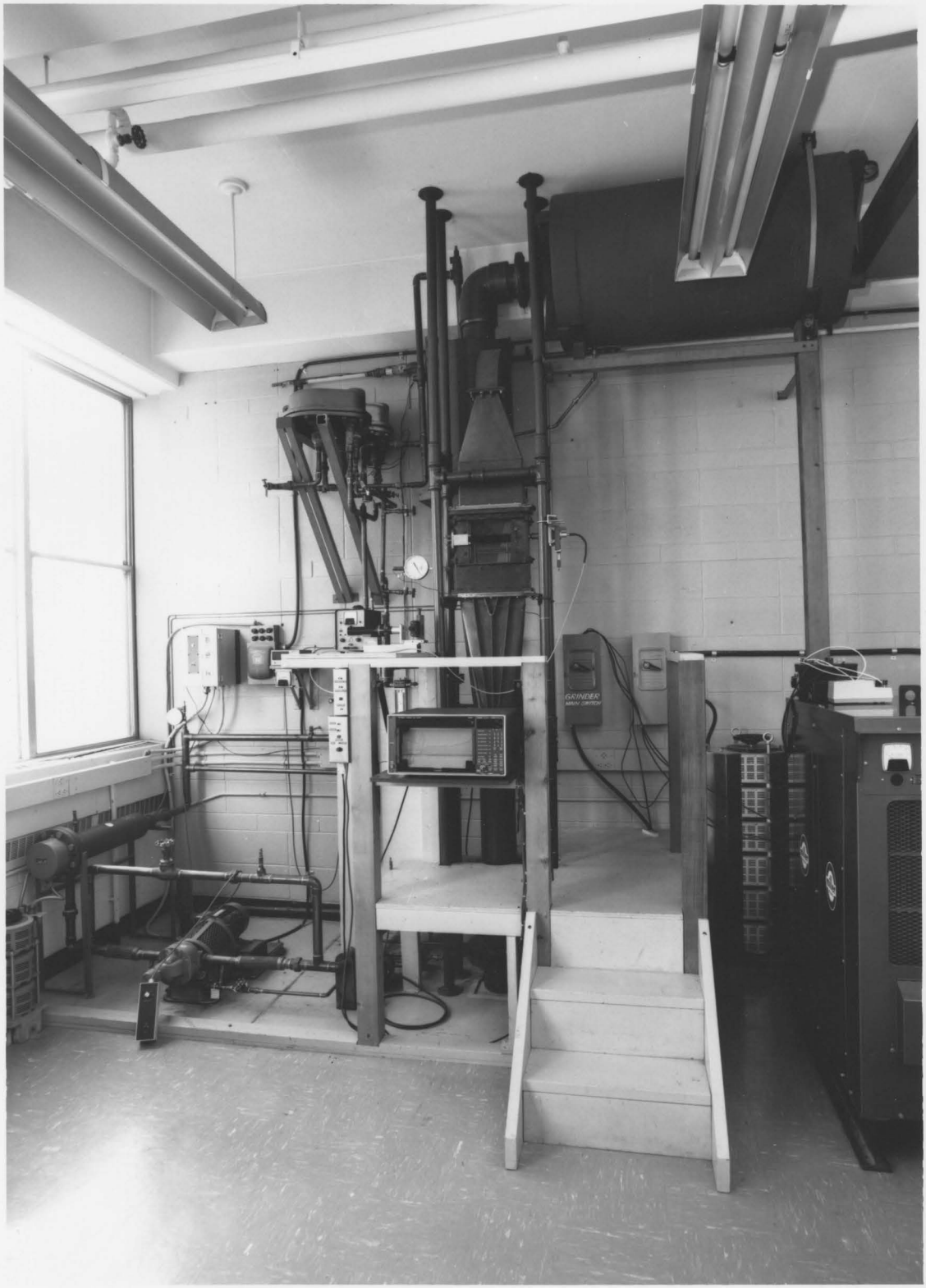

Figure 3.1 Picture of the Complete Two Phase Flow Loop

MAIN FLOW SUBLOOP

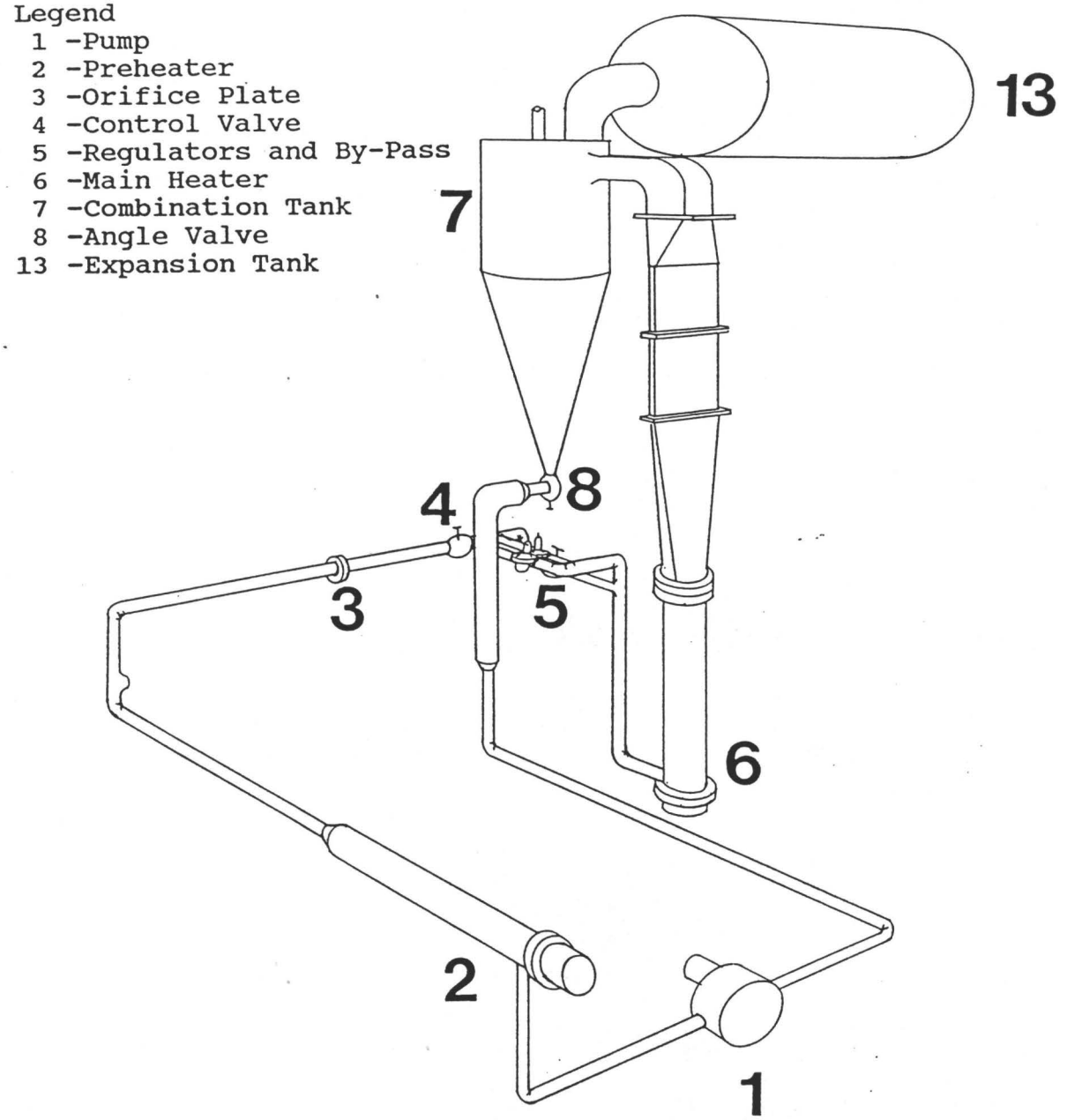

Figure 3.2 Main Flow Subloop

3.1.1.1 Pump, Preheater, Regulators & By-Pass

The Worthington Gear Pump provides the driving force for the entire flow of the two phase flow loop, and is therefore a logical place to begin the tour of the individual subloops. From the pump the fluid passes into the preheater. It is now known that there is no necessity for the preheater, although the original design with the pressure regulators would have made it useful in bringing the flow up to saturation conditions prior to the main heater. Since the regulators have been shown to operate as flow smoothing valves only, the preheater input may generate problems at the lower operating pressures that the loop now uses.

After passing through the orifice plate, the main flow encounters the pressure regulators and by-pass valve. Initially, the regulators were intended to provide a constant inlet pressure to the heater. However, the basic operation of the regulators requires a constant back pressure in order to provide constant pressure to the heater inlet. Investigation into the operation of these devices has shown that the regulators simply provide a frictional pressure drop directly proportional to the square of the flowrate. This discovery does not render the regulators redundant, since it is possible that they could provide some flow conditioning. However, at higher temperatures and flowrates signs of cavitation were noted when the regulators were in use.

The net effect of the regulators was to reduce the

attainable flowrate at the design temperature and pressure. Therefore, the loop was modified by installing a by-pass around the regulators with a valve to control the relative flowrate distribution between the regulators and the by-pass line. This modification has become one of the major control functions of the loop. When fully closed, stable single phase flowrates are more easily maintained. Manipulating the by-pass valve during two phase operation allows for greater pump efficiency at higher potential flowrates through the adjustment of the pressure seen by the pump.

3.1.1.2 Main Heater

After passing through the regulators and by-pass, the flow now enters the main heater, which is designed to provide 48 KW of heat input over its length. Since the equipment required to control this amount of power was unavailable, the heater was rewired to provide 19.2 KW, which is the maximum power output that can be obtained if a balance between the phases is maintained and the number of heater elements within each phase is equal.

This level of heat input still allows the generation of two phase flow. Through the use of a variable transformer, it is possible to vary heat input for the various conditions as required. The original heating capacity was intended to match the heat removal capability of the loop, including heat loss to the room. However, experience has shown that the natural

convection component of the heat loss was over estimated. At present, the capacity of the cooling units approximately equals the capacity of the main heater as it is currently configured. Consequently, any increase in the heat input desired for future stages of the project will also require additional cooling capacity to be created. The necessity of additional heat must yet be determined.

3.1.1.3 Test Section

The heater is intended to provide sufficient energy to generate the two phase flow, which then passes through the tube bundles of the test section. This is the central concern of the project, and the flow conditions here are critical. While the pump provides the pressure head, and the heater provides the needed energy for two phase flow, the pressure in the tanks above the test section must be maintained in conjunction with these inputs to attain the desired conditions in the test section. Therefore, all the components described before and after this point operate together so that useful data can be collected from the test section. This is a simple, but important concept in the understanding of the tradeoffs involved in the operation of the loop.

The flow entering the test section is modified by homogenizing bundles that are designed to create bubbly homogeneous flow conditions. These have been redesigned as will be discussed in chapter 5. In addition, the exterior

structure has also been redesigned to meet the requirements of the loop from a flow conditions perspective and a mounting stress point of view. These modifications will also be described in chapter 5.

3.1.1.4 Expansion & Combination Tanks

There are two tanks into which the flow now enters. First, the combination tank sees both phases of the flow, from which the vapour is allowed to flow into the second tank, the expansion tank. This is the one component that both subloops use, which does not appear to directly affect the flow. The existence of the expansion tank accounts for the possibility of sudden vaporization of a large quantity of liquid. The resulting expansion in fluid volume would generate extreme pressures if there were not space for the vapour to expand into. The expansion tank provides the necessary volume to reduce the effects of such an occurrence.

The combination tank was originally intended to promote the separation of the liquid from the vapour phase in order that the vapour might flow through the condensers. However, as a result of the unsteadiness of the vapour flowrate, the energy in the vapour phase could not be removed continually in this way. Consequently, control of the loop conditions was erratic. The principal of loop operation is to maintain a constant or controlled pressure in the expansion and combination tanks while the heat input is increased, resulting

in the generation of two phase flow. It was intended that the vapour be removed from the tanks directly, but since this method proved unreliable, the loop was modified to remove energy from the liquid phase instead.

Consequently, cold liquid is introduced into the combination tank to combine with the main fluid flow. The result is that some vapour is removed by the cooled liquid spray, some is condensed before it leaves the fluid and some is condensed by contact with the cooled liquid mixture. In this manner, the vapour is removed indirectly.

3.1.1.5 Back to the Pump

The remainder of the main subloop is designed to provide the necessary head for the pump to provide the required pressure and flowrate combinations. The flow now returns to the pump where the discussion began. From this point, the tour of the heat removal subloop can begin.

3.1.2 Heat Removal Subloop

The heat removal subloop takes a portion of the fluid flowing in the main loop and passes it through heat exchangers to remove the excess energy from the system. This loop is comprised of eight components, many of which are included in the main subloop and will be mentioned for completeness.

HEAT REMOVAL SUBLOOP

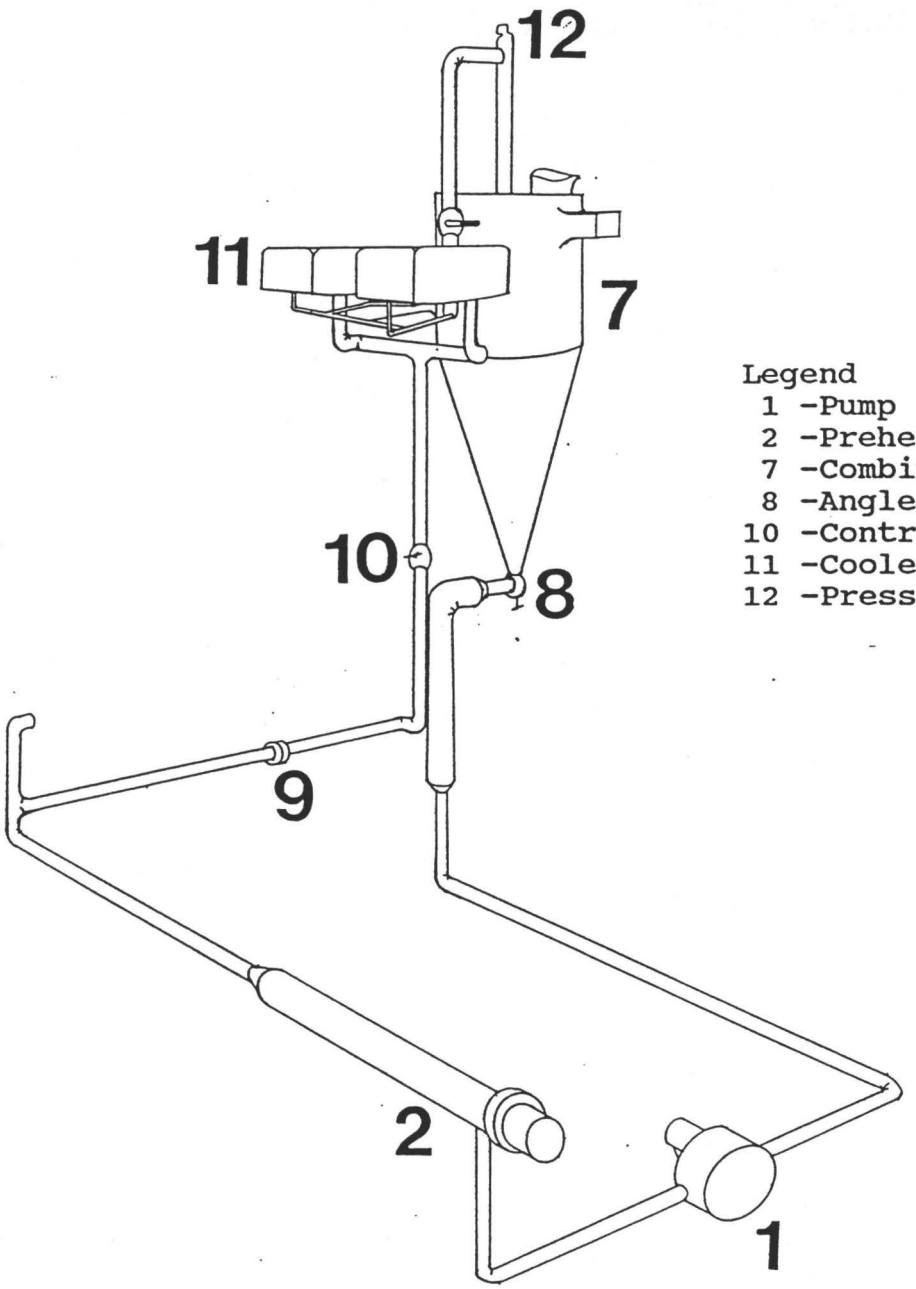

Legend
1 -Pump
2 -Preheater
7 -Combination Tank
8 -Angle Valve
10 -Control Valve
11 -Coolers
12 -Pressure Relief Valve

Figure 3.3 Heat Removal Subloop

3.1.2.1 Pump

The flow does not split until after it has passed through the preheater. Once split, the heat removal flow uses a line that initially was intended for use with small flowrates. However, the variable speed pump and the numerous control valves made this unnecessary. Therefore, when the search for a secondary pump to provide head for the heat removal subloop proved to be extremely difficult, it was suggested that some of the flow be diverted from the main flow. This would be satisfactory provided the pump had sufficient capacity and this did not create any complications for control of the loop. Neither of these concerns has proven to be significant, and therefore the main pump supplies the flow to both subloops.

3.1.2.2 Control Valve

The primary flow control valve for this subloop is a gate valve located upstream of the coolers. This valve acts against or in conjunction with the by-pass control valve from the main subloop. It is a simple task, using these valves, to balance the resistance between the two loops to attain the relative flow rates that are desired.

3.1.2.3 Coolers

Following the control valve, the coolers receive the flow to remove the heat. The coolers were originally intended to condense vapour. However the necessary pressure drop could not

be generated. The problem was associated with a build up of liquid in the helicoils of the coolers. To nullify the effects of gravity, the coolers were repositioned on their sides. This did not solve the problem and consequently further modifications were introduced so that the coolers now operate to cool liquid. The consequence of this change is that the mass flowrate through the coolers required to remove the heat is increased considerably. This is a result of the less efficient process of removing heat from liquid as opposed to that of condensing vapour. The liquid flowrate was calculated to be approximately 4.2 USGPM using a method similar to that used by Westermann (1987). However, the loop operation required a flowrate of approximately 10 USGPM at maximum conditions. This discrepancy is most likely due to the approximate form of the calculations and the inefficiencies observed within the heat exchangers. Fortunately, the modifications made also improved the potential flowrate capability. Therefore, the loop can still achieve the design flowrates. Additionally, the heat removal subloop flowrate is well within the design specifications of the two heat exchangers.

3.1.2.4 Combination Tank

The cooled liquid Freon 11 then flows into the top of the combination tank, where the vapour is condensed. From here the flow is once again united, flowing back to the pump to repeat

the cycle.

3.1.3 Water Line and Service Loop

To provide the cooling for the condensers, water is brought in from the University's water supply. The water loop is composed of a by-pass for cooling and controlling the flow variability of the incoming water, an orifice plate, control valve, drain valve, and a drain. The operation of this loop is described in appendix III along with its pertinent special features.

The charging and discharging of the Freon 11 is accomplished through the operation of the service loop. Again, for a description of its operation and characteristics, refer to the appendix. The one important capability that is not noted there, is the ability to charge and discharge particular areas of the loop without affecting other areas. In particular, the calibration of the gamma densitometer, which is used for the measurement of the loop's void fraction in the test section, requires that the test section be alternately empty and then full. The charging system allows this to be accomplished in a very short period of time.

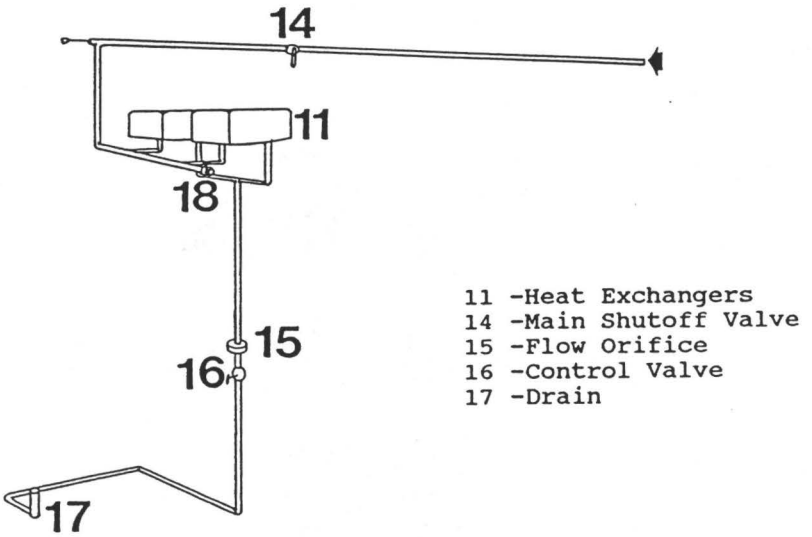

Figure 3.4a

Water Line

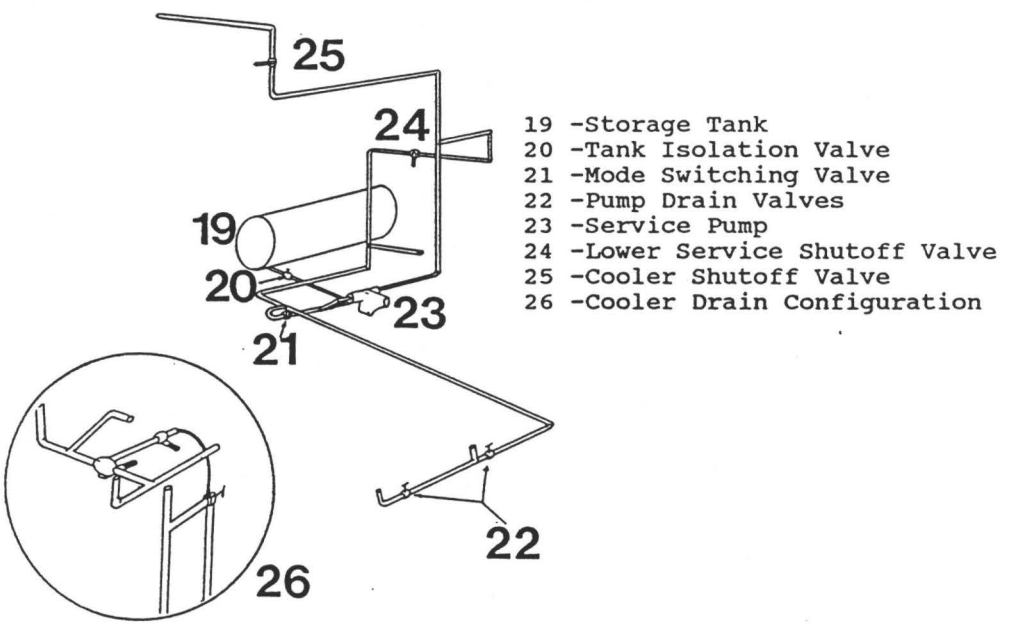

Figure 3.4b

Service Loop

3.2 Instrumentation and Special Controls

Instruments were installed to provide information on pressure, temperature, flowrate, and current. Moreover, some controls have been put in place to guard against the possibility of burnout. This section will provide a brief overview of the instrumentation and controls employed in the loop.

3.2.1 Temperatures

Temperatures are measured in the loop through the use of 12 E type thermocouples. The output of these thermocouples cannot be directly input into the Phillips PM 8237 A Multipoint Data Recorder, which is being used, since it does not have the capability to provide an electronic reference point for E type thermocouples. Therefore, it is necessary to use an ice bath as the reference temperature, and as a result the recorder provides output in millivolts. The outputs are then converted by means of charts.

Presently, the recorder has the following 12 channels dedicated to monitoring the following thermocouples:

Channel	Location
1.-	Test Section
2.-	Immediately Upstream of the Pump
3.-	Immediately Downstream of the Pump
4.-	Water Line - Post Coolers

5.- Heat Removal Line- Pre Cooler

6.- Water Line - Pre Coolers

7,8,9.- 1/4 Power Heater Elements

10,11,12.- Full Power Heater Elements

In addition to the digital recorder, there is a duplicate system using less advanced technology. This system is housed in the console that accompanies the loop. Originally intended to be the loop's control centre, the console contains all the wiring and electronics necessary to monitor the twelve thermocouples and to duplicate the alarm capabilities of the Phillips recorder. The actual plotting of temperatures is accomplished through a Honeywell recorder found in JHE-206. The original input hardware for the console has been changed to serial plugs, therefore allowing the use of the existing connectors for input to the digital recorder to be easily plugged into the console if the need arises.

3.2.2 Pressure

The loop uses pressure gauges to monitor the pressure at 7 locations around the loop. To suppress the occurrence of random fluctuations in the gauge readings, miniature control valves were installed between the gauges and the flow being measured. Consequently, the readings are the average pressures at the specific location. Should a particular gauge appear either to have a slow response or to have stopped responding

altogether, the setting of these valves should be checked before the actual gauge is considered. Furthermore, should a particular gauge require removal, the valves can be shut off to allow easy removal without loss of fluid or necessitating the discharge of the loop.

The most accurate gauge provides measurement of the pressure in the test section. The pressure in the test section is one of the parameters that is controlled when operating the loop. Therefore, this gauge must be closely monitored while making adjustments in order to attain specified conditions, or determining the response of the loop as specified conditions are approached.

There is a set of two gauges to monitor the pump head, although each also provides information concerning the flow conditions in other parts of the loop. Monitoring these gauges aids in the most efficient operation of the loop pump.

A second set of gauges monitors the pressure drop across the regulators. This was important in the past, but their use is now relegated to providing information on the pressure of the flow as it enters the heater section, and the pressure drop that the by-pass is creating.

The sixth gauge measures the pressure in the heat removal subloop. This reading is of concern when adjusting the relative flowrates of the subloops. The change of either flowrate will affect the pressure seen at this point in the loop.

The final gauge measures the pressure of the vapour in the upper tanks. This pressure can also be considered the loop back pressure. It is through the control of this pressure that the fluid can be forced into two phase flow conditions. A gauge with a large and easily read face was chosen for this purpose.

3.2.3 Flowrate

Each subloop and the water line have orifice plates to monitor the flowrate in that loop. The larger of the two Freon monitoring plates is situated in main subloop line. A differential pressure (DP) cell, which monitors the pressure drop across the plate, is calibrated to indicate the flowrate. The output, read on channel 1 of the Validyne display, corresponds to one inch of mercury per unit on the readout. The actual conversions to be used are provided in the manual.

The second orifice plate is mounted in the heat removal subloop, and as before, a DP cell is used to measure pressure drop. The output, read on channel 2, corresponds to one half inch mercury per unit on the readout.

The DP cells are mounted in manifolds that allow the proper installation of the cells and also allow the easy removal of the cells. The readout has been calibrated using Heise mercury pressure gauges, which are considered very accurate. However, the scales selected for the DP cell readout were chosen such that the readout may not remain zeroed for

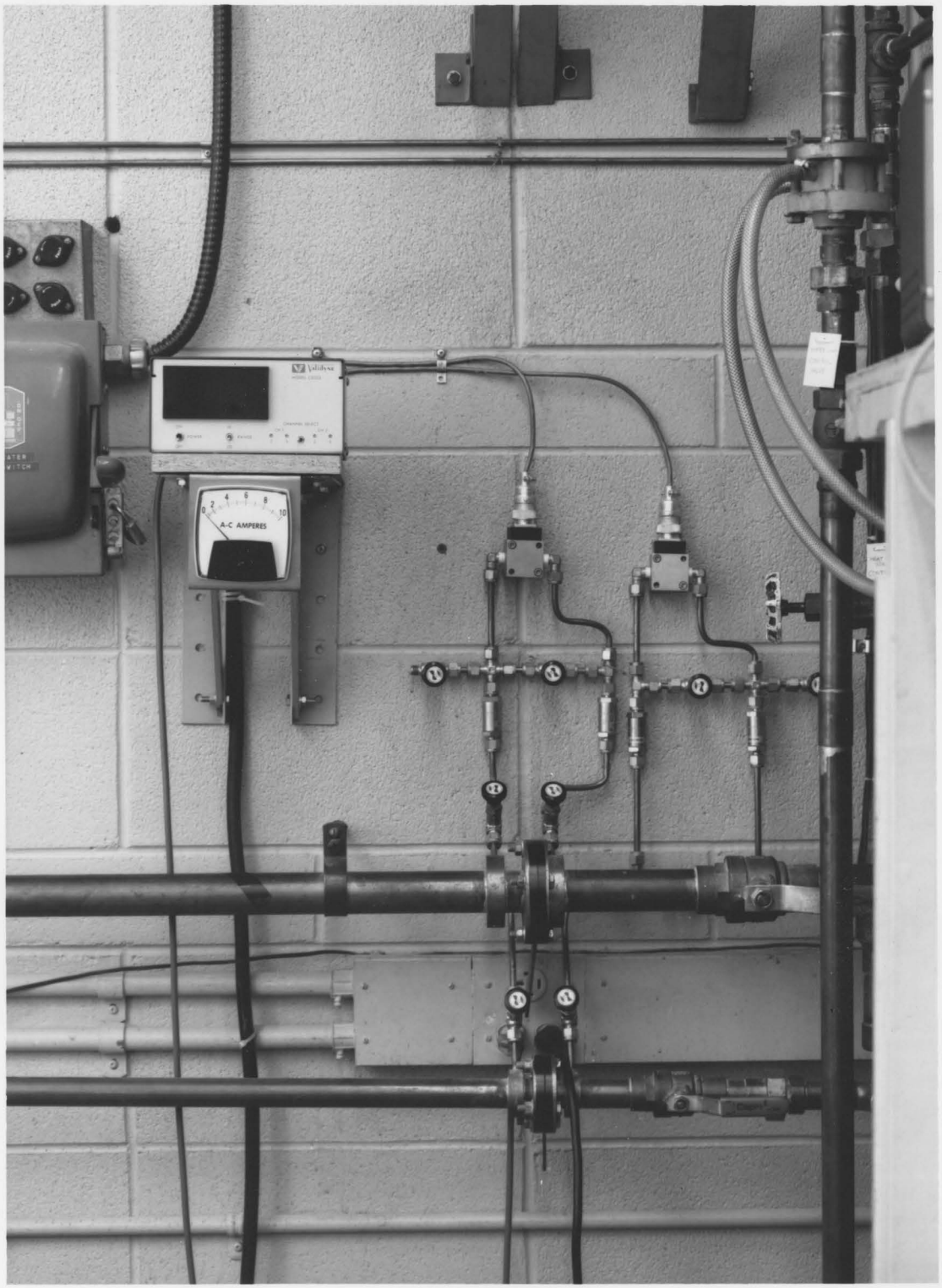

Figure 3.5 Picture of DP Cells and Manifold

long periods of time. The tradeoff is a more sensitive scale reading to allow greater accuracy in the flowrate determination. Moreover, this variation is small and can usually be corrected using the zero control screws on the readout device.

The final orifice plate can be used to determine the water flowrate. The experiments discussed in chapter 6 used cooling flowrates easily measured by the manometers connected to this orifice. The determination of the actual flowrate can be accomplished by using a graph found in the thesis by Westermann (1987).

3.2.4 Controls

There are basically two areas of concern when discussing the loop controls. Primarily, the heater can result in the greatest problems, and therefore several automatic devices have been installed. Secondly, there are the manual controls for the general operation of the loop.

The phenomenon which the heater is subject to is referred to as burnout. Should the critical heat flux be reached, the heater elements could be subject to a sudden temperature rise of approximately 1000 degrees Fahrenheit. The digital recorder, mentioned earlier, monitors all the thermocouples simultaneously and can be set to send an alarm signal if the preset maximum or minimum are reached. Therefore, the six heater thermocouples are set to trip the alarm should the

temperature exceed 100 degrees Celsius, which is roughly twice the maximum operating temperature. The alarm signal is used by a control circuit to trip the breaker for the heater power. Consequently, the phenomenon of burnout can be avoided.

The same control circuit is used to turn the breaker on and off at the desired times. To operate the heater, the control circuit must be activated, and the start button pushed. Additionally, a circuit has been installed that also cuts the heater power if the power to the motor controller should be interrupted. This circuit is activated automatically when the controller is turned on.

The concern over burnout is largely a fear of the unknown. First, it is not known whether or not the inconel heater elements could sustain the temperature change as a result of burnout. Second, Freon 11 was chosen partly for its low latent heat of vaporization, which results in an intuitive concern when boiling this fluid. However, a study done previously, using a number of different correlations, showed that there was little possibility of burnout occurring.

The secondary controls of the loop are manually controlled. These are the Variacs and the motor controller. There are two variacs used to control the preheater and the main heater respectively. A new 48 KW Variac has been installed to replace the present 24 KW Variac used to control power to the main heater. This will allow the reconfiguration of the heater to its original 48 kW output capability.

To monitor the power consumption of the pump and the main heater, gauges have been installed to measure current and voltage. The current entering the pump motor is of interest when operating near the motor rated current levels. Therefore, an ammeter measures the current of one phase of the motor, which is used to govern the pump speed being used.

The power consumed by the main heater is a parameter used when determining void fraction, as outlined later. To measure the power, two watt meters are required for a three phase delta connected load. The theory behind this measuring technique is provided in the appendices. Presently, an ammeter and a voltmeter are being used, which requires the inclusion of the appropriate phase factor in the multiplication of the two readings. This system will be replaced by a permanent system involving the use of wattmeters in the future.

3.2.5 Vibrations

The last instrumentation deals with the measurement of tube vibrations. Several problems, as outlined in the subsequent chapter, led to the development of a new measurement technique. Using a modified flashlight as a light source, light is passed through a tube and onto a sensor array. The sensor then provides a signal that can be monitored to determine both the direction, magnitude and frequency of the vibrations. The development and detailed operation of the instrumentation is discussed in the following chapter.

3.3 Summary

The modifications to the loop center largely around the attainment of "user friendly" control. The heat removed from the Freon 11 vapour is now taken from the liquid. This method of control still allows the control of the vapour back pressure that develops in the expansion and combination tanks. It was determined that control of this pressure was the key to providing a high level of control over loop conditions. The results described later in chapter 6 will confirm that this analysis of the situation is correct, and the loop conditions are easily manipulated as a result.

In addition, the final instrumentation for the purposes of experimental measurement and loop control have been installed. As outlined, temperatures and pressures around the loop are well displayed. Moreover, automatic controls have been installed to prevent dangerous accidents. Consequently, the use of the loop is relatively simple and can be used as an effective experimental facility.

Chapter 4

Vibration Monitoring Using Light

4.1 Introduction

Traditionally, vibrations have been measured in one of two ways, using accelerometers or strain gauges. The method chosen is primarily dependent on the vibration to be measured and the availability of the equipment required to analyze the resulting electrical signals. In flow induced vibrations research it is necessary to monitor vibrations on particular tubes in rod bundles. The size of the rods and the type of mounting used usually determine the best method for obtaining data. Moreover, the environment to which the tubes are exposed has a bearing on the technology used.

During the test section design stage of the present two phase flow induced vibration project, the following situation had to be considered. First, as a result of limited funding, the physical scale of the model had to be reduced below those scales normally employed in this field. Secondly, changes in state within the two phase flow are of interest in this project, but again the construction of a loop using water would be beyond the resources available. Therefore, Freon 11 was chosen as the operating fluid, which imposed some significant constraints on the choice of instrumentation to be used.

The resulting tube configuration did not permit instrumentation within the tubes. Furthermore, the mounting of external instruments created two problems. First, the instruments could not be permitted to interfere with the flow patterns in the vicinity of the tubes, nor affect the natural response of the tubes. Second, the environment to which the tubes are exposed is hostile to most commonly used plastics and adhesives. The first problem eliminated the use of accelerometers, which meant that strain gauges were the best alternative. The second problem made the longevity of the gauges uncertain. The use of an external coating for protection was an alternative, but finding a suitable protectant was difficult.

Consequently, an alternative means of measuring the vibrations was sought. Acting on the suggestion that light could be used, instrumentation was developed that enabled measurement of both the frequency and the magnitude of the vibrations in two directions. One unexpected benefit was that there was no requirement for amplification of the signal. Although there were some technical problems to be overcome in the development, these have been solved as will be discussed in the following pages.

4.2 General Design

Light has been used in obtaining vibration data previously, but inevitably the method required the use of

laser light and some means of optically manipulating the beam so that a photo sensitive device could determine either the location of the beam or the frequency. Furthermore, methods using light tend to measure magnitude in one direction only. The technique developed here is based upon the same basic idea, but the use of a laser was eliminated for cost reasons. Instead, a relatively inexpensive light source was used to do the same job.

The general concept behind the technique is the passage of light through one of the vibrating tubes which is intercepted by a photo sensitive device. The movement of the tube causes the pattern of light on the sensor array to move, resulting in variations in the intensity of the light impinging on stationary photo sensitive devices. These variations can then be used to induce variations in voltage and as a consequence, frequencies can be easily measured. Position can also be measured using a simple extension of this concept. Through the use of several photo sensitive devices and simple circuitry, the exact position can be determined.

4.2.1 Getting Light In and Out - Fibre Optics

Two methods of passing the light through the tube were considered. The first method was to use a directed light source that could introduce sufficient light into the tube to provide significant intensity upon emergence from the tube. There were some difficulties in obtaining the light intensity

desired with this method. The directed light source was manifest in the form of a flashlight, but the beam had to be focused onto the tube end. A penlight equipped with a lens end bulb could provide the same result, but requires that the light be placed in contact with the entrance of the tube.

The first method required less power for the light source than the second method, as will be described subsequently. However, there are drawbacks. If the tube is not perfectly circular at or near the open end, then the light spot produced will be irregular in shape (a problem addressed later). Moreover, the intensity varied with the direction of the flashlight, which is more difficult to aim than might be expected. Finally, the light had to pass through the tube unimpeded, which is important if other objects, such as electrical wires, are to be introduced into the tubes.

It was this last problem that led to the final design utilizing fibre optic technology. The future of the project allows for the possibility of generating heat within the tubes, which would require the introduction of wires into the tubes. Therefore, the light would be blocked. Alternatively, a fibre bundle could carry light along side a wire providing current. However, there are some problems that must be addressed when using fibre optics.

The advantage of using fibre optics is the highly efficient manner in which light can be guided through nonlinear paths. The use of this technology relies on the

ability to introduce the light into the fibre and the subsequent collection at the other end. Using a parabolic mirror and a lens, a light source can be focused onto the end of the fibre. The amount of light that successfully enters the fibre will be a function of the ability to focus the light and the nature of the fibre itself.

The choice of fibre depends upon the nature of the light being transmitted. For this design, white light was used, and the fibre operates as a light guide only. The introduction of the various light frequencies simultaneously, as is found in white light, requires a larger acceptance angle. That is, the core of the fibre must be larger to accept the light efficiently. Furthermore, to provide for the introduction of more light, a larger fibre is intuitively more applicable. The larger area can be accomplished by using a fibre optic bundle. However, the emerging light will tend to resolve itself into individual spots of light upon focusing, which is undesirable. Therefore, a single plastic fibre, 0.056 inches in diameter, was chosen. Plastic fibre was found to be sufficiently efficient for light transmission and also allowed for simpler manipulation of the fibre when it came to providing square ends after cutting.

Once the light carrying medium was chosen, the light had to be introduced into it. A parabolic mirror behind a light source can be commonly found in a standard hand held flashlight. Replacing the batteries with a constant D.C. power

supply eliminates the slow decline in battery voltage level over time. Furthermore, the power available can be varied to allow the use of a light bulb with higher power requirements, and consequently higher power output. The bulb chosen was a 4.42 Watt halogen flashlight bulb. The light pattern of this bulb has been designed to have high intensity over a wide area, therefore the placement of the focusing lens was moved almost directly in front of the bulb itself as seen in figure 4.1. The lens used was 25 mm in diameter with a 65 mm focal length.

Although the light was focused onto the end of the fibre, another spherical lens, specifically designed for optic fibres, was used to improve the efficiency of the light introduction process. Figure 4.1 shows the second lens mounted on an X-Y translator, which makes it possible to align the lens for maximum light intensity. Additionally, several of these lens can be mounted adjacent to each other, therefore providing the ability to supply different optic fibres with high intensity light individually.

Having successfully introduced the light into the fibre, the next problem was the collection of the light as it leaves the fibre. The light has the tendency to scatter randomly as determined by the surface of the fibre end. Polishing the ends can improve the concentration of the light, but the reduction in light intensity will be significant. Therefore, a method of collimating the light is necessary. Standard collimators

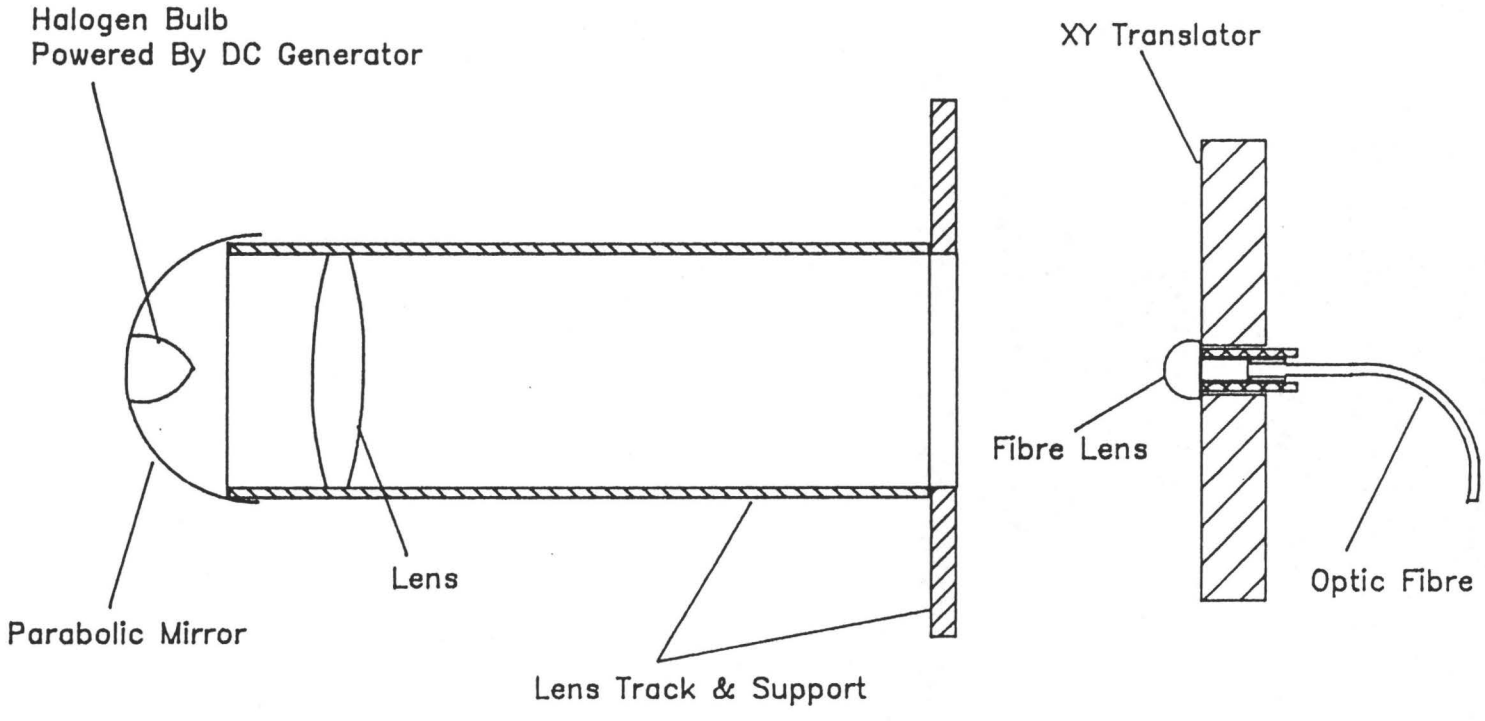

Figure 4.1 Light Input Apparatus

were not acceptable since the introduction of significant mass to the tube was undesirable, and the small size of the tube made this solution impractical. To solve the problem, the tube must be made into a collimator itself as shown in figure 4.2. This was done using a 5 mm plano-convex lens placed at the end of the fibre. Consequently, all the light leaving the fibre is forced to follow a trajectory which is closer to the centre line of the tube itself. Although the light is not a true column, the confinement of the beam is such that a spot of significantly higher intensity light can be maintained for a useful distance from the tube.

4.2.2 The Light Spot

The subsequent step in the design of the system was the development of a means to monitor the moving light beam. This was accomplished using four phototransistors, mounted such that two provided information on horizontal displacement, and two provided information on vertical displacement. Zero for each direction is defined as halfway between the corresponding pair of transistors. If the transistors are mounted as in figure 4.3, then zero is located at the centre of the array.

The spacing between the phototransistors was dependent upon the size of the transistors themselves. The spacing is the physically tightest spacing possible without contact between adjacent transistors. The response of the transistors is dependent on the variation of light intensity as the tube

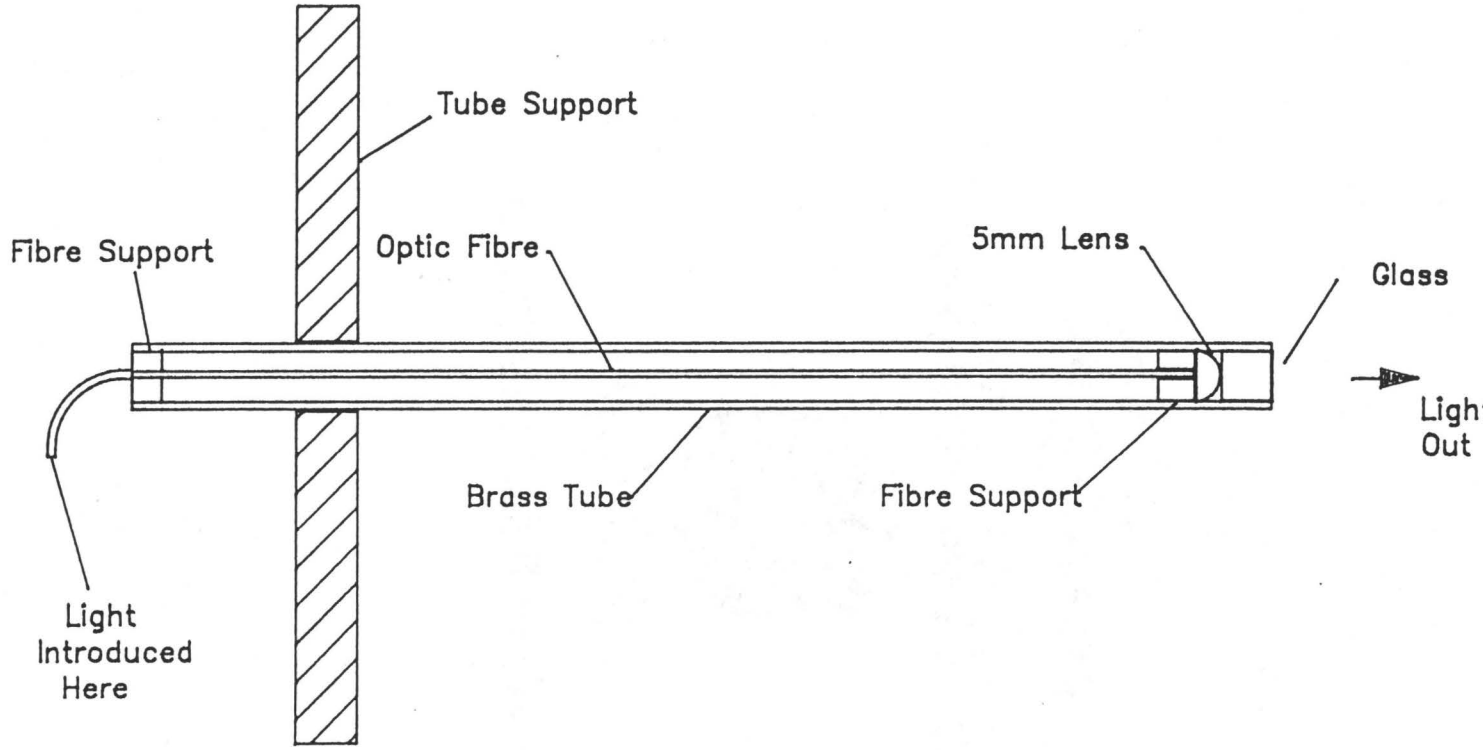

Figure 4.2 Tube With Optic Fibre & Collimator

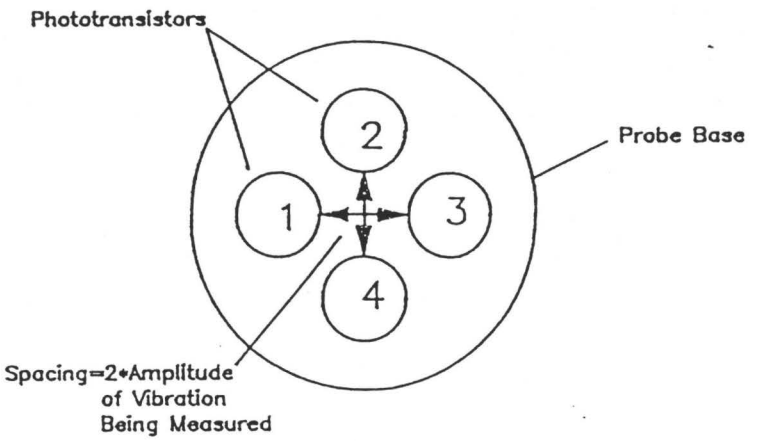

Fig. 4.3 Probe Layout for Light Instrumentation

end vibrates causing the light beam to move. As the beam moves across the array, the location of the tube end is measured by the difference in potentials induced by the phototransistors. The intensity of the spot of light, although it appears uniform, varies significantly. Furthermore, the use of the two transistors for each direction creates a much larger response than a single transistor.

A problem arises in the determination of the ideal light spot diameter. This can be best discussed by an example. Consider a light spot divided into several concentric areas spaced equally in the radial direction. Moreover, assume each area to have a constant light intensity, with intensity varying between areas so that it decreases linearly from the centre. Finally, assume the area outside the spot to be constant in intensity.

Using this model, several points can be noted. First, as the spot moves horizontally to the left, as in figure 4.4a, we see that transistor 1 is exposed to higher intensity light as transistor 3 is exposed to lower intensity light. There are two possible limiting cases for this movement. First, when the spot moves to the left far enough that transistor 1 passes the centre, and second, when the spot moves far enough to the left so that transistor 3 is outside the spot of light. In the former case (figure 4.4a), the potential difference does not change as it did prior to passing the spot centre. This is not desirable. Therefore the spacing of the transistors must be such that with the maximum tube movement possible, this situation is not allowed to happen. Consequently, transistor spacing along an axis must be greater than twice the maximum amplitude of the tube motion.

The latter case also results in a discontinuity of response which is, again, undesirable. Therefore, the spot diameter must allow the full tube vibration to occur while both transistors remain in the light spot. Since any vibration amplitude of the tube can be described in terms of its radial component, the size of the light spot must be greater than the diameter of the array, as seen in figure 4.4a, by an amount equal to or greater than the maximum amplitude of the spot motion. Otherwise, the situation seen in figure 4.4b will arise.

The second point to be noted in this example concerns

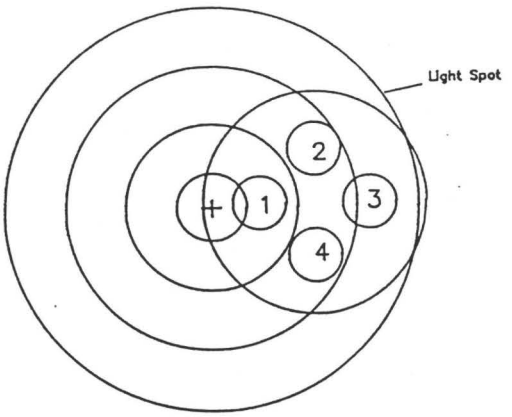

Figure 4.4a

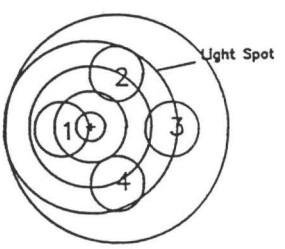

Figure 4.4b

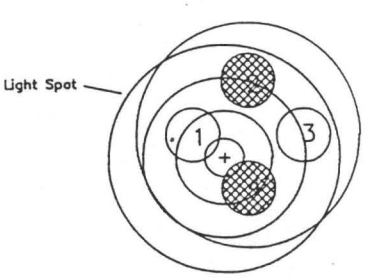

Figure 4.4c

Probe Function Example

what happens to transistors 2 and 4 as the spot moves to the left. Since each transistor passes through intensities 180 degrees from each other at an equal radius from the zero point, the response will remain balanced (figure 4.4a and 4.4b). However, as the spot moves downward, there is a change in the intensity seen by each transistor (figure 4.4c). The difference in intensities seen by transistors 2 and 4 will vary as the spot moves to the left. As the spot moves down, the variation will be greater as the spot moves left. Fortunately, the vibrations monitored are radial in nature, and therefore the extremes of the problem are never encountered (ie maximum tube amplitude in both the x and y direction simultaneously). Regardless, this is a concern to be addressed through experimentation. Testing indicated a maximum error of approximately 3% for extreme cases, which is acceptable. This error is a composite of both the instrumentation error and the error associated with movement of the XY translator. This small error level supports the assumption that the instrumentation will remain calibrated for small changes in overall light intensity. Therefore, this result suggests that for small variations in light intensity resulting from either a poor alignment of the apparatus or small changes in power level in the light source, will have insignificant consequences.

This example has several implied assumptions in addition to those stated outright. The assumption of a linear

distribution of light intensity is not valid, although it has its advantages in simplifying the problem. There are some problems associated with the creation of a nonlinear response to the tube movement. However, this is not the only source of possible nonlinearities. Regardless, the final calibration of the device has shown that the response was relatively linear for the range that would be used in the experiment. Therefore, the problems associated with nonlinearity can be alleviated by the instrument circuitry for the small vibration amplitudes being dealt with here.

The second implied assumption is that the spot of light is perfectly circular in shape and that the intensity of the light at a given radius is independent of circumferential angle. The first design alternative for light introduction, described earlier, did result in nonuniform spots. However the configuration using fibre optics had no such problems. Furthermore, the symmetry of response obtained from the apparatus in its final form indicates that the intensity is independent of angle, or that the differences can again be alleviated by the circuitry. Therefore, this assumption is also a valid one.

The final assumption introduces the discussion of the circuitry used to condition the signals provided by the phototransistors. It is implied, throughout the previous discussion, that the four phototransistors respond to light intensity in exactly the same fashion. Although it is true

that the characteristic behaviour has similar trends, the level of response is significantly different in any two transistors. Therefore, something has to be done to adjust this response and tailor it to the needs of the apparatus.

In addition, any uneven response can be partly attributed to the lens built into each of the transistors. This causes the probe to not necessarily be centered on the light spot when the probe output is balanced. Consequently, the physical layout rules, described previously, should be augmented to allow for the additional space required as a result of this possibility. That is, the spacing will generally be larger than that determined by the layout rules.

4.2.3 The Basic Circuit

The circuit illustrated in figure 4.5, is the basic circuit used to monitor the response of the phototransistors. The potential differences between points A & B, and points C & D provide the output for monitoring. This circuit, although useful for determining the required resistor values, assumes that the phototransistors have equal response to a given light intensity. To remedy the problem of unequal responses involves taking advantage of the fact that these devices are transistors. Therefore, the response curve can be manipulated in two ways. If the base of the transistors is used, the response curve (figure 4.6a) of the transistors can be manipulated (figure 4.6b). More precisely, the response will

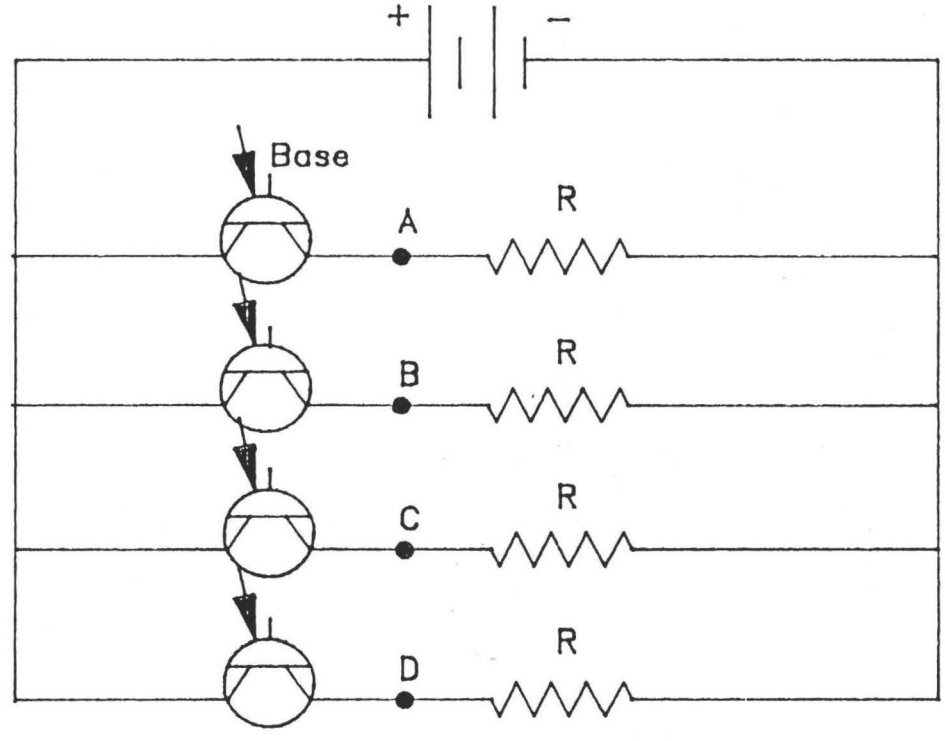

R — Resistor

Figure 4.5
Basic Circuit

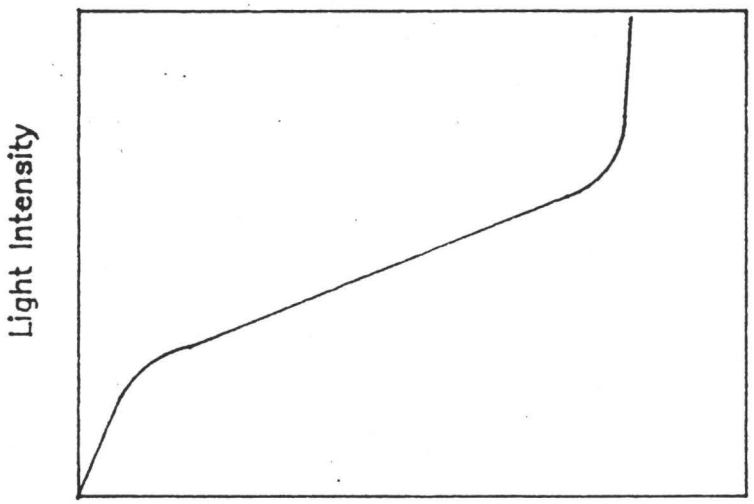

Figure 4.6a Typical Response Curve of a Phototransistor

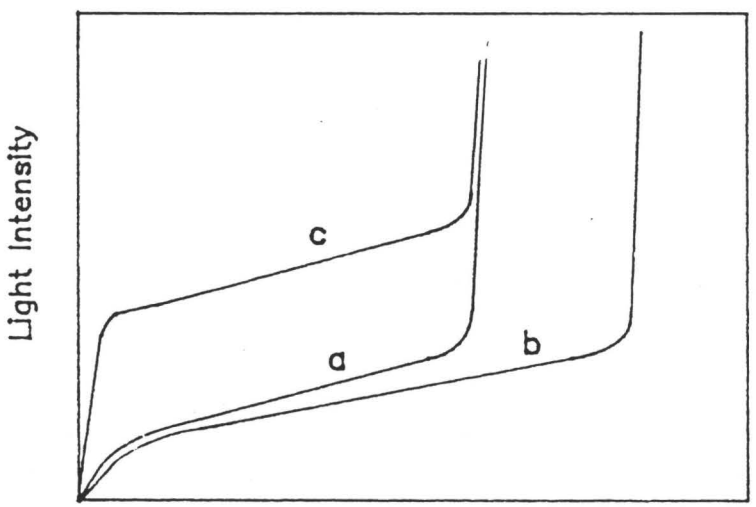

Figure 4.6b Manipulations of the Typical Response Curve

a) Typical Response Curve
b) Varying Resistance after Phototransistor
c) Varying Bias Resistance

follow a similar curve to that it previously followed, but the level of response can be scaled (figure 4.6b). If the resistance in the connection to the base is made infinitely large, then the original circuit is attained. Therefore, as this resistance is increased the current passing through the transistor is proportionately larger for a given light intensity. Determination of the suitable level of resistance is a function of the response curves presented in figure 4.6. Note that there is an intermediate linear region in the curve, with sharply curving regions at either end. The linear region is the desired response for the transistor. The target resistance is such that the light intensity is always within the linear region of the curve.

A tradeoff was observed between the slope of the linear region and the ability to get the light intensity high enough to reach the linear region. That is, the response curve did not only shift upwards, but also showed a slight change of slope in the linear region. The phototransistors chosen were selected for their higher current increase between the off and on states. Therefore, for a given increment in light intensity the increase in current passing through the transistor is larger. However, obtaining enough light intensity was more difficult than expected. This was primarily a problem observed when applying a bias to the base of the transistors, making them less sensitive to lower light intensities. Consequently, obtaining both the largest and most linear response could be

achieved only without any bias being applied to the base.

The problem still remains then, that the individual phototransistors behave in slightly different ways and this must be compensated for. Fortunately, transistors can also be thought of as current gates. That is, the transistor controls the current passing through it, but does not act as a variable resistor to do it. Therefore, if the response is in the linear region, the slope of the response curve can be changed by varying the resistance across which the voltage drop is being measured. (Compare circuit diagram figure 4.5 & figure 4.7) Since the total voltage change between the two phototransistors is being measured, the task of balancing the two channels is relatively simple.

4.2.4 Final Circuit

The circuit in the form shown in figure 4.5 provides four voltage signals. Monitoring the differences, as noted previously, will provide the necessary output. However, the majority of reading devices require that each channel of output have a common ground. To accommodate this need, the output was modified by a differential operating amplifier. The sole purpose of this amplifier is to provide the common ground. There is no gain applied to the signal, but there are other implications. The amplifier serves to eliminate any noise in the circuit that may be picked up by connected cables and wires. The use of a ground point between batteries has

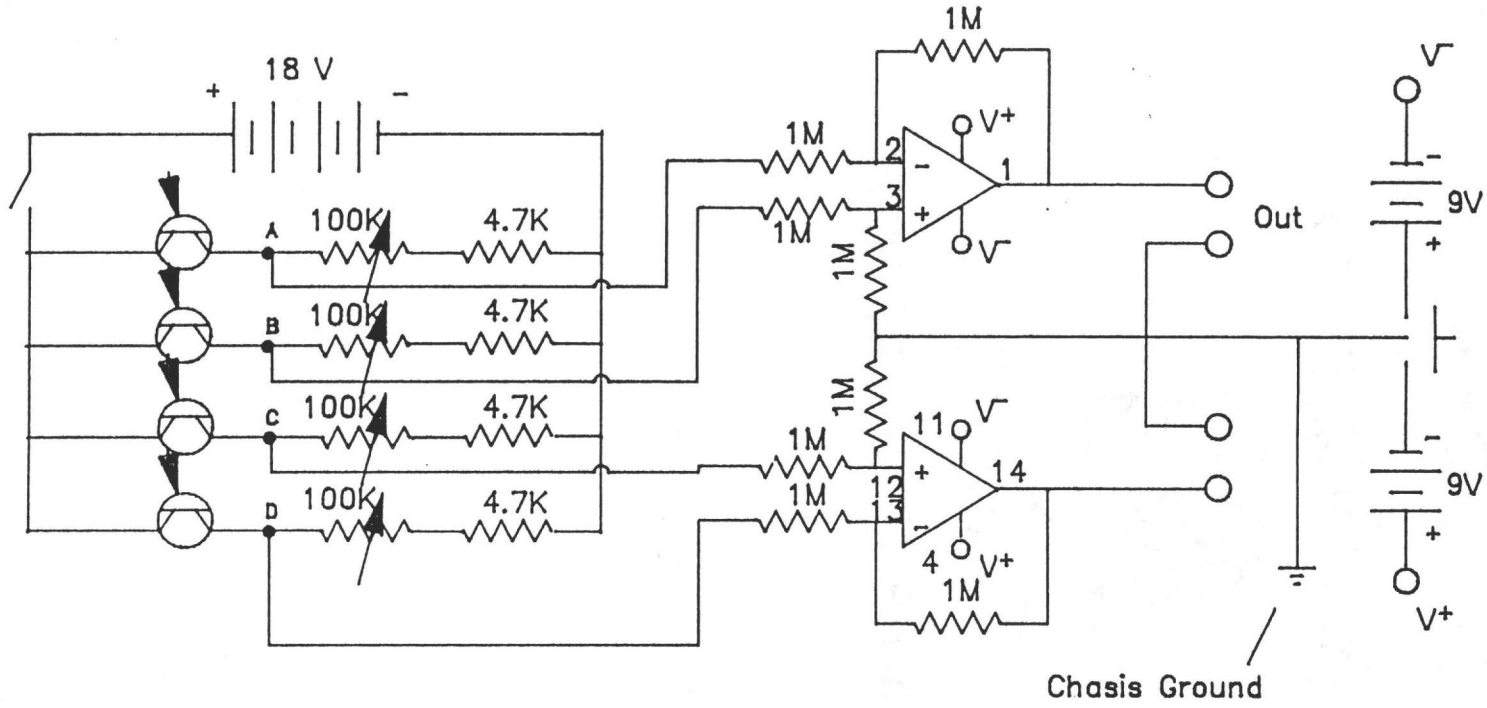

Figure 4.7 Final Circuit

proven sufficient to reduce the noise to insignificant levels. However, the conversion of the circuit to an A.C. power supply was still considered advantageous. Therefore, the final version employs power from a wall socket. This circuit has proven itself to be more consistent over time, which makes the instrumentation more practical to use.

4.3 Results

The calibration curve, shown in figure 4.8, illustrates the closely linear response of the apparatus to tube movement. To attain this curve one assumption was made, which is that the displacement of the tube end is small enough to permit the effects of the angle of the tube end to be ignored. Performing a simple calculation, using an energy method, the error in this assumption for the final configuration of the apparatus was found to be 5.6% (see appendix A), which is acceptable. Furthermore, the calculation does not take into account the effect of the indices of refraction as the light passes from the Freon 11 to the glass, and finally to the air. As a result, the mean slope of the light path as it travels from the tube to the probe is actually less, resulting in a lower error. Therefore, calibration becomes a simple exercise of moving the probe (with the phototransistors on it) in precise increments. This is facilitated by the X-Y translator on which the probe is mounted. The micrometer controls allow the determination of probe position precisely, while measurements

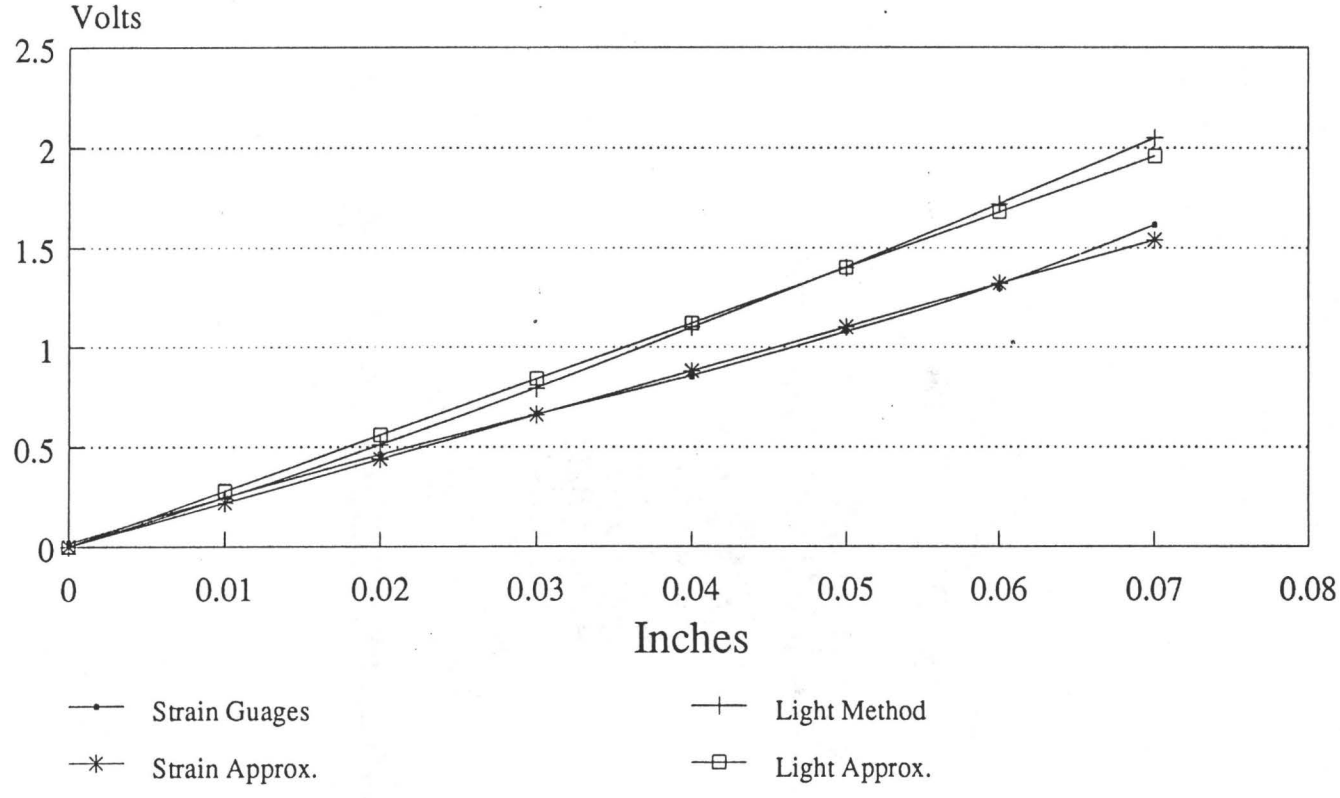

Strain Gauge Gain=900

Figure 4.8

Light vs Strain Calibration

can be taken numerically from a digital voltmeter. Note that this arrangement also allows for recentering once the inevitable displacement occurs due to the flowing fluid.

Since the phototransistors can be expected to be equal in response with the accompanying circuit, centering the probe is accomplished by zeroing the response. However, centering does not ensure that the probe is orientated so that horizontal responses in reality are horizontal. The probe could be rotated relative to the translator, and therefore the same method used to calibrate the apparatus can also be used to square the probe correctly.

The calibration is performed by observing the responses resulting from moving along one axis in both directions (i.e. positive and negative directions), beginning with the zero point. The interaction of horizontal movement and the vertical movement becomes important here. If there were a problem, the movement along an axis would cause apparent movement along the second axis. However, the movement along the second axis would be in the same direction regardless of whether the movement is on the positive or negative side of the first axis (See figure 4.9a). Moreover, if the probe is not orientated correctly, the response on the second axis will be positive for one direction and negative for the other direction on the first axis (See figure 4.8b). Assuming the translator to be properly orientated, the necessary correction in the probe orientation can be easily accomplished.

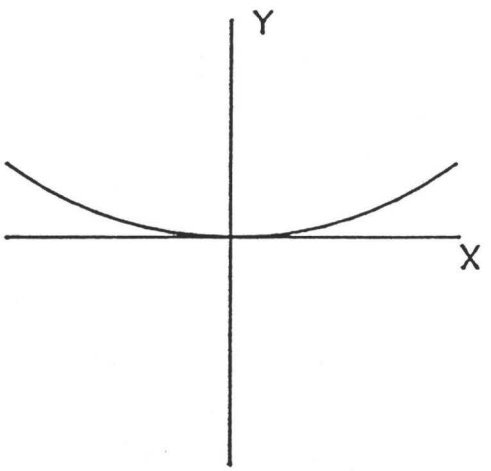

a Response Resulting From Unequal
Phototransistor Response Curves

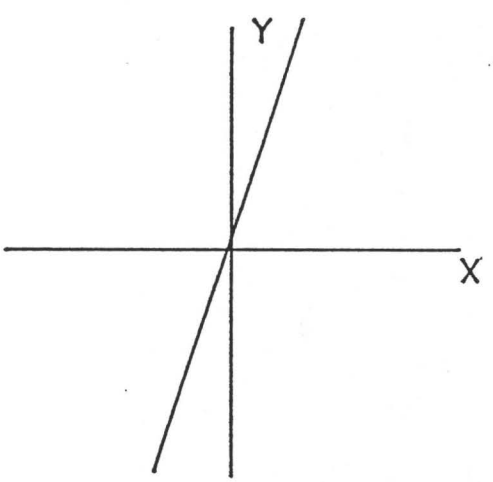

b Response Resulting From Improper
Allignment of Probe

Figure 4.9
Examples of Configuration Problems

It should be noted that the interaction of channels was insignificant relative to the magnitude of the displacement. Therefore, the problem of differentiating between improper orientation and the potential error in the response is not an important one. Moreover, it was ascertained that the large signal response obscures any noise in the circuit. The final form of the apparatus has the advantages of simple calibration, and has a high signal to noise ratio, even for small responses. However, this sensitivity has one other implication, which is related to the fact that the intensity of the light impinging upon the probe may vary from one day to the next. Therefore, the apparatus should be checked by making a quick calibration at one or two points. The use of a higher powered halogen flashlight bulb with a DC generator power supply, allows the accommodation of small variations in light intensity, which should be sufficient.

The only unknown at this stage of the discussion is the effect of the fluid flowing between the end of the tube and the end window. To test the apparatus, a strain gauge set was also installed on the monitored tube. The gauges were protected with a microcrystalline wax recommended by the strain gauge manufacturer. It was suspected that the wax would not survive Freon 11 exposure, but it was still used. The manufacturer also claimed that the wax was not necessary if the Freon were pure.

The calibration of strain gauges resulted in the

determination of the appropriate gain, which was 900. This provided a response very similar to the response of the light instrumentation with a reduced sensitivity, a comparison of which is seen in figure 4.8. The wires for the gauges were Teflon coated to ensure the greatest endurance of the strain gauge system.

To compare the responses of the two sets of instruments, two experiments were conducted. First, the loop was run in single phase flow and the instantaneous spectral density plots were compared. The plots, shown in figure 4.10a, are for comparable channels of the two systems. It can be seen that the plots are very similar, and closer analysis shows that the peaks correspond exactly according to frequency, with slight variations in amplitude. The one exception is the peak seen at 28 Hz that is only registered by the strain gauges. Further investigation has revealed that this is one of several peaks found throughout the frequency spectrum as a result of interference by the motor controller. Therefore, this peak is extraneous and only serves to demonstrate an advantage of the light instrumentation.

Having demonstrated that the light instrumentation works in single phase, the last concern is the effect of two phase flow. If the flow patterns brought significant amounts of vapour past the end of the tube, the intensity of the light would be affected as a result of the optical variations. It is acknowledged that the problem is inevitable once the void

fraction approaches 100 %. However, the void fraction will not approach this value by design, and therefore the only concern is the flow pattern of the two phase flow.

Consequently, a second experiment was run with the dual purpose of generating visible two phase flow for the first time, and subsequently evaluating the instrumentation. The results were less favourable this time. Two phase flow was easily generated, but the flow pattern was such that vapour found its way past the tube ends. Monitoring the tube response on the oscilloscope became more difficult as the void fraction increased. However, it was postulated that the bubbles were causing low frequency responses in a random manner. Therefore, the RMS frequency response should be unaffected. Figure 4.10b shows the comparison of the strain gauge and light instrumentation responses in frothy flow. It is apparent that the bubbles do not significantly affect the signal, since the first mode response is virtually identical. In fact, the light response is smoother, possibly as a result of the lower noise level on the signal.

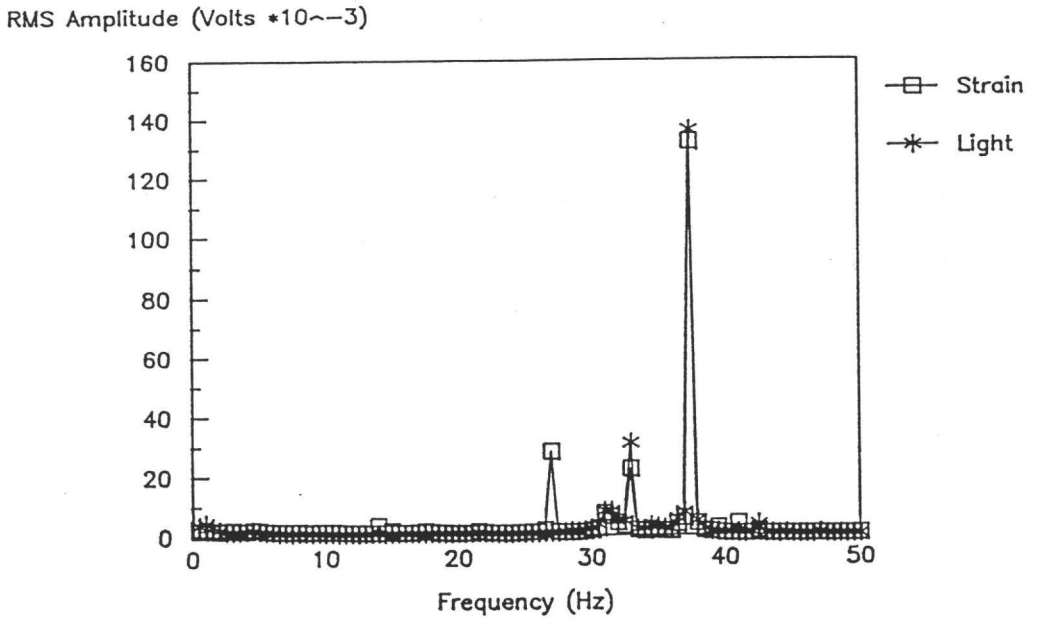

Figure 4.10a

Light vs Strain Comparison of

Single Phase Frequency Response

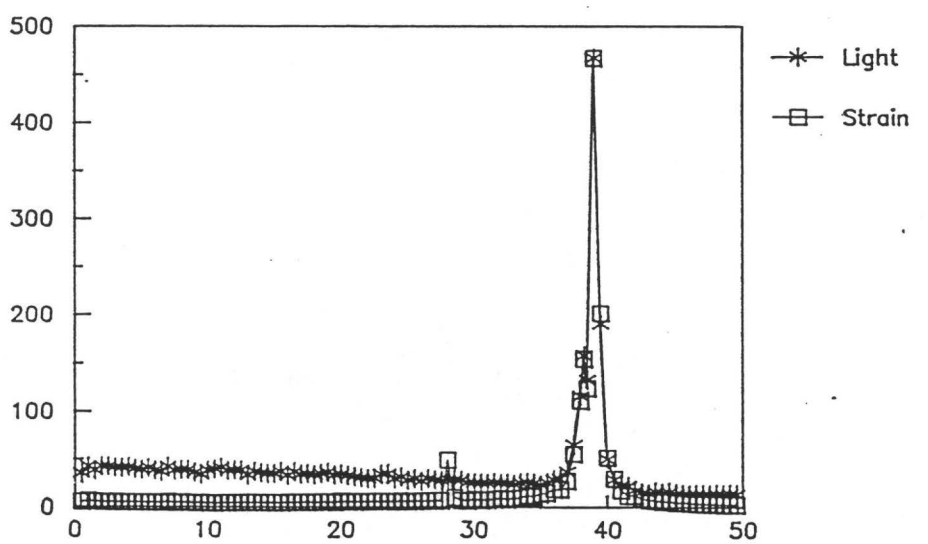

Figure 4.10b

Light vs Strain Comparison of

Two Phase Frequency Response

4.4 Conclusion

The results show that the developed light instrumentation is a practical method of measuring tube vibrations. In addition, the method has some inherent advantages. Namely, the lack of amplification contributes to a high signal to noise ratio. This is compounded by the fact that the system response is more sensitive than the strain gauges as set up for these experiments. If greater sensitivity is desired, there is the possibility, either through circuit conditioning or increased light intensity to accommodate this need. The present setting is at the limits of the physical construction. That is, the tolerances on the X-Y translator and the probe support are inadequate for greater sensitivity. However, it is possible to replace these components with more expensive parts with higher tolerances.

The low noise levels were maintained even though a simple DC circuit was used. The batteries provide a satisfactory grounding system, which eliminated all perceptible noise from the response signal. This is particularly apparent when comparing the frequency response of the light instrumentation to the strain gauges. However, the batteries do tend to lose power over time, and it has been found that the calibration of the instrumentation becomes more difficult as this occurs. Therefore, it was recommended that the circuit be reconfigured using an AC power source. This suggestion has been acted upon.

The system presented may require calibration (i.e.

ascertaining the present response slope) more frequently, but this is inconsequential since it is much easier to perform the calibration. Furthermore, the X-Y translators, which contribute to the ease of calibration, allow the movement of the probe to other tubes. As a result, a number of tubes can be monitored using the same instrumentation. Once calibrated, this means that the tubes will all follow the same response curve.

From these attributes, it can be ascertained that the light instrumentation is a useful means of obtaining vibration data. The advantages described here show that this technique may even prove to be preferable in some instances. Further development for applications on larger scales combined with its already high degree of flexibility, could make it a preferred means of measuring vibrations.

Note: Figures 4.11 and 4.12 are provided to show the final form of the mounted instrumentation.

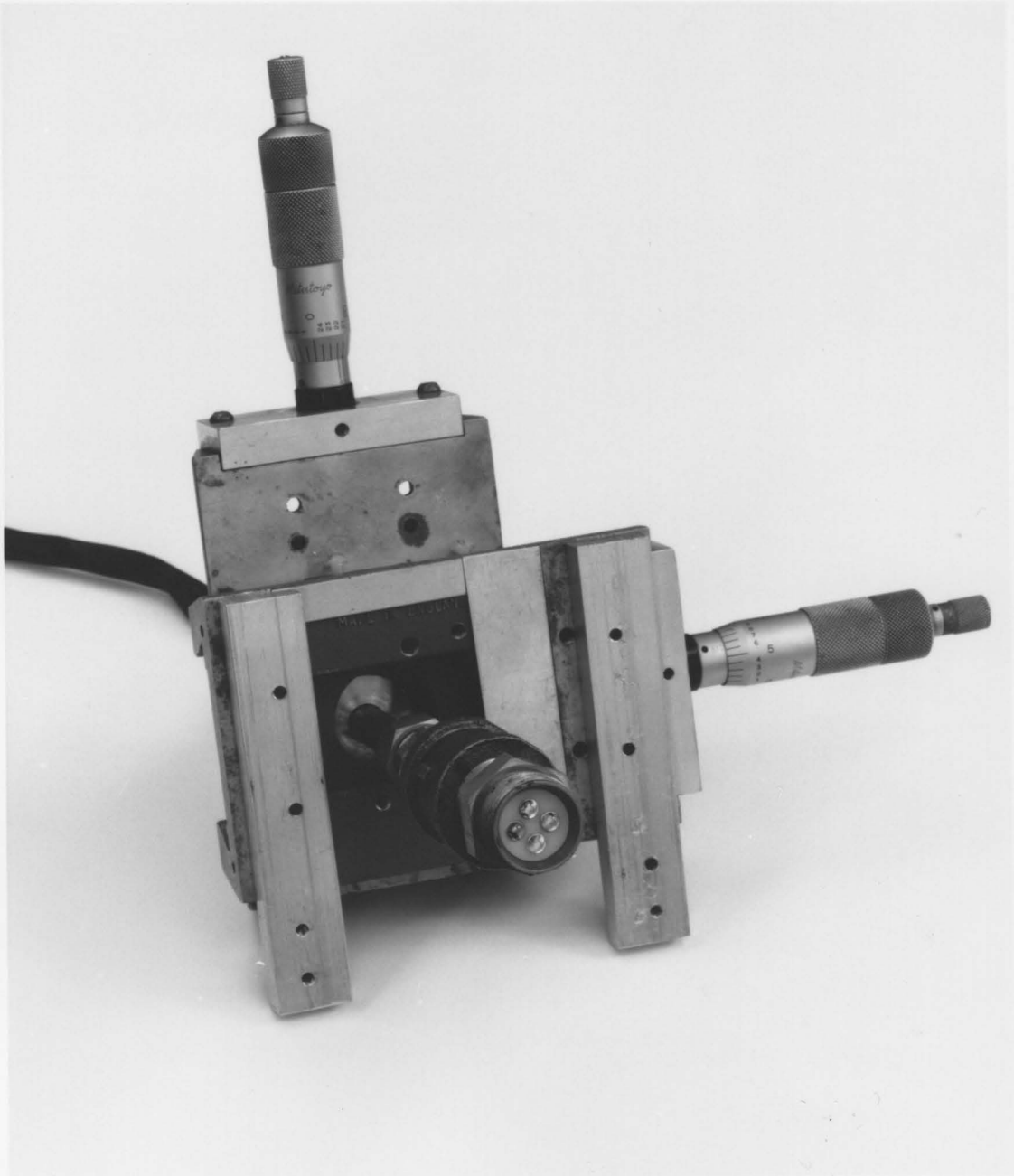

Figure 4.11 Picture of Probe Dismounted

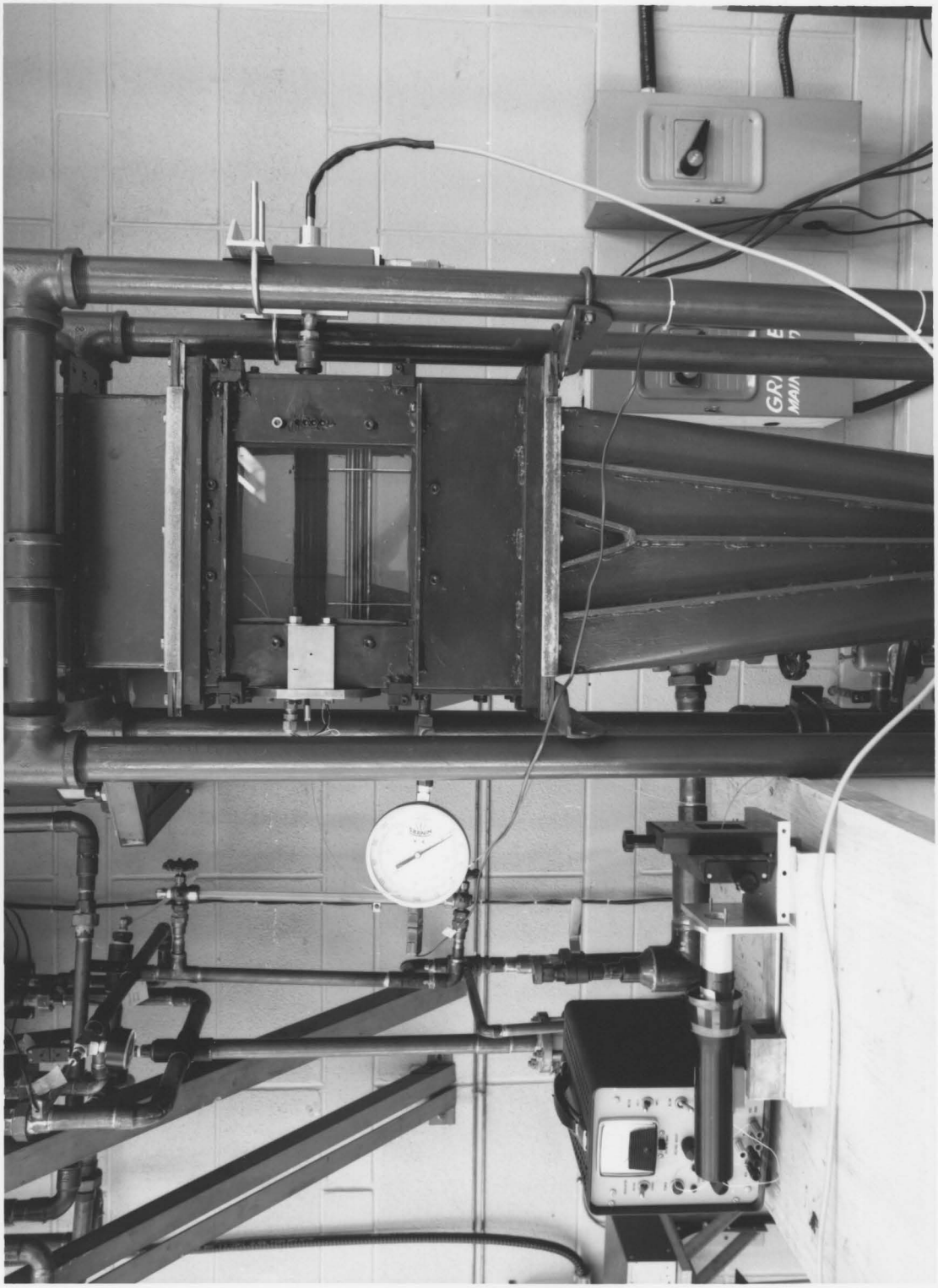

Figure 4.12 Picture of Instrumentation Mounted

Chapter 5

Test Section Redesign

5.1 The Original Test Section

As a result of his work on the two phase flow loop, Westermann designed and built a test section for the study of two phase flow induced vibrations. The section was designed to meet specifications resulting from the modelling analysis outlined in the thesis "The Design & Construction of a Flow Loop for the Study of Two Phase Crossflow-Induced Vibrations of Heat Exchanger Tubes", written by Westermann. In summary, a parallel triangular array of cantilever mounted tubes is expected to reach fluidelastic instability upon interaction with a flow rate of 2.25 kg/s. Moreover, the loop is designed to generate two phase flow at a pressure of approximately 20 psi and 47 degrees Celsius, and the flow rate previously noted. Eventually, it was hoped to generate an 80% void fraction at maximum conditions.

Although less power is available, the design conditions can still be met according to preliminary results. Moreover, this implies that the important design forces are in existence and the test section must be able to absorb these forces. One other feature of the test section is the placement of viewing windows to allow visualization studies of the tube movement. The windows introduce the main difficulty associated with the

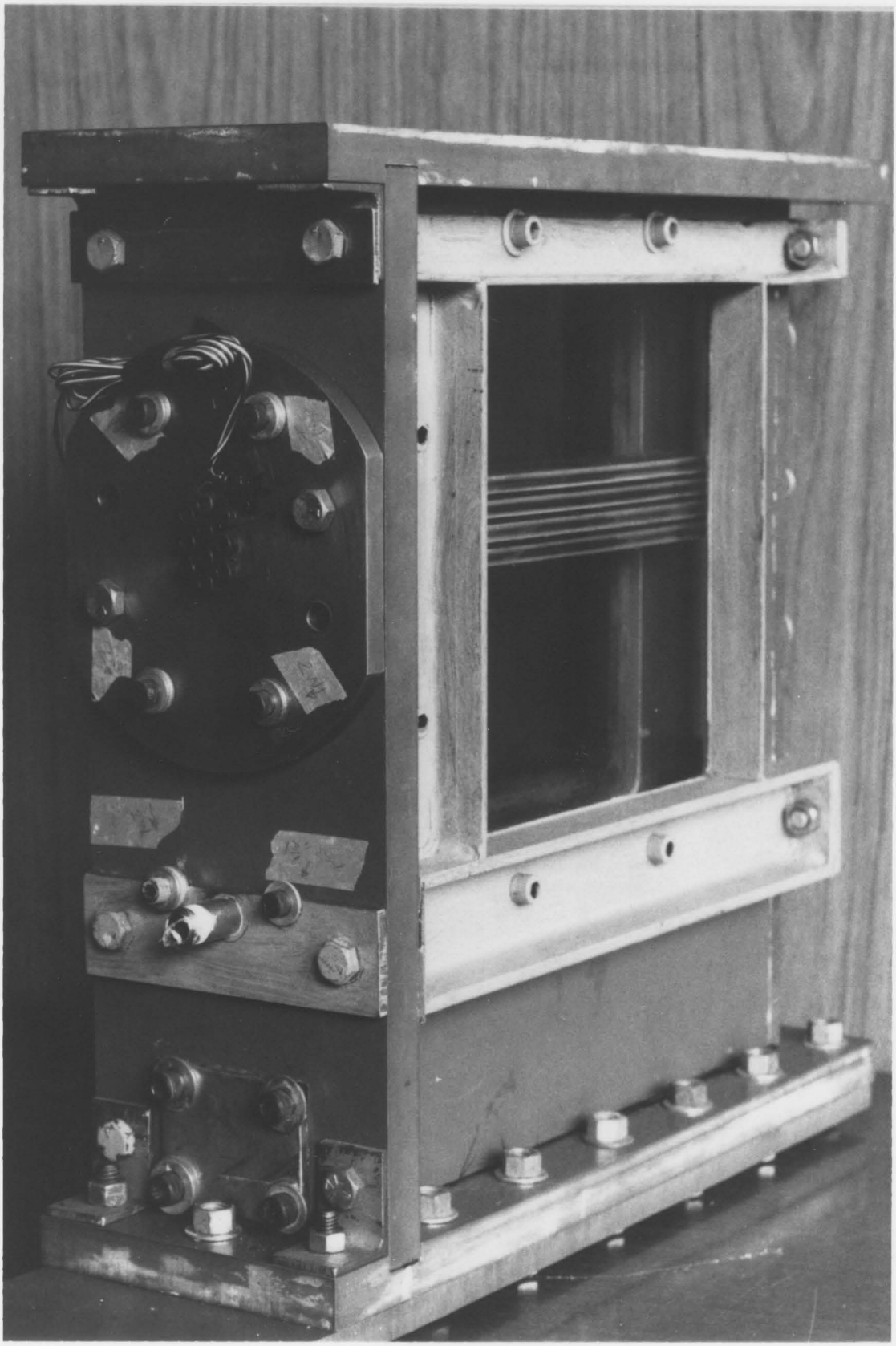

Figure 5.1 Original Test Section Design

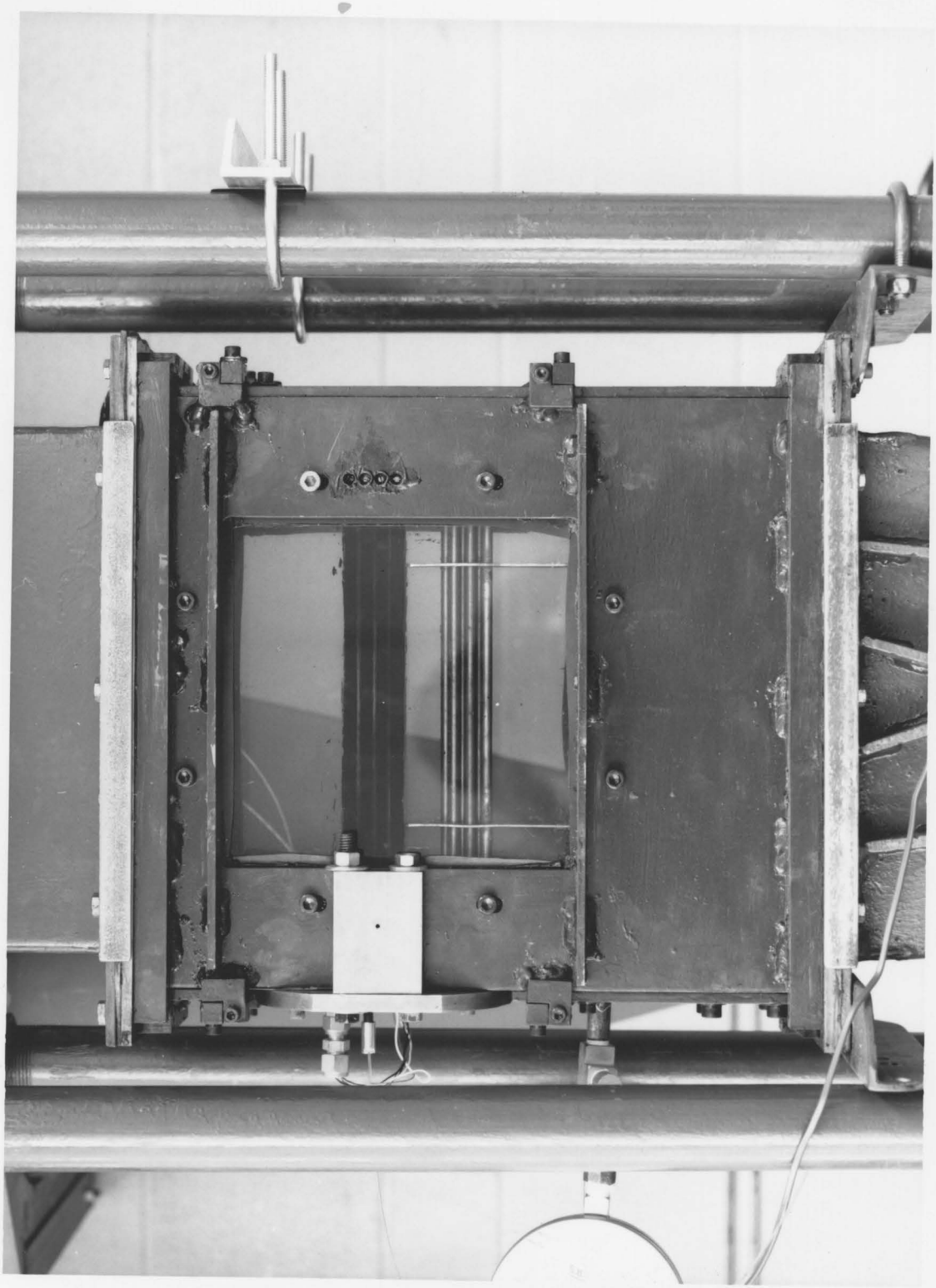

Figure 5.2 New Test Section Design

design of the test section.

Upon completion of his work, Westermann had pressure tested the test section at 30 psi, and had found that the test section had passed the test as far as structural integrity was concerned. Unfortunately, one of the windows was still leaking at this point. Additionally, the mounting flanges of the section were constructed of nonplasticised PVC and relied on a sealant/adhesive for transmitting forces to the body of the test section. This adhesive provides excellent sealing capabilities, but possesses only moderate strength as an adhesive. Therefore, upon insertion of the test section into the loop, the stresses introduced likely would have resulted in failure. Although Westermann had built a superstructure (an external steel skeleton) for solving this problem, it was deemed to be inadequate for the task.

5.2 Objectives

There were two objectives at the outset for the redesign of the test section. First, the structure had to be modified to allow safe mounting of the test section in the existing two phase flow loop. Second, the leak problem had to be remedied. It was also considered appropriate for the new design to take advantage of the considerable work and analysis involved in the original design. Consequently, the redesigned test section was intended to improve on the structural properties of the original test section by building on the existing structure as

much as possible.

5.3 Alternatives

There were two alternatives considered for the problem. These were as follows:

1. The existing structure was mainly deficient in the strength of the flanges. The superstructure did provide the strength required for pressure forces, but there were limited connections provided for extension of this structure to the PVC flanges. Consequently, it was considered that the superstructure be extended by increasing the number of connections to the flanges.

Advantages: This solution would have been the cheapest and the quickest. There would be no problems associated with construction, with the possible exception of the limited space available between the bolt holes of the flange and the side walls of the test section. This imposes a limitation on the thickness of metal that could be used for connecting purposes, which would be a problem in any solution. However, this design would demand a great deal of rigidity from the steel structure, which is a function of the material thickness.

This design modification utilizes the entire test section as it exists and therefore would save considerable work.

Disadvantages: There is a question of strength when the flanges are connected at discrete locations. However, the number and size of the locations could be increased.

There is another significant difficulty that lies in the sealing of the window sections. This design modification does nothing to improve the existing sealing system, which relies primarily on epoxy. To remedy this problem, the existing frame would have needed redesigning to allow for the inclusion of a gasket. Consequently, the superstructure would require total rebuilding, which meant that less of the original work could be saved.

2. The second alternative, a sleave that the existing section, with some modifications, could fit into, takes the first alternative to the limit. This would require the construction of a steel shell and the removal of external pieces of PVC from the original test section. Moreover, the flanges could be totally replaced by steel flanges. As a result, the interior of the test section would remain untouched, but the external and mounting surfaces would be redesigned with strength as the primary concern.

Advantages: The greatest advantage lies in the strength to be derived from the resulting structure, since welding could be used to create a continuous shell of steel. This modification would allow the bolt hole problem, mentioned earlier, to be solved since the steel could be easily threaded to allow for thicker material in the shell body. Furthermore, window gaskets can be easily incorporated into the design.

Disadvantages: This solution would take considerably more

time to complete and cost more. Moreover, there were some design difficulties associated with the fitting of an existing object into something which is to be built. Since it is desirable to have the surfaces in intimate contact, the design and construction have some inherent difficulties.

5.4 Solution - F.E.M. Analysis

Since both designs would require the redesign of the superstructure, and strength is the most important objective, the second alternative was chosen. The physical measurements of the test section made it possible for 1/8 inch steel to be used and the bolt problem could be avoided. To analyze the design in more detail, finite element analysis was undertaken by Aneesh Chopra as part of an undergraduate course at McMaster University. The goal of the analysis was to ascertain the desired thickness of the steel, the pressure distribution along the window edge, and the stress distribution within the windows to determine a factor of safety.

5.4.1 Assumptions

To model the problem, several simplifying assumptions were made. The greatest deflection and the greatest stresses were expected in the sides of the test section where the main windows are located. Consequently, the model could be simplified by considering only one face with the appropriate boundary conditions. Furthermore, the windows are not symmetrically orientated, but were modelled as such. The resulting symmetry allowed the modelling of only one quarter of the face as seen in figure 5.3.

The actual design called for the mating of two surfaces fastened to each other by bolts. Modelling of bolts is difficult, and can unnecessarily complicate the model.

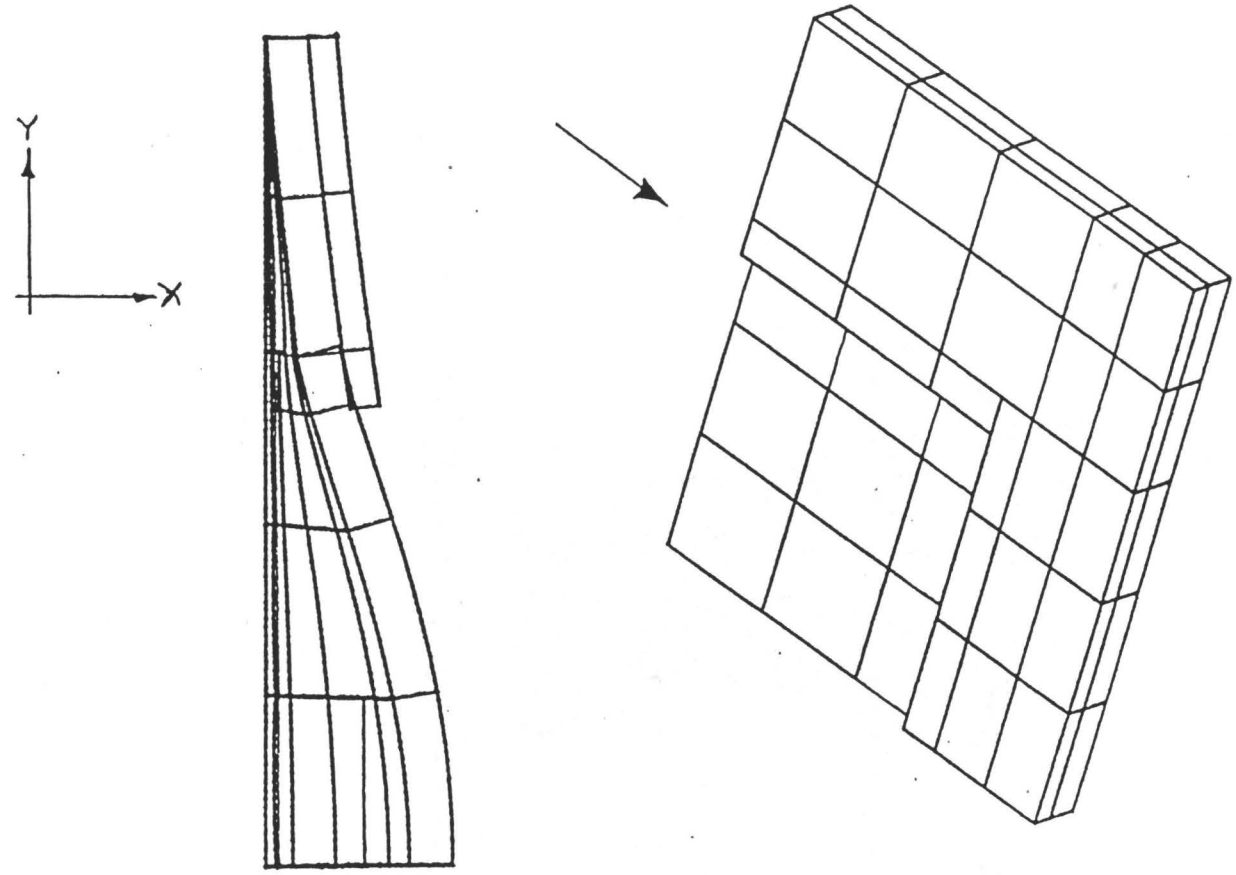

Figure 5.3

Finite Element Model Mesh and Sample Deflection

Therefore, the two surfaces were fixed to each other by common nodes at the interface. For the glass and steel interface, the surfaces were left unattached. This required that a force be input for these nodes. The resulting equilibrium forces would then represent the forces the gasket would see.

These assumptions have implications that provide conservative results in some cases and nonconservative results in others. The fixing of the PVC and steel interface gives a nonconservative result. Moreover, the stress distribution in the steel and PVC components will not be correct in detail. However, this stress pattern, and the internal stress distribution of the PVC, are not the main concern. Moreover, the test section has bolts threaded through the PVC edges, which increase the strength of the PVC, the exclusion of which is conservative when considering test section deflection. Knowing that the original test section can handle the pressure loads, the model is intended to duplicate the deflection characteristics as opposed to the exact stress distribution. That is, the average stress conditions are modelled resulting in what should be a reasonable deflection model. Therefore, the PVC and steel are modelled such that they provide the correct constraints on the glass, which is the weakest point of the structure.

The centering of the windows moves the point of maximum deflection and will shift the stress distribution. However,

the maximum deflection point will remain in the window and the stresses introduced are primarily a result of the steel and glass contact. Therefore, the model should give a good indication of magnitude and location of the greatest tensile stresses, since they will still occur within the window. Moreover, the contact forces and their distribution should also give reasonable magnitude values, since the shift is in the vertical direction only. It is not expected that this slight adjustment will generate great errors within the results.

5.4.2 F.E.M. Results

Initially, the steel thickness was modelled as being 1/8 inches. The results from this model were compared to the results of 1/4 inch steel model. The results indicated that the 1/8 inch steel was adequate, however, for safety reasons, the much improved strength of the 1/4 inch steel was considered more desirable. Moreover, the design called for the welding of the plate steel, which would result in greater distortion problems if the 1/8 inch steel plate were used. Additionally, the 1/4 inch steel plate allows for the machining of slots to contain the gaskets.

Table 1 is taken from the final report written by Aneesh Chopra. It presents the forces between the contact nodes of the gasket surface, as seen in figure 5.4, resulting from the use of both 1/8 and 1/4 inch steel. The pattern that arises

Node Pair (See Fig. 5.4)	1/8 Inch Steel Pressure Psi	1/4 Inch Steel Pressure Psi
1	450	700
2	20	20
3	450	700
4	20	20
5	400	650
6	20	20
7	400	650
8	20	20
9	0	0
10	20	20
11	500	800
12	20	20
13	500	800
14	20	20
15	500	800

Table 5.1

Pressure Forces Along Gasket Surface at the Nodes Identified in Figure 5.4

is echoed in the maximum and minimum stress plots shown figures 5.5 & 5.6 respectively. Generally, the pressures are of the same magnitude as expected. Moreover, this magnitude is more than sufficient for sealing purposes since the gasket pressures are more than 20 times the internal test section pressure.

Moving to the stress plots, it can be seen that the maximum tensile stress reduces in the corner region and under the steel, as a result of the increased structural support, whereas, the tension rises to a peak in the centre of the glass where the maximum deflection occurs. Moreover, there are

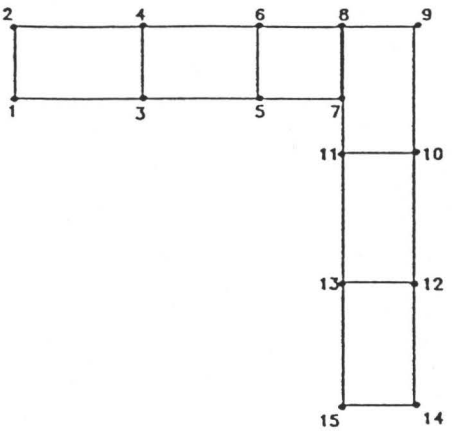

Figure 5.4

Gasket Surface Nodes

pockets of increased tension seen close to the steel support. These concentrations correspond to the deflection profile seen in figure 5.3 where a point of inflection is observed near the corresponding high tension points.

The maximum compression seen in figure 5.6 shows an opposite trend, where higher compression is seen on one edge in particular. However, the general trend is that the compression is higher under the steel support than in the central region where the greatest deflections occur. This is as one would expect for a problem such as this. Higher stress levels found at an axis of symmetry can be explained by the added restrictions seen by the material at these locations. Since nodes can only move along the plane of the axis, stress is added in the form of a restraining force or fixity. Consequently, the increased compression found on one side is expected.

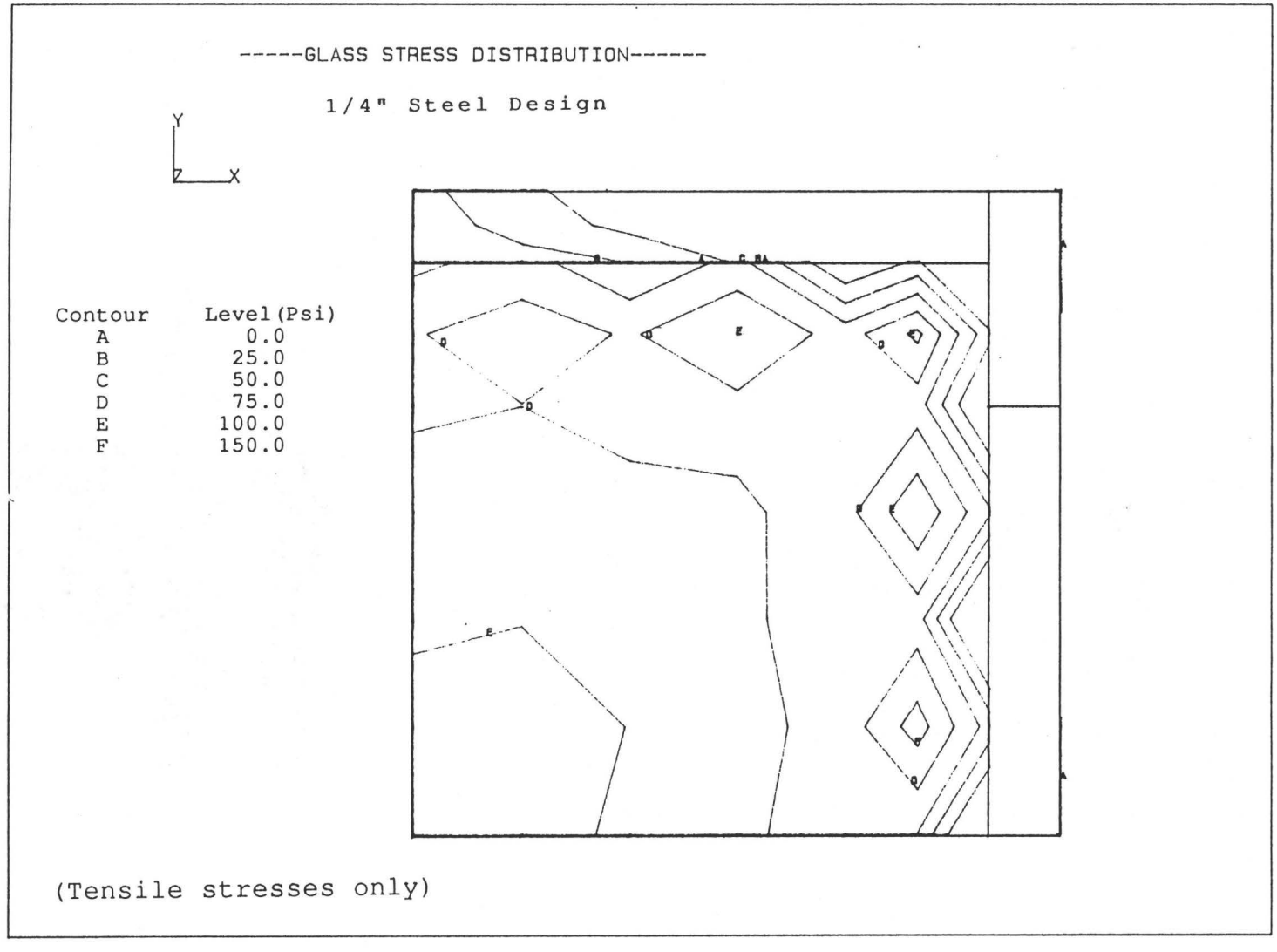

Figure 5.5
Maximum Principle Stresses of
The Test Section Window

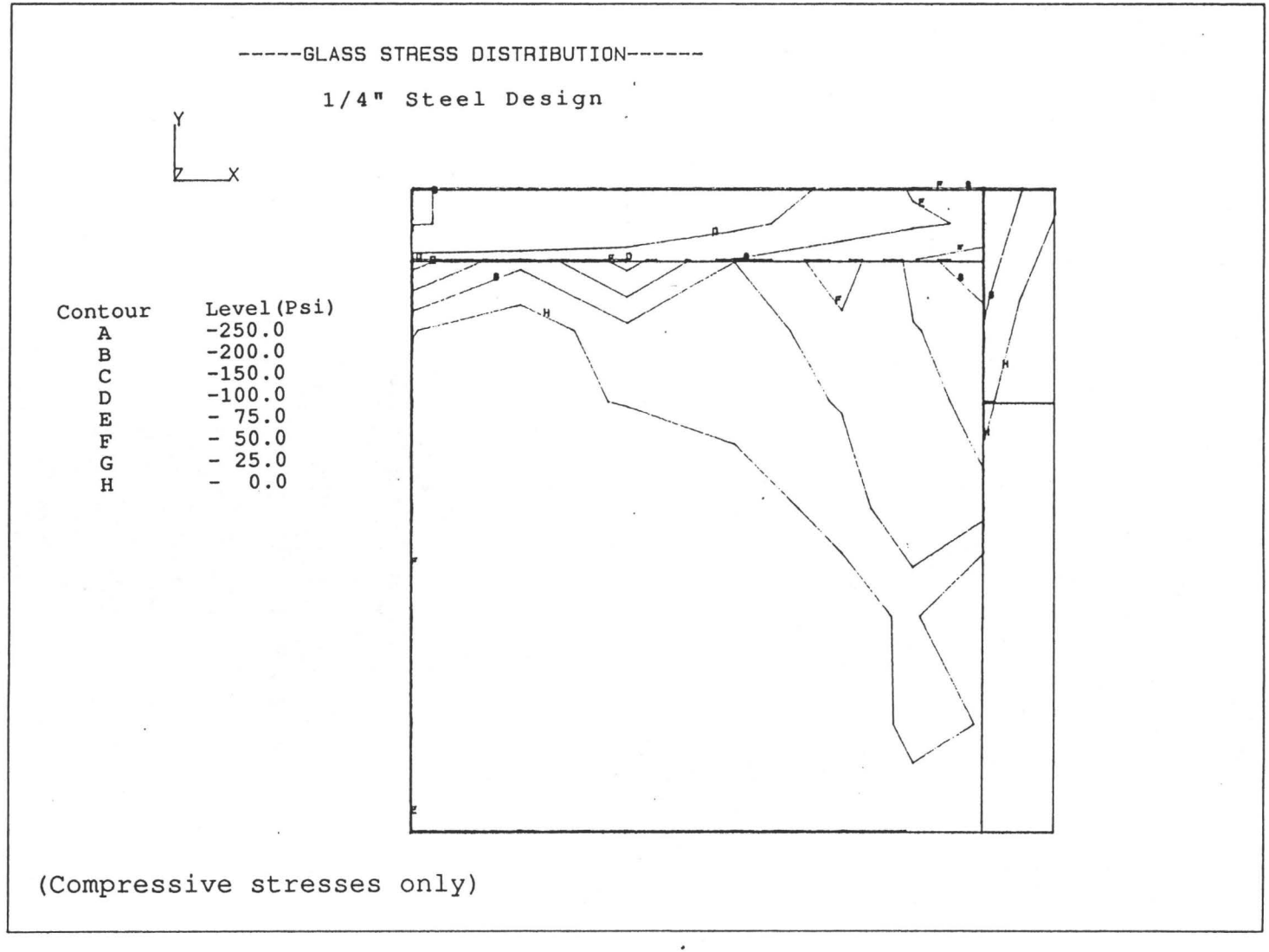

Figure 5.6
Minimum Principle Stresses of
The Test Section Window

This explanation, although useful for explaining the patterns observed in the stress plot, is not entirely necessary since the overall level of the stresses, whether tensile or compressive, is small. The stress patterns are useful in confirming that the finite element modelling has provided a reasonable result, but the stress levels are the prime concern. To totally explain the stress distributions observed in the plots would require looking at the overall stress patterns of the three dimensional model. This was done using computer simulation, and as expected the model results were found to be reasonable in light of the overall behaviour of the modelled structure. Consequently, the slight differences observed on individual edges are not of any concern.

The model performance leads to the conclusion that the finite element modelling has successfully modelled the test section. Additionally, the gasket pressures are seen to be adequate, and the window stress levels are not significantly high. To verify that the stresses are acceptable a factor of safety should be calculated.

A survey of various sources of material properties did not reveal an exact tensile or compressive yield strength. However, there was a range given of 5 to 10 ksi. From the stress plots the largest principal stress is less than 250 psi in compression. A conservative estimate of the factor of safety is 20 based on these figures. For a pressure vessel

with glass walls, this is an acceptable value.

The model incorporates many assumptions as noted previously. The effect of these assumptions appears to be minimal in light of the good overall performance of the model, and the low stress levels observed in the critical area, namely the glass. The proper placement of the window may introduce slightly higher stress levels on the upper edge, but this is not a significant concern. A criticism of the model is that the glass appears to be given greater flexibility than in reality. The apparent flexibility in the sample deflection seen in figure 5.3 results from the scale of the deflections. To make the deflections observable they are multiplied by a large scaling factor. The low stress levels found in the glass indicate that the bending is acceptable in the model.

5.4.3 Conclusions from F.E.M.

The deflections resulting from the analysis appear reasonable, therefore the stress distribution that results in the glass can be used to ascertain the validity of the design. The factor of safety derived from the analysis, which is approximately 20, indicates that the design will work. This conclusion is supported by the successful pressure testing of the test section.

Furthermore, the pressure distribution along the window edge assures us that the gasket will have sufficient pressure to seal the windows. The nonsymmetric location of the window

is not expected to result in a serious lack of gasket pressure. The only unknown that remains concerning the gasket, is its ability to deform and seal against a smooth surface such as the glass. This is a greater concern when it is considered that the glass will not push into the gasket as firmly at lower pressures. The modelling of the window as a free body being pushed against the steel is truer than the hinged model used in this analysis. Unfortunately, this could not be ascertained until actual pressure testing was conducted.

5.5 Modifications to The Design

5.5.1 Materials

Construction of the sleave for the test section resulted in several design modifications. A material supply problem meant that hot rolled steel had to be used for the plates on the sides with the large windows, while the remainder of the pieces could be comprised of cold rolled steel. This is significant since cold rolled steel is considerably flatter than the hot rolled steel. Therefore, the ability to provide a good contact between the steel and the glass or PVC was in jeopardy. To help with the problem, bars were welded along the window edges to force the window contact area to be relatively flat. Moreover, after welding, the plates were physically manipulated to encourage a consistently flat surface. The resulting pieces were adequately flat to continue with construction.

5.5.2 Assembly

Initially, the design called for seam welds to connect the various components. However, a fear of distortion resulting from the welding process prompted a redesign. Instead of seam welds, clamps were built that pulled the two components together from two directions. Additionally, to combat the distortion problem further, 3/4 inch bars were welded to the bottom edges of all the components to form a 1 inch thick base on which the flanges could sit. These bars

were also drilled and tapped to receive the mounting bolts. The resulting design improved the flatness of the plates and provided stiffer surfaces for fastening purposes.

As a result of this latest modification, the original steel flanges became merely dummy flanges that had two functions. First, they increased the mating area between the test section and transition sections, which provides an increased sealing area. Second, they acted to ensure flat mating surfaces, which also encourages a better seal. This second function was aided by milling the bottom surface of the 3/4 inch bars.

Earlier, the question of how the gasket material would deform under pressure was mentioned. During the assembly process the answer was found. The 1/8 inch gaskets being used to seal the window edges were found not to deform as much under the imposed forces as expected, and consequently the gasket would not allow the steel to come in contact with the PVC. Moreover, the windows tended to give under the gasket pressure, moving inward and bending the Lexan half tubes. To remedy the situation, pieces of sheet metal were placed between the PVC and the steel plate on the sides. This provided adequate contact between the surfaces, and reduced the imposed pressure on the gasket. This in turn lowered the pressure on the windows, yet provided reasonable forces on the gasket for sealing purposes.

The behaviour of the gasket material resulted in one

other modification. The pressure testing procedure showed that there were two areas where leaking was likely to occur. The windows, which were not sealed by the mounting epoxy, would still leak with the gasket in place. Therefore, to ensure a seal, the same adhesive sealant used with the PVC was used in conjunction with the gasket material to seal the windows. This is not an unusual practice when using gaskets to seal connections.

The second area of concern was the mounting flanges. The interface between the steel flange and the PVC is 3/8 to 3/4 of an inch from the interior surface of the test section. The gasket material, while sealing well, given the full width of the flange, did allow some fluid to penetrate to the interface. This provided a secondary path for the fluid to escape through. This problem was solved by again using the sealant/adhesive used for the PVC to seal the interface between the PVC and the steel flange.

Although the gasket material did not deform well for the windows, the gasket material was seen to squeeze out from between the mounting flanges. Consequently, the tightening of the bolts produced limited improvements when sealing minor leaks. To remedy the problem, containment brackets were fabricated that forced the gasket material to remain between the flanges. This solution has sealed this area of the loop properly.

5.5.3 End Window Redesign

The final modification to the test section structure itself was the redesign of the small end window. As a result of forces introduced by the two way clamps and the homogenizing bundle in the test section interior, stresses were introduced into the glass that caused it to repeatedly fracture. Two adjustments were made to solve this problem. First, the glass area was shrunk to ensure the glass would not be subjected to the area where the stress problem was suspected to be critical. Second, part of the problem was attributed to the lack of flexible material in contact with the glass to absorb some of the stresses. This softer material could be used to act as a gasket simultaneously. This resulted in the final end window design having a gasket and smaller surface area.

While reconstructing the end window, careful analysis of the bolt locations in the end of the test section showed that some holes provided the opportunity for other leak paths. Since it was ascertained that these bolts were redundant in a fastening capacity, they were replaced with brass rods that could be sealed into the PVC. These rods still provide the strength needed in the sides to improve bending strength, but also sealed small leaks that were forming in some of the holes.

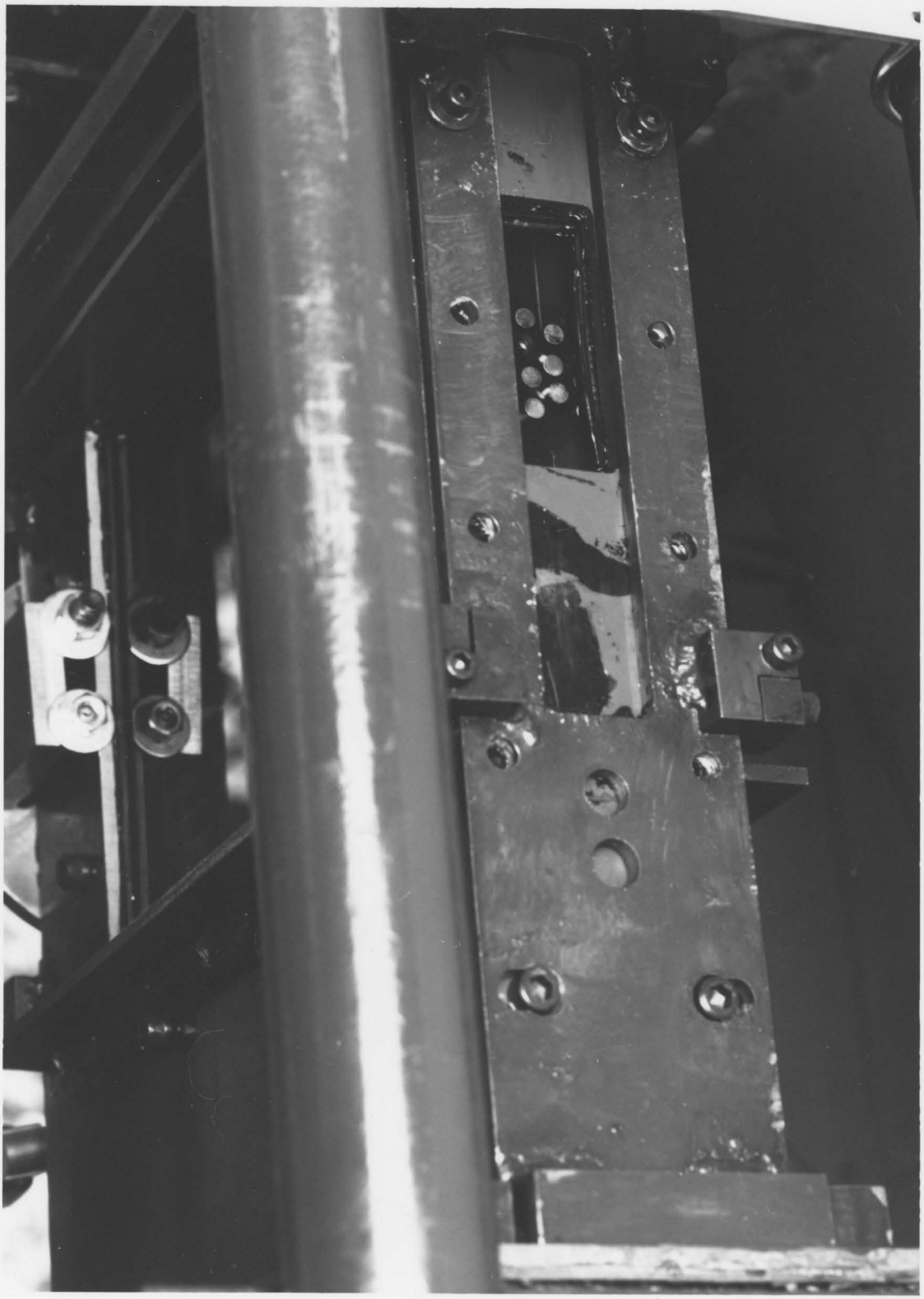

Figure 5.7 Picture of End Window Redesign

5.5.4 Test Results

Once these modifications to both the actual structural components and the assembly procedures were completed, the final test section was assembled. After subjecting the test section to a pressure 1 1/2 times that of the design pressure (20 psig), the test section was ready for installation. The mounting of the section uncovered no other leaks and showed no signs of deformation under the mounting forces. Therefore, from a structural perspective, the design is a success.

5.5.5 Homogenizing Bundle Redesign

The state of the art in two phase flow, as discussed in an earlier chapter, is such that there are still concerns over the actual modelling of the two phase flow. This was one of the primary concerns that prompted the initiation of this project. Therefore, it was prudent to include some ability to change the test section to account for some different conditions. Moreover, it would be useful to be able to ascertain the effects on tubes in many different locations in the bundle.

When analyzing two phase flow, it simplifies the work considerably if the flow can be assumed to be homogeneous. It can also be argued that due to the sheer number of tubes found in a steam generator and the small spacing between these tubes, that the chances of the flow being anything but bubbly and homogeneous in the U-bend region is unlikely (except for

the first few rows possibly). Consequently, it is advisable to ensure a bubbly two phase flow in the test section.

The test section for this project has two homogenizing bundles. The first bundle is found near the base of the test section, with the tube array being shifted slightly in relation to the instrumented tube bundle. The second bundle acts as a continuation of the instrumented bundle. This second bundle, as a result of its location, can have the top 5 rows removed to create a break between the instrumented bundle and itself. This allows the position of the monitored tubes to effectively be moved within the bundle. This assumes that tubes far downstream of a particular tube have little effect on its motion.

In addition, these removable tubes allow the study of the effect of the relative position of the homogenizing bundle. Of concern is the possibility of standing waves between bundles, and whether the spacing affects the composition of the two phase flow and the subsequent tube reaction. To supplement the removable tubes, two tubes found in the first homogenizing bundle can be removed to allow movement of the entire homogenizing bundle assembly. These two tubes can be placed in three different positions relative to the test section itself. Therefore, the spacing between the instrumented and homogenizing bundles can range from 0 to 9 tube rows.

To provide the capability of having the second final homogenizing bundle close to the instrumented bundle, splitter

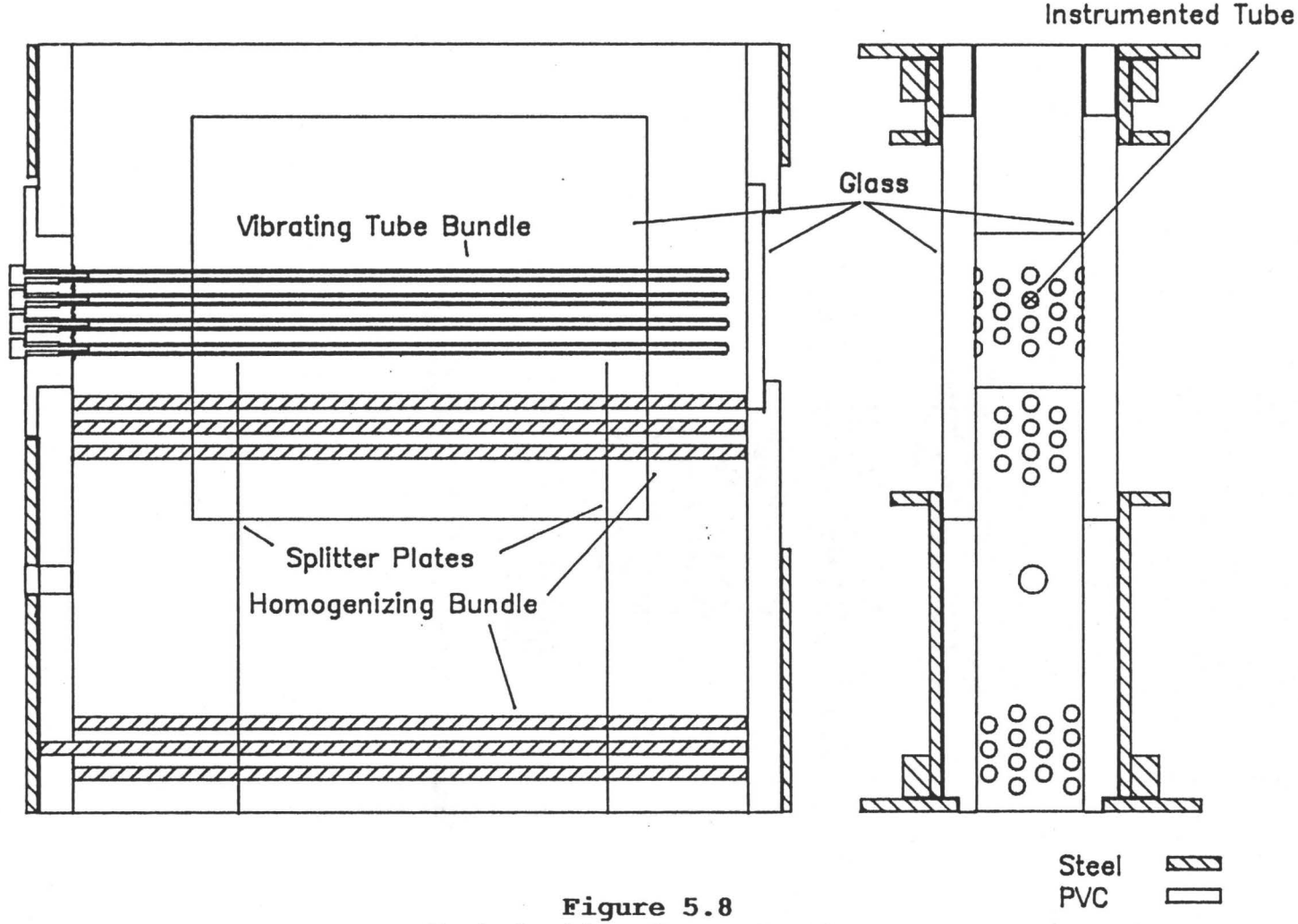

Figure 5.8
Test Section Cross Section
and Homogenizing Bundles

plates were used as supports. The assumption is that the flow will be uniformly distributed upon entering the first homogenizing bundle, where the breakup of large bubbles is initiated. Therefore, the flow between the plates will be more or less uniform, resulting in no further error associated with the assumption of a highly correlated force along the tube length. The plates will obviously introduce some boundary effects, but since they are very thin, they should be essentially invisible downstream.

5.5.6 Lexan Half Tubes

Following the successful completion of the single phase experiments, the two phase flow experiments began. However, after only two runs it was observed that the Lexan half tubes had broken free and were interfering with the vibrating bundle. Closer examination has shown that the epoxy absorbed some of the Freon 11 and subsequently lost its adhesive power. As a result, it was decided to have brass half tubes made that could be attached from the outside.

The design uses machine screws to fasten each half tube at either end. The screws are passed through holes in the PVC and sealed against the exterior of the PVC with Hypalon gaskets. To ensure that the flow does not pass under the half tubes, sealant is used to provide contact between the interior of the test section with the backs of the tubes. This also ensures that the test section remains sealed.

Consequently, the semi transparent Lexan tubes are now replaced by brass tubes with a black sealant that can be seen from the outside. Therefore, light has greater difficulty passing through the tube bundle. However, the scale of the tube bundle would have made visual studies through the bundle impractical, although visual studies from the end of the bundle are not affected in any way.

5.6 Summary

This chapter has discussed the redesign of the test section from the point of conception to its final use. The only topic not mentioned is the results from vibration experiments. The following chapter will provide information in this area.

The F.E.M. analysis proved to be extremely useful in confirming that the design was practical. The detailed accuracy of the modelling may be questioned, but the design was not expected to fail since results from the original design pressure testing showed that structural integrity already existed. Furthermore, the analysis can be considered very general in light of the many modifications that were made. The final design is clamped in specific locations, and support bars have been welded in place that improve the strength further. The conclusion is that the model is very conservative. However, the stresses found within the glass are useful in ascertaining the possibility of a problem at the sections weakest point. Therefore, generating a model that provided reasonable results was adequate. This approach was supported by the successful testing and implementation of the new design.

Chapter 6

Preliminary Results

This chapter contains both a qualitative and quantitative discussion of preliminary results obtained to evaluate the experimental performance of the new test facility. Although problems prohibited the acquisition of final results, there is comparability with results seen in past studies as outlined in chapter 2. Moreover, two phase results also show promise, but there are basic questions yet to be answered.

The single phase analysis is presented in the form of reduced velocity vs RMS amplitude plots and frequency vs amplitude plots. Moreover, there are a number of assumptions implicit to the analysis. Consequently, the definitions and equations used in the analysis will be outlined first. Although many of the definitions are repeated from chapter 2, they are presented in a more explicit form here. Following this presentation, the results will be considered.

6.1 Calculations

As just mentioned, analysis of the experimental data obtained for single phase results is presented on plots of reduced velocity versus the RMS amplitude of the tube response. The amplitude can be easily provided by a Nicolet

FFT analyzer, which breaks the down the RMS response by frequency and then numerically integrates the response over the stipulated frequency range to obtain the RMS voltage amplitude. Knowing the response characteristics of the instrumentation, the final RMS amplitude can be presented in μm. For analysis purposes, the presentation uses a dimensionless amplitude by dividing the absolute value by the diameter of the tube.

Determination of the reduced velocity is considerably more involved. The method of calculation is described in the following discussion.

6.1.1 Calculating Reduced Velocity

The calculation of V_r begins with knowing the void fraction. Determination of the void fraction is essentially performed through an energy balance.

$$E_{in} = E_{out} \tag{6.1}$$

where $E_{in} = Power_{in}(W) + \dot{m}(kg/s) * Enthalpy_{in}(J/kg)$

and $E_{out} = Power_{Lost}(W) + \dot{m}(kg/s) * Enthalpy_{out}(J/kg)$

Substituting and rearranging we get,

$$Enthalpy_{out} = (Power_{in} - Power_{Lost})/\dot{m} + Enthalpy_{in} \tag{6.2}$$

Defining these variables in the context of physical components of the loop, the following equation results:

$$h_{test}=(P_h - P_L)+h_{f2} \qquad (6.3)$$

h_{test}- enthalpy of flow in the test section (kJ/kg)

h_{f2}- enthalpy at a point immediately prior to the heater (Kj/kg)

P_h - specific power input by heater (Kw/kg)

P_L - heat lost to the ambient (kW/kg)

The right side of equation 6.3 represents inputs from the various readouts of the loop monitoring system. First consider the enthalpy immediately upstream of the heater, h_{f2}. This value can be determined from the temperature measured at the location, assuming that it is approximately equal to the liquid saturation enthalpy for the temperature, which is an acceptable assumption.

Second, the power of the heater can be measured by two wattmeters as shown in the appendix. Since the volt and ammeter allow for both higher precision and accuracy, the following equation was used to determine the power input:

$$P_h=(V_1*I_1+V_2*I_2)*\cos(30) \qquad (6.4)$$

P_h - heater power input in watts

V_1, I_1, V_2, and I_2 are obtained from the appropriate meters as shown in figure II.1. (V and Amps)

Moreover, there is significant heat transfer to the environment for some loop operating conditions. Therefore, in order to accommodate this heat loss, 'P_L', the area between the thermocouples was considered to be composed of four sections. The areas of each section is approximate. When obtaining information about a data point, the surface temperature of each section was measured. This information was used in the following equation:

$$P_L = h_T * (A_1 * \Delta T_1 + A_2 * \Delta T_2 + A_3 * \Delta T_3 + A_4 * \Delta T_4) \qquad (6.5)$$

P_L - heat lost in surroundings (W)

h_T - heat transfer coefficient, which is estimated to be about 6 $W/(m^2K)$. This was determined over the past three years to be a reasonable estimate of the heat transfer coefficient.

A_x - section areas (m^2)

ΔT_x - temperature difference between individual section temperatures & the ambient temperature (°C)

To obtain the specific power input, the power is divided by the flowrate, which must be calculated. Appendix III gives the equations for the flowrates in each subloop based upon the differential pressure cell readings. However there is some error associated with changes in the fluid density. Recalculating the parameters according to the calculations

performed by Westermann, the following equation resulted:

$$Q=0.02671*\rho_L^{.5}*H^{.5} \qquad (6.6)$$

Q- flowrate (kg/s)

ρ_L- saturated liquid density for liquid temperature (kg/m^3)

H- reading from channel 1 of the DP cells (in. Hg)

Although flow related energy losses do exist, they are assumed insignificant. Therefore, the net energy transfer can now be calculated as follows:

$$P_{net}=(P_h-P_L)/(1000*Q) \quad (KJ/Kg) \qquad (6.7)$$

This gives the energy of the flow as it passes through the test section, as given in equation 6.3. The next step is to estimate the quality. The quality 'x' is given by:

$$x=(h_{TEST}-h_{fT})/h_{fg} \qquad (6.8)$$

h_{fT} - saturation enthalpy at test section temperature (kJ/kg)

h_{fg} - latent heat at test section temperature (kJ/kg)

Having established the quality, the next step is to determine the homogeneous density, for which some assumptions must be made. These also extend to the determination of the

void fraction. The two predominant assumptions are:

1) There is no slip between the phases, and

2) The flow is well mixed and can be assumed to be homogeneous with regard to its properties.

Slip is defined as the ratio of velocities between the phases. In equation form:

$$S_l = W_v / W_l \qquad (6.9)$$

S_l= Slip

W_v= vapour phase velocity

W_l= liquid phase velocity

This can be shown to result in the following equation:

$$S = x/(1-x) * \rho_f/\rho_g * (1-\phi)/\phi \qquad (6.10)$$

ρ_g - saturated vapour density at test section temperature (kg/m^3)

ρ_f - saturated liquid density at test section temperature (kg/m^3)

ϕ - void fraction

Assumption 1 implies that the value of S is 1.0, which corresponds to the homogeneous assumption. Based on these assumptions the homogeneous density is:

$$1/\rho_h = x/\rho_g + (1-x)/\rho_f \qquad (6.11)$$

ρ_h - homogeneous density (kg/m^3)

This value is calculated separately since it is used later. It is also used here to calculate the void fraction as follows:

$$\phi=(x/\rho_g)/(1/\rho_h) \qquad (6.12)$$

Although useful for classifying the flow, the void fraction does not explicitly figure into the remainder of the calculations. To obtain the reduced velocity, it is necessary to go back to the homogeneous density.

$$V_u=Q/(\rho_h*A_{XT}) \qquad (6.13)$$

V_u -flow velocity in the test section upstream of the test bundle (m/s)

A_{XT} - test section cross sectional area

$= 0.009680\ m^2$

The velocity of interest is the pitch velocity defined as:

$$V_p=V_u*P/(P-d) \qquad (6.14)$$

V_p - pitch or gap velocity (m/s)

P - tube pitch =9.16 mm

d - tube diameter =6.35 mm

Finally, the reduced velocity can be calculated as follows:

$$V_r = V_p/(f_a d) \qquad (6.15)$$

V_r - reduced velocity

f_a - tube natural frequency in air (Hz)

This definition is consistent with the format adopted by Weaver & Fitzpatrick (29), and the format of the plots found later in this chapter. In past studies, as noted in chapter 2, some results have been plotted using the natural frequency of the tube in two phase flow. To establish this value, the natural frequency was calculated using the following equation:

$$f_n = A*(k/m)^{.5} \qquad (6.16)$$

f_n - tube natural frequency (Hz)

A - constant=$\epsilon^2/(2\pi L^2)$ (m^2)

ϵ =1.875

L -tube length=.300 m

k - tube stiffness=7.4 (Nm^2) (measured)

m - equivalent mass per unit length (kg/m)

If A and k are assumed constant properties of the tube, then adjusting the mass per unit length for the added mass associated with the various fluid densities will allow the estimation of the appropriate natural frequency. The equivalent mass of the tube can be calculated using:

$$m_{eq} = m_T + m_{added} \qquad (6.17)$$

m_{eq} - equivalent mass (kg/m)

m_T - tube mass=.171 (kg/m)

m_{added} - hydrodynamic mass (kg/m)

Pettigrew et. al. 1985 suggest the following equation for the hydrodynamic mass:

$$m_{added}=c_m\rho_h\pi d^2/4 \qquad (6.18)$$

where: $c_m=((D/d)^2+1)/((D/d)^2-1)$ (6.19)

: D/d=1.7*P/d for triangular arrays

These equations allow the simple adjustment of the homogeneous density to be translated into an estimate of the tube natural frequency in two phase flow.

A complementary method of representing the results is to plot the critical reduced velocity (velocity at which instability occurs) as a function of the mass damping parameter. This parameter is defined as:

$$m_d=m_{eq}\delta/(\rho_h d^2) \qquad (6.20)$$

The only undefined value in this equation is the damping value δ. The logarithmic decrement of damping of the instrumented tube measured in air is .010 +/- .001. This value can be used for future plotting of the results as done by Weaver & Fitzpatrick. However, most of the data in the

literature are plotted with an estimate of the value for the two phase damping. Westermann 1987 suggested scaling the study damping results of Pettigrew et al 1985, using the following equation:

$$\delta_P=\delta_M(d_P/d_M)(m_M/m_P)(f_M/f_P) \qquad (6.21)$$

M - refers to the data of Pettigrew et al(1985)

P - refers to the data from this experiment

The use of this equation assumes that the scaling used in single phase can be extended into the two phase region. The remaining analysis predominantly relies on the calculations presented here.

6.2 Procedure

6.2.1 Single Phase

The purpose of the experiment is to determine the effects of different flowrates on the tube response, which implies that the only parameter varied is the flowrate. However, maintaining pressure and temperature constant may not be necessary for the single phase case. In light of this possibility, two approaches were used in the single phase experiments. They are:

1) using the heat removal subloop to cool and control loop pressure and temperature below room conditions, and
2) allowing the loop to increase in pressure and temperature naturally as the experiment progresses.

The second approach is considerably simpler to perform and would therefore be preferable if there are no observable differences in response between the two procedures. To date, there have been no discernable differences, but further work must still be done to directly evaluate the effects.

In general the procedure can be summarized as follows:

i) Set pump speed as required for the desired mass flowrate.
ii) Allow time for the loop to settle into its steady state mode which can be determined by a consistent temperature, pressure, and a consistent RMS frequency

response on the Nicolet FFT analyzer.

iii) Take final reading of the RMS response and integrate over the peak responses to determine the RMS amplitude.

iv) Take a reading of the flowrate.

v) Determine the next flowrate desired and repeat i through iv.

vi) Repeat until instability portion of curve has been established.

Note: To avoid hysteresis problems, the proper procedure is to begin at a low velocity and move towards the point of instability.

6.2.2 Two Phase

The two phase procedure was similar to that just described for the single phase except that greater effort was required to generate the desired conditions and more readings are necessary.

The procedure was as follows:

For the first point only:

i) Determine the flowrate, temperature of test section, temperature difference between the test section and heater entrance, the corresponding heater input power, pressure, and quality desired for the test point.

ii) Set the flowrate by adjusting the pump speed.

iii) Initiate the heat removal subloop flow.

iv) Once the main flow begins to cool, introduce the heater power by beginning with approximately 10-20% of the final power.

v) Readjust the heat removal subloop flow to bring the temperature rise under control and to create the desired temperature difference between the test section and heater entrance.

vi) Repeat ii through v until the desired conditions are reached.

For all points:

vii) Allow steady state to be achieved and then proceed to read the following inputs:

1) flowrate,
2) test section pressure,
3) test section temperature,
4) temperature prior to heater inlet,
5) four surface temperatures to evaluate the heat loss,
6) heater power, and
7) the RMS frequency response and amplitude. In cases where the gamma densitometer is used, it too must be used at this point.

viii) To move to the next higher mass flowrate, the required increase in heater power must be calculated.

ix) The flowrate is increased and then the heater power is increased.

x) The loop is allowed to achieve steady state at the new flowrate. To maintain conditions identical to those of the previous point, the subloop may need to be adjusted.

xi) Repeat vii through x until several unstable points have been achieved.

The key to the two phase experiment is to maintain a constant temperature distribution, which allows the quality in the test section to be controlled by maintaining the flowrate to heater power ratio at a constant. Generally, 8-10 points were taken in the initial experiment to map out the response. A second experiment was then performed to fill in the points of interest. This served to verify the repeatability of experiment as well. To do this, the first point in the second experiment had to be identical to a point in the initial experiment.

The preceding description outlines the procedure recommended when conducting two phase experiments. Conducting a subsequent experiment to compliment the first is a little easier to start since the initial conditions are well defined. The initial experiment requires an estimate of the loop

conditions necessary to achieve a given quality at a desired pressure. With experience this problem alleviates itself, but the problem could still exist for first time users. This situation could be eliminated if the loop were well mapped out according to the control settings necessary to generate a variety of conditions.

The procedure outlined here assumes a general knowledge of the loop controls. For details of these controls, the reader is referred to the appendices where the operating manual is reproduced.

6.3 Test Results

To demonstrate the experimental validity of the loop, experiments were conducted at two sets of conditions. The first experiment, as discussed in the subsequent pages, considers the test facility performance for single phase conditions. The second experiment, to be discussed in a later section, deals with conditions at the design quality, which corresponds to 80% void if the assumptions outlined in the calculation section are valid. Consequently, the performance for the loop can be ascertained at extremes of the designed range of the loop. However, this does not necessarily imply that the entire range of potential conditions are within these two boundaries, as will be explained in section 6.4.2 on range limitations

The original intention to ascertain the validity of the

loop performance can have several outcomes. If the results are totally as expected and explainable, then benchmarks will result. Should anything questionable about the results arise, then the problem must be explained and rectified. This last scenario occurred with the single phase experiments. Consequently, the results discussed in the single phase section are intended to provide a general understanding of the behaviour exhibited by the test bundle in the loop. Future efforts will be required to obtain benchmark results.

6.3.1 General Tube Response

The natural frequency of the monitored tube was determined by experiment and through calculations. Using equation 6.16 and measured values of stiffness and mass, while assuming the added mass in air is insignificant, the tube natural frequency is calculated as 40.90 hz. This compares favourably with the measured value seen in figure 6.1 of 40.0 hz. The difference can easily be accounted for by a slight variance in the tube length. This slight variance has physically changed the tube frequency itself, since the tube originally measured 41.2 hz and was lengthened slightly to obtain the 40 hz measurement.

The purpose of the reduction in the tube natural frequency was to provide a closer match to the rest of the tube bundle measured to be 39 hz. Although the tubes only varied in length by up to 2 millimetres throughout the bundle,

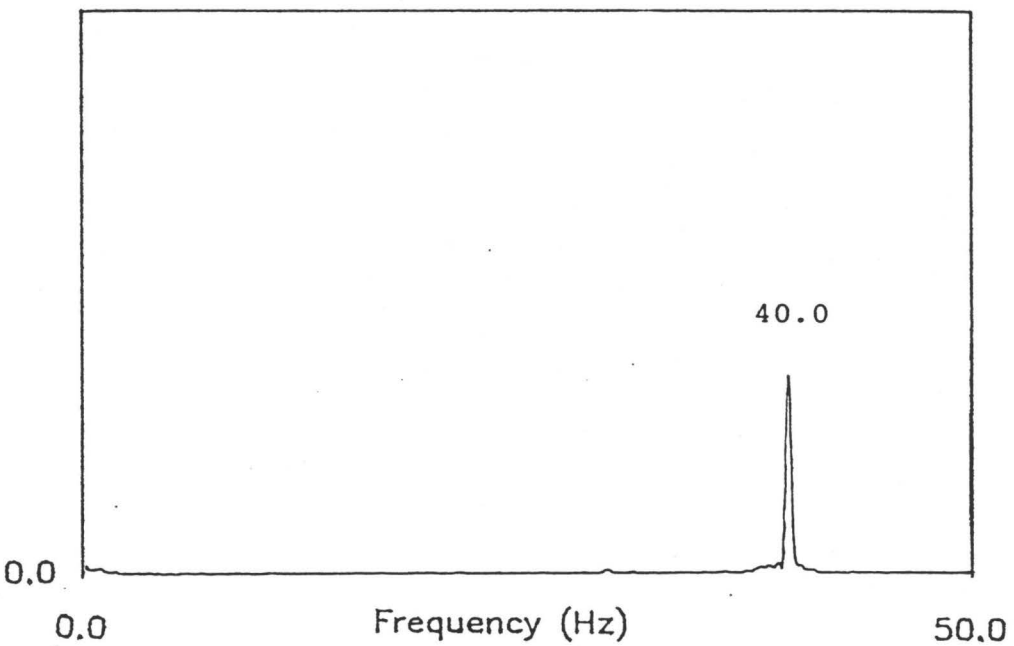

Figure 6.1

Natural Frequency in Air

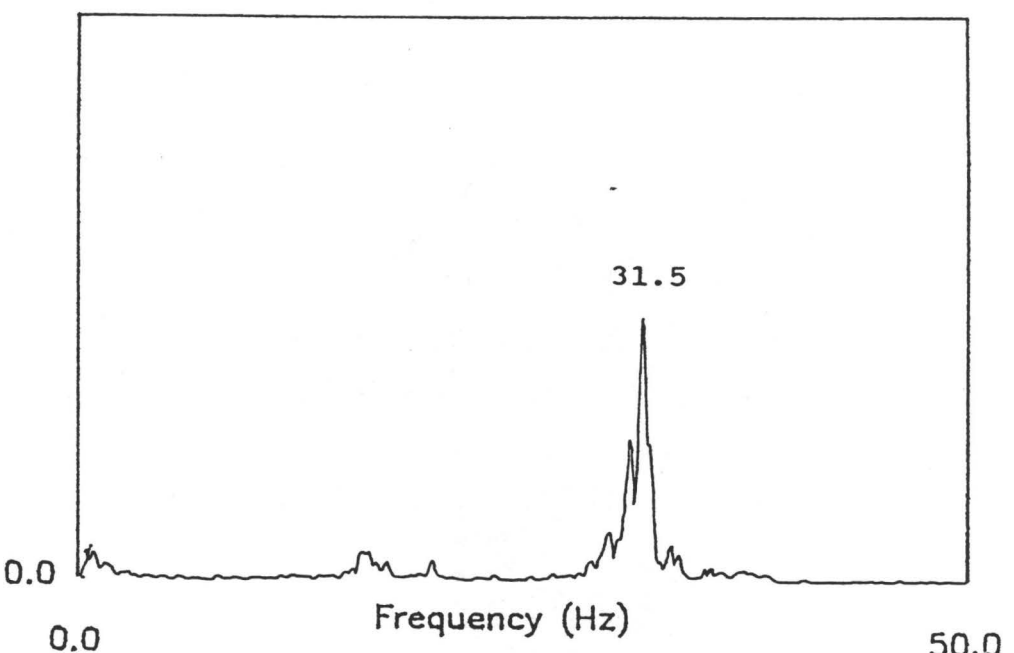

Figure 6.2

Natural Frquency in Liquid

there was a 2.6% difference between the monitored tube and the remainder of the bundle. The source of the difference was suspected of being the brass end plug removed from the instrumented tube to insert the collimator, which is composed of glass and nylon. To confirm this possibility, a second equation was employed to calculate the effects of the brass end plug found in the remainder of the bundle.

From Blevins (1979), the following equation is obtained to account for an end mass on a cantilever tube:

$$f=1/(2\pi)*\{3EI/(L^3(M+0.24M_b)\}^{.5} \qquad (6.22)$$

M=mass of plug (kg)

M_b=mass of tube (kg)

The mass of the tube can be calculated using:

$$M_b=m_T*L=.0513 \text{ kg}$$

The volume of the plug is considered to be the portion of the tube that was filled with brass. The size of the plug was measured to be 3.85 mm in diameter by 7.94 mm in length. The density can be calculated from the tubes measured mass per unit length as approximately 8540 kg/m^3. This results in a mass for the plug of:

M=.000789 kg

Substituting into equation 6.22 the frequency for the

remainder of the bundle is calculated to be 39.87 hz assuming a tube length of 0.3 metres. Therefore, there is a net change in the frequency of about 1.0 hz which is comparable to the frequency difference measured.

Having evaluated the tube response in air, a similar analysis is required for liquid "Freon 11". To obtain the frequency, the test section was struck, as it was with the frequency in air measurement, and the response recorded on the Nicolet FFT analyzer. Figure 6.2 shows the single peak at the tube natural frequency of 31.5 hz. To calculate this value, the added mass coefficient must be determined. To provide a better estimate of the coefficient in quiescent fluid, the length should be determined that provides the 40 hz result in air. Using equation 6.16 again, the length is approximately 303 mm.

Equation 6.19 gives an added mass coefficient of 1.4. However, this corresponds to a natural frequency of 34.1 hz. Working from the measured frequency the added mass coefficient is estimated to be 2.26, assuming the fluid to be at 25 °C. This value seems slightly high, but as will be shown, there is a change in this value in flowing fluid. The value could be large as a result of the method of measuring the frequency, where the striking of the structure may produce different results than if the tube itself were tweaked. Additionally, the added mass is partially a function of the tubes interaction with its neighbours, resulting in a band of

frequencies at which a tube can vibrate, depending upon the mode of vibration. This concept will be expanded upon in a later discussion.

6.3.2 Single Phase Experiments

Several single phase experiments were run, of which typical results are presented in the following sections. The repetition of the experiment served to reevaluate the results after a small change in the test section had taken place. Since several changes were made over the period during which the experiments were carried out, many different experiments were needed to ascertain the effects. Generally, the frequency spectrum response followed the same pattern, although a slight shift in frequencies occurred when the monitored tube was tuned to 40 hz from 41.25 hz in air, as would be expected. The results presented for the test section are with the natural frequency of the monitored tube in air approximately equal to 40 hz.

More significant variances were seen in the reduced velocity plots. Slight changes in approach flow angle caused the streamwise and transverse curves to vary in the steepness of the curve after instability was reached. Moreover, the change in frequency of the monitored tube caused the critical reduced velocity to rise by approximately 0.3. Regardless, the changes did not introduce any further unexplainable results. Generally, the behaviour always fell within the criteria set

out by the results of other studies, as outlined in chapter 2 and utilized in the upcoming discussion.

6.3.3 Single Phase Frequency Spectra

Figure 6.3 and 6.4 present the frequency spectra for a range of flowrates leading up to fluidelastic instability in the transverse and streamwise directions respectively. The plots are characterized by one or two solitary peaks that increase slightly in frequency as the flowrate is increased. Unusual features are noted in three of the plots.

Figure 6.3b shows a small peak in the 22 hz range, which further investigation revealed to be the natural frequency of the test section itself. Figures 6.3d & 6.3e show the emergence of a second frequency at approximately 37 hz. Although there is a continuous increase in frequency throughout the experiment, the 37 hz frequency constitutes a discontinuous jump from 33.5 hz. Other than the discontinuous jump, the response is classical, showing responses at the natural frequency only. A characteristic of parallel triangular bundles is the lack of a Strouhal peak. The same result was observed for the single phase experiment discussed here.

6.3.4 Explanation

The only identifiable source of the discontinuous jump is the fact that the monitored tube is detuned with respect

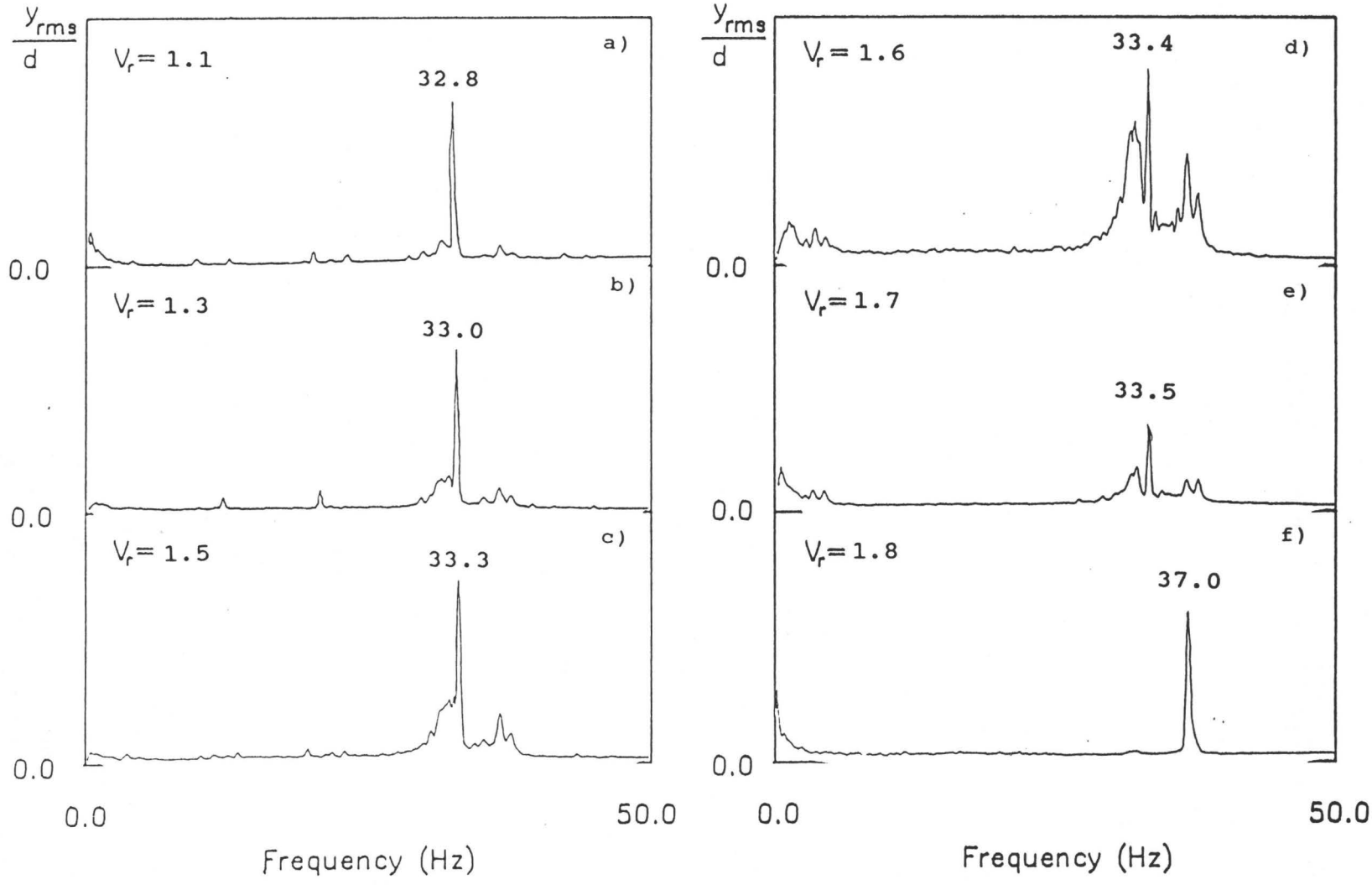

Figure 6.3

Transverse Frequency Spectra

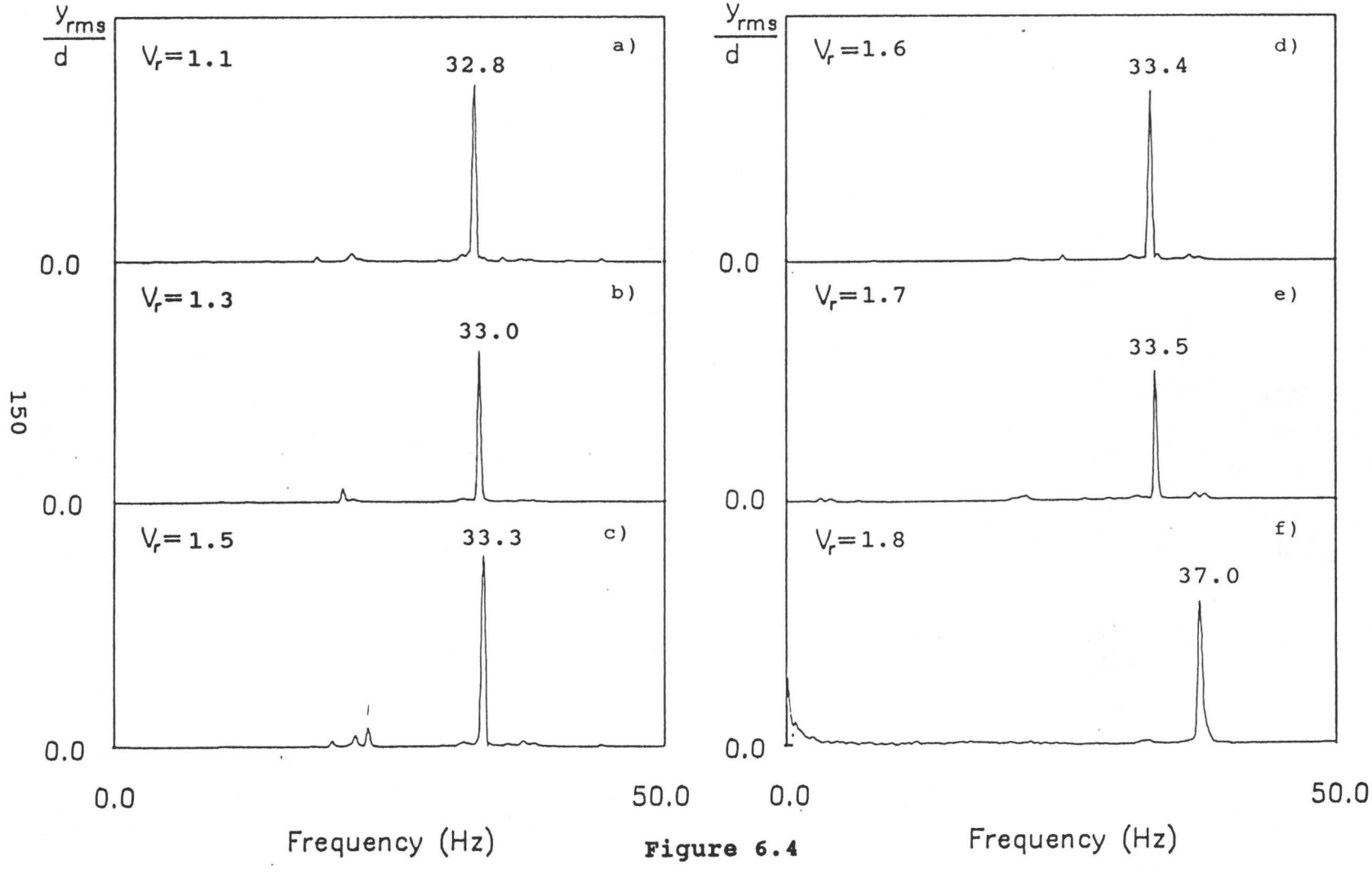

Figure 6.4

Streamwise Frequency Spectra

to the rest of the bundle. The flow is characterized by broad band turbulence causing the tube to respond at its natural frequency. As the flow increases there is increased turbulence and the possible variance in added mass. However, the change to 37 hz is discontinuous, and this frequency begins to appear as a separate response at a reduced velocity of 1.6. The tube goes unstable at V_r=1.8 and the frequency is isolated at the 37 hz frequency. It can be concluded that the natural frequency of the tube is not varying, but the exciting force is changing.

The large change in frequency makes the possibility of the tube mode changing an unlikely explanation. Alternatively, the detuned tube may be experiencing a unique environment where its neighbours are exciting the flow and in turn the monitored tube at a different frequency. That is, the bundle predominantly vibrates at lower frequencies than the monitored tube, exciting the flow at those frequencies. The tube experiences a force at a dominant frequency other than its natural frequency. As the flow velocity approaches the critical velocity for instability, the lower frequency tubes are expected to go unstable first, assuming that all the tubes in the bundle will go unstable at the same reduced velocity. Therefore, the majority of the bundle will reach larger amplitudes earlier than the instrumented tube, enhancing the dominance of the bundle response over that of the single tube. As the isolated tube approaches instability, the response of

the tube to the broad band component of the excitation begins to grow. Finally, at instability the tube responds at its own natural frequency since the fluidelastic phenomenon dominates.

The strength of hydrodynamic effects are well documented in the literature, as noted in chapter 2. These same effects have not been studied on a single detuned tube in a dense fluid, but have been looked at for detuned rows in a gas flow by Lever and Weaver (1977). The effects described here were not evident in these studies, although the critical reduced velocity was affected. The frequency spectrum was most likely unaffected since the hydrodynamic effects are not as strong in a gas flow. Regardless, the hypothesis presented should result in visual evidence in the test section.

To further analyze the response of the bundle, a single phase test was conducted using a strobe to isolate the frequencies of the individual tubes. Conditions were chosen to provide a response where the instrumented tube was vibrating at two frequencies simultaneously. The upstream tubes responded as expected in the 33 hz range, while the instrumented tube was seen to whirl slightly, affecting the other tubes as it passed close to them. The surrounding tubes tended to shift frequencies constantly, making them difficult to monitor. This response is what would be expected if the postulate is correct. It is not expected that the there would be strong interaction between the upstream tubes and the

instrumented tube. However, the tubes surrounding the instrumented tube show a strong fluid coupling with the detuned tube, as expected. Since the instrumented tube is surrounded by tubes with the lower natural frequency, it is expected that at lower velocities they would dominate the single tubes response.

Lever and Weaver (1977), while studying the effects on the critical velocity of detuning rows of tubes, noted that the detuned tubes would alternately have the maximum amplitude response with the base frequency tubes. That is, if the detuned tubes showed large amplitudes, the tuned tubes responded at suppressed amplitudes. In the present case of discussion, a single detuned tube is surrounded by an entire bundle of tuned tubes, which would lead to the speculation that the single tube may be constantly dominated by the surrounding tubes. The strobe experiment did show that the instrumented tube appeared to show consistently lower amplitude vibrations.

These observations, although useful, are inconclusive and further analysis is required. There is one further point that must be addressed if the hypothesis is to be accepted. The tube natural frequencies can be reasonably predicted in quiescent fluid, as seen earlier. It has been noted in past studies that hydrodynamic effects are strong within a bundle, and would be stronger in a fluid of higher density, such as Freon 11. Further, the observed response of the tubes follows

a predictable pattern as determined by implications of what has been learned in these same studies. Still, there is one implication that has not been addressed, which is that 37 hz must be the natural frequency of the monitored tube.

Using the same analysis as that used earlier to consider added mass coefficients, the added mass coefficient at 37 hz is 0.64. This value is difficult to accept since it is below 1.0. The variation in the added mass coefficient is shown in table 6.1 for the various frequencies shown in figures 6.3 & 6.4. Although values are calculated for each frequency for both the instrumented and uninstrumented tubes, the explanation put forth here dictates that frequencies prior to 37 hz are only applicable to the bundle tubes, whereas the 37 hz frequency is applicable only to the monitored tube. The value of 1.45 for the bundle tubes at 33.5 hz corresponds very well with the 1.4 value calculated using equation 6.19. Chen (1987) notes that although m_{added} varies with flow, values in quiescent fluid give good results in a flowing fluid.

In his analytical model of added mass coefficients, Chen determined that there is band of coefficients as a result of the hydrodynamic effects between every tube in the bundle and the one of interest. As seen in the graph reproduced in figure 6.5, a value of 0.64 is above the minimum values calculated by Chen. The derivation of the equations used identifies that the added mass coefficient is mode dependent, with coupled modes providing the extreme cases.

Table 6.1
Table of Added Mass Coefficients vs Frequency of Tube Response

Bundle Tubes		Monitored Tube	
f(hz)	C_m	f(hz)	C_m
39.0	0.00	40.1	0.00
31.5	2.15	31.5	2.28
32.6	1.75	32.6	1.88
33.0	1.62	33.0	1.75
33.3	1.52	33.3	1.65
33.4	1.48	33.4	1.62
33.5	1.45	33.5	1.59
37.0	0.49	37.0	0.64

Note: Calculations based on density at 25 °C.

Furthermore, Chen shows that there are 2n eigenvalues between these limits where n is the number of tubes in the bundle. Each eigenvalue represents an added mass coefficient resulting from the interaction of a pair of tubes. The added mass coefficient is broken down into two components, namely the self added mass $\propto_{11}$, and the added mass due to interaction with another tube $\propto_{12}$. The total added mass coefficient is found to be:

$$C_m = \propto_{11} + \propto_{12} \qquad (6.23)$$

The value $\propto_{11}$ can be represented experimentally as a flexible tube in an otherwise rigid bundle in quiescent fluid. The definitions provided here correspond to a triangular

array, which result in the simplified representation given. The theoretical calculations provide favourable results for the self added mass coefficients as shown figure 6.6. Here Chen plots results from Moretti and Lowry (1976) against the predictions from his model.

Chen's model demonstrates that the added mass is only significantly affected by a tube's nearest neighbours, which has been verified in other studies. Consequently, there is considerable experimental support for Chen's model of the added mass coefficients. This partially validates the added mass coefficient found for the instrumented tube. Chen also noted that the extreme values of added mass were obtained for coupled modes of vibration. Whether or not this is the case for the instrumented tube is debatable since there is no clear evidence to support such a claim.

The added mass coefficient is clearly within the realm of possibilities, but there are other effects that should be considered. The apparently reduced added mass could also be partially attributable to the low latent heat of Freon 11, which creates the possibility of cavitation in the flow surrounding the tube. Moreover, past tests on detuned tubes do not correspond directly to the high density and the single detuned tube case. These effects provide other potential explanation for the reduction in the apparent added mass of the tube.

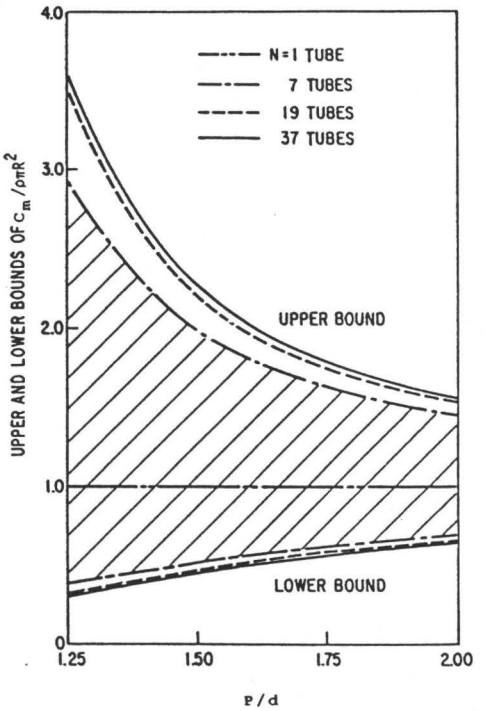

Figure 6.5

Added Mass Coefficient (C_m) Chen (1987)

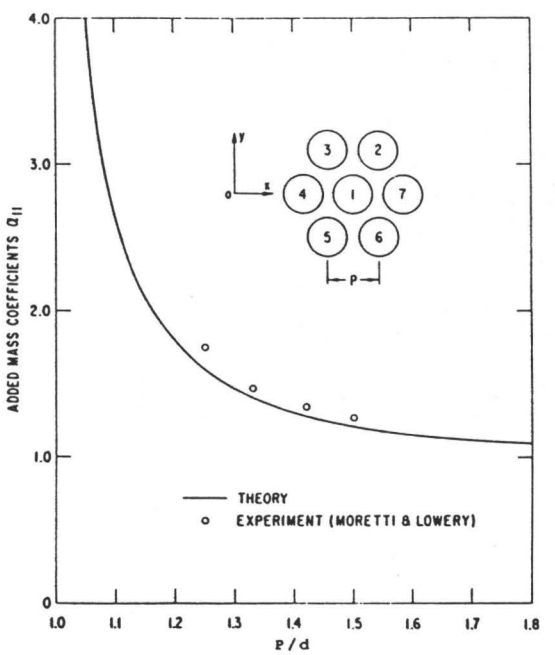

Figure 6.6

α_{11} vs Moretti & Lowry (1976) ref. Chen (1987)

The most important observation of the previous discussion is that the upstream tubes behave in a classical manner, going unstable at a predictable natural frequency. Since it is expected that these tubes will not be influenced strongly by the detuned tube, they demonstrate the behaviour of the tubes under normal conditions where all the tubes are tuned to the same frequency. This suggests that tuning of the instrumented tube will rectify the present situation. The occurrence of this phenomenon indicates an interesting effect to be studied in the future. Any modifications to the tube bundle should allow for the bundle frequencies to be easily manipulated.

6.3.5 Single Phase Amplitude Response

Although the frequency spectra appears to significantly deviate from the expected results with respect to the discontinuous jump, the amplitude response as a function of reduced velocity (eqn. 6.15) follows expected trends. The single phase experiment was run several times with small variations between each test situation, as noted previously. Although some changes were observed, the overall performance possesses the same characteristics. From figure 6.7 it is seen that the tube response becomes unstable in a classic manner in both directions. In an experiment done earlier, the streamwise direction showed the largest amplitudes and the sharpest increases in amplitude response as a result of instability. The difference between experiments can be attributed to slight

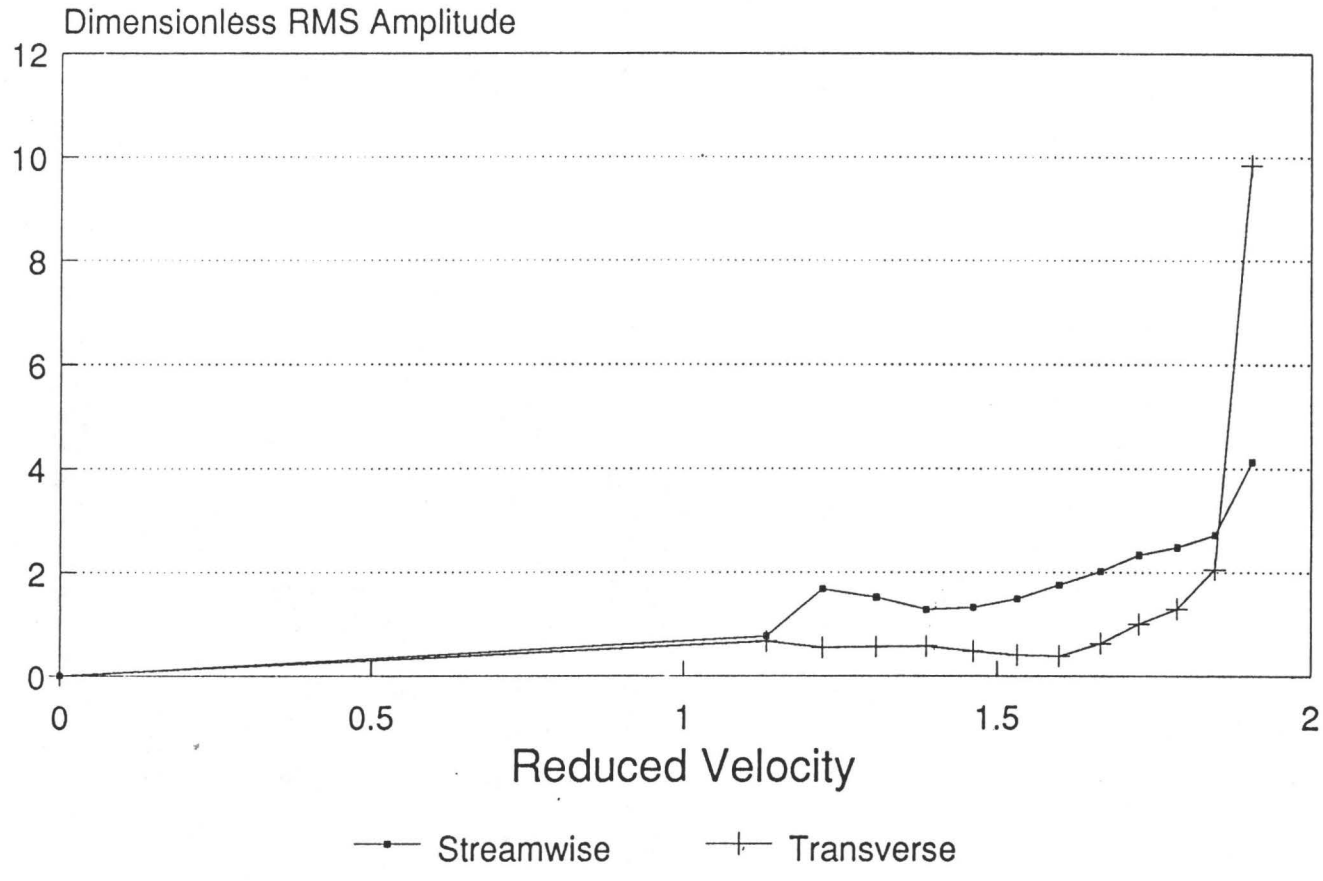

Figure 6.7

Single Phase Amplitude Response

variations in the tube bundle orientation, a phenomenon studied by Yeung and Weaver (1983). Three experiments were run, each after the tube bundle had been removed for repairs or modifications to some portion of the loop. Each experiment showed slightly different response characteristics. A latter modification involving the reconstruction of the tube bundle sealing gasket and the replacement of the lexan half tubes by brass half tubes alleviated this problem. The resulting configuration is more exact in dimensions and allows for easier mounting of the tube bundle in an identical orientation should the tube bundle be removed again.

The final modification involved repairs to the instrumented tube. The result was a change in the natural frequency of the monitored tube from 41.25 to 40 hz. This did cause a slight shift in the frequency observed at instability, but no perceptible change in the lower flow frequencies. Simultaneously, a new bundle gasket was again made which may have affected the ability to maintain the orientation of the bundle in the exact position prior to the repairs. Although there were changes noted between experiments, the characteristics used for comparison varied insignificantly. The discussion turns to these considerations at this point.

Instability clearly begins around a value of reduced velocity of 1.8. Comparison to previous studies shows reduced velocity values ranging from 1.0 to 3.0 for mass damping values up to 0.1 (figure 2.4). Using a density of 1480.74

kg/m^3 and an added mass coefficient (C_m) of 1.45, a mass damping value of .040 is obtained. For a C_m of .64 the mass damping parameter value of .034 is obtained. Therefore the tube is achieving instability in a predictable range regardless of the which set of tube characteristics are chosen.

The value of 1.8 is 0.3 higher than in each of the previous single phase experiments performed with the loop. The difference may be attributable to the adjustment of the monitored tube frequency. Lever and Weaver (1977) showed that the critical velocity could be delayed when detuning tube rows by small percentages, as shown in figure 6.8. The case of 41.25 hz (5.8%) is on the downward sloping portion of the curve, whereas the 40 hz case (2.6%) is on the upward sloping portion and close to the maximum at 3%. The curve of figure 6.8 indicates a tuned critical reduced velocity of approximately 1.25. The scaling doesn't correspond perfectly, but within the error associated with reading the graph and determining the critical reduced velocities, the results of Lever and Weaver appear to fit quite well. This provides further support for the explanation given for the discontinuous jump.

When evaluating the critical reduced velocity (reduced velocity at which instability begins) a criterion is needed. A definition commonly used to show that instability has begun is the RMS response of the tube being 1 to 2% of the tube

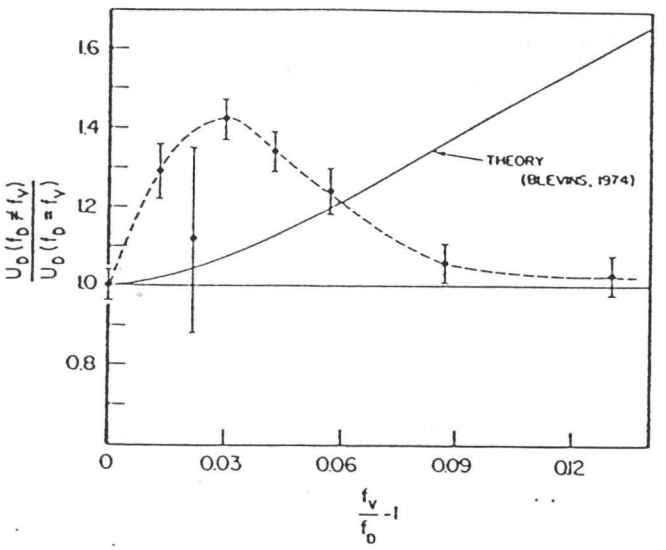

Figure 6.8
Change in Critical V_r with Detuning
(Weaver and Leaver (1977))

diameter. If the analysis given so far is correct, than the actual amplitude at instability is somewhat obscured, as is common in liquid flows. However, if lines are extended representing the turbulence response and the unstable response, their intersection would be found to be approximately 1%.

It should also be noted that, although there were two dominant frequency responses, all other frequencies registered insignificant response levels. Therefore, the discontinuous jump is the only abnormality observed. Furthermore, the two frequencies in question were close together which creates the effect of a much wider range of higher response levels, as opposed to a single peak. Therefore, it should not be surprising that the tube amplitude response is reasonable. However, the discontinuous jump cannot remain if future

experimental findings are to have meaning.

6.3.6 Single Phase Conclusions

The amplitude response characteristics of the tube in single phase are comparable to those found in previous experiments. The frequency response shows a discontinuous jump in frequency as instability is reached. This is postulated to result from the monitored tube responding at a different natural frequency than the balance of the bundle. Observations have shown this to be a plausible explanation. Ultimate proof can only be obtained through the tuning of the bundle. The occurrence of this phenomenon has not been studied in depth and perhaps this facility could be used to provide more insight into the effects of detuned tubes.

Tuning of the bundle is expected to rectify the present situation. This will allow proper benchmark test results to be obtained. There is some concern over the effects of bundle removal. If the present configuration is maintained, that is the gasket design is not changed, then bundle removal will not significantly change the bundle response. Consequently, the only concern for the single phase case relates to the bundle tuning which can be corrected. The facility performs in all other respects in a predictable and reliable fashion.

6.3.7 Implications of Calculations on Void Fraction Determination

There are a number of assumptions implicit to the calculations, most of which are associated with approximations made to provide information for values not readily obtainable. However, the largest error can be attributed to the calculation of the homogeneous density (eqn. 6.11). A small error in this calculation results in a significant error in the velocity calculation (eqn. 6.13). This is most prominent for void fractions lower than 70%, and at lower pressures and temperatures, where, when using the homogeneous assumption, an extremely high change in void fraction results from a small change in quality.

The implication is that small errors in determining the input parameters for the calculations can have a significant effect on the calculated quality, and in turn the void fraction. As the equations used in the calculations demonstrate, the resulting density and void fraction will affect the presentation of the results in a nondimensional form. To compensate, a high degree of accuracy in the experimental procedure must be ensured.

The no slip assumption has similar ramifications, although these cannot be alleviated through carefully carrying out the experiment. Slip can be accounted for, however there

are implications on the presentation of the results as will be discussed later. At this point, it is sufficient to note that the error associated with this assumption is potentially more significant than the error associated with the inaccuracy of input parameters.

To evaluate the slip ratio, the void fraction must be directly measured. In this case, the most easily applied apparatus for measuring void fraction was a gamma densitometer. However, a problem was detected when the pump motor controller interfered with the results produced. Subsequently, two undergraduate students, Francois Kneppert, and Paul Feenstra, were asked to solve this problem. Through an improved ground and high frequency filter, consistent performance was reestablished. Although the gamma densitometer results have not been confirmed, the conditions calculated to produce 80% void at 49 °C, were measured to produce a 45-50% void fraction. The inclusion of the +/- 5% error expected on the reading does not alleviate the concern over the high degree of slip (5.0) that this measurement indicates.

Bergles et al (1981) present several slip models with their experimentally determined errors. Two recommended models were provided by Smith(1969) and Chisholm(1973). These models have a standard deviation on the error of the mean density of 20 -30 %, but they are easy to use and correspond well with each other. These equations are plotted with the homogenous assumption for void as a function of flow quality in Freon 11

at 49 °C in figure 6.9. The slip models coincide quite well, but are significantly different than the homogeneous curve for low qualities. For the conditions measured by the gamma densitometer, the quality was approximately 3.5%. From the plot it can be seen that the slip models predict void fractions in the 60-65% range. Although, higher than the gamma densitometer, it is closer to 50 than to 80%. The significance of this value will be considered further in the following section.

Since the gamma densitometer readings were suspect as of this writing, the void fraction measurement must yet be confirmed. Moreover, the error in the slip models is significant, which is due to the nature of the two phase flow. However, sufficient information has been provided to warrant changes in the presentation of the two phase results. For this reason, the results presented for the two phase test will be presented in the form of mass flowrate versus dimensionless amplitude for a known average quality as opposed to void fraction.

The implications discussed in this section are not intended to demonstrate a limit on the usefulness of the experimental facility. These problems can be accounted for, and removed from concern in the future. The important point is that they be identified so that proper conclusions may be made from future experiments. Moreover, the slip problem has implications on all the results obtained in two phase flow.

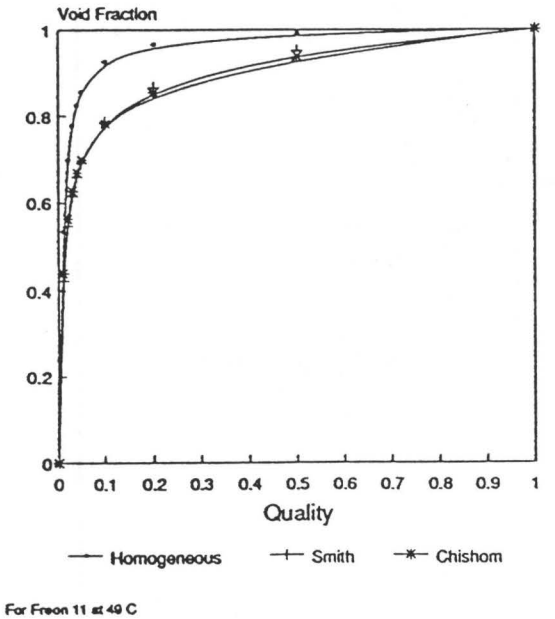

Figure 6.9
Quality vs Void Fraction
Homogeneous vs Slip Models

A no-slip assumption is the norm amongst researchers in the field. Consequently, the problem of how to properly describe the flow conditions must be solved.

6.3.8 Two Phase Frequency Spectrum

The twin peak phenomenon, that appeared in single phase flow, was not present in the two phase frequency response. This is most likely a result of the reduced hydrodynamic effects present in the two phase flow. A typical response from

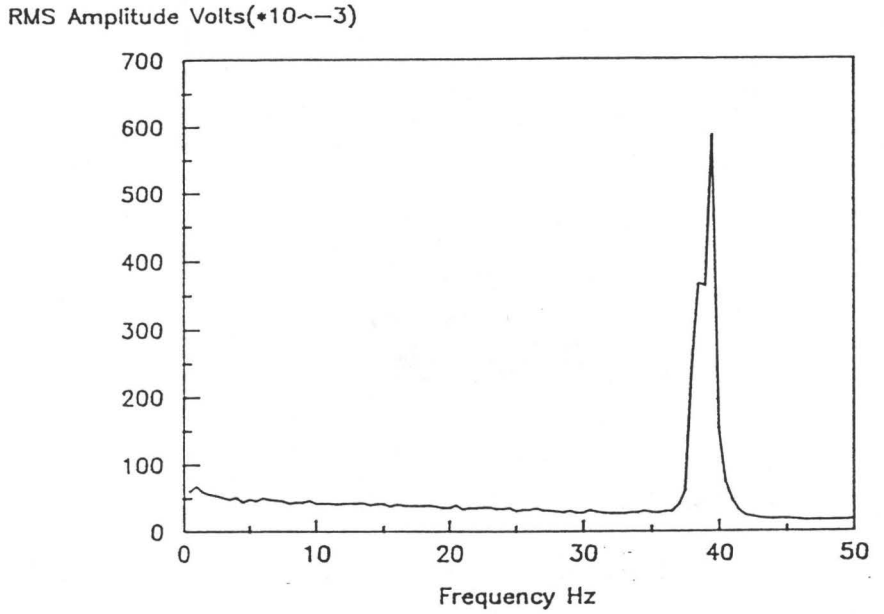

a) Transverse Frequency Response

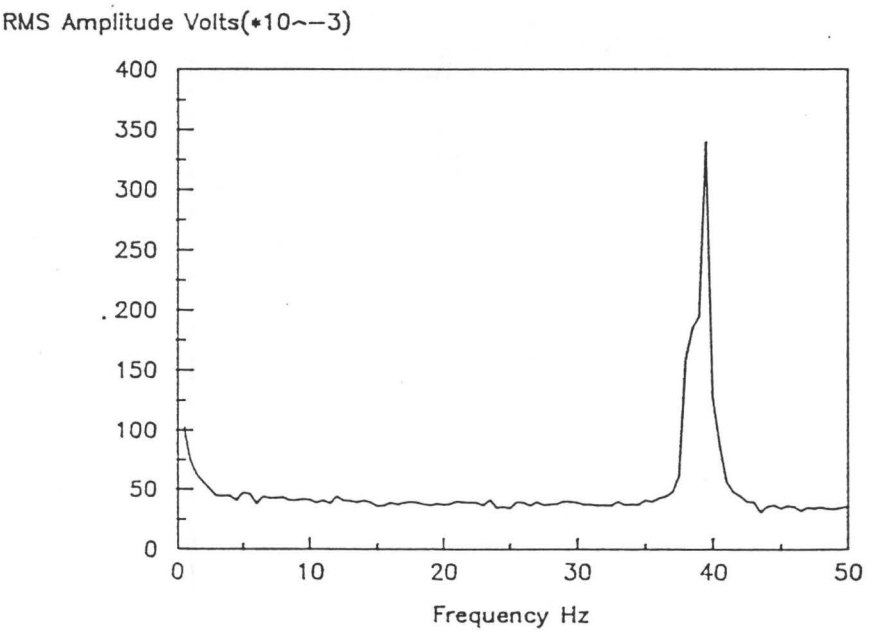

b) Streamwise Frequency Response

3.5% Quality

Figure 6.10

Frequency Spectrum for Two Phase Response

an experiment at 49 °C with a flow quality of 3.5% is shown in figure 6.10. The peak frequency is seen at 39 hz. The remainder of the response is broad band noise exhibiting response levels significantly higher than that observed in single phase flow. This is attributed to the generally higher turbulence level found in two phase flow. The bundle response is typical of that observed in other studies.

The size of the peak grows with increased mass flux. For lower velocities, the peak is not observed. Pettigrew et al. (1985) present plots that follow this pattern, but also had growing low frequency response as the void fraction was increased. Although this phenomenon was observed for some conditions, the strength of the responses at these frequencies was not significant as compared to the peak response. Consequently, future experiments will have to consider this problem more carefully.

The lack of low level peaks may be attributed to the homogenizing bundle, which tends to break up the vapour into smaller bubbles. Therefore, the vibrating bundle never sees the effects of larger bubbles. These larger bubbles may cause the low frequency vibrations observed by Pettigrew et al. An alternative explanation is that the void fractions determined by the energy balance are incorrect and that the readings of the gamma densitometer are correct resulting in a significantly lower void fraction. Then the low frequency response is not different from that observed by Pettigrew et

al.

Accepting the lower void fraction value poses some problems with the peak frequency. The response, as depicted in figure 6.10, consists of broad band turbulence and one dominant peak. This peak is expected to be occurring near the tube natural frequency. Using equation 6.16, the implied density of the fluid can be determined. This provided a result of 68% void fraction assuming an added mass coefficient of 1.4. The calculated void fraction without slip is 75 %. Referring to the slip models noted earlier, the 68% void fraction is also close to the 60-65% prediction they provide. Although this appears to suggest that the void fraction is closer to that calculated by the slip models than the gamma densitometer would indicate, there is some question over the added mass coefficient. The reduced coefficient seen in the single phase could be affecting this result as well. This indicates the need to reevaluate this argument after the bundle has been tuned.

6.3.9 Two Phase - Amplitude Response

Figure 6.11 shows the amplitude response of the instrumented tube as a function of the pitch mass flux as defined by:

$$G_p = P/(P-d)*G \qquad (6.24)$$

where: $P = 1.443*d$ (m)

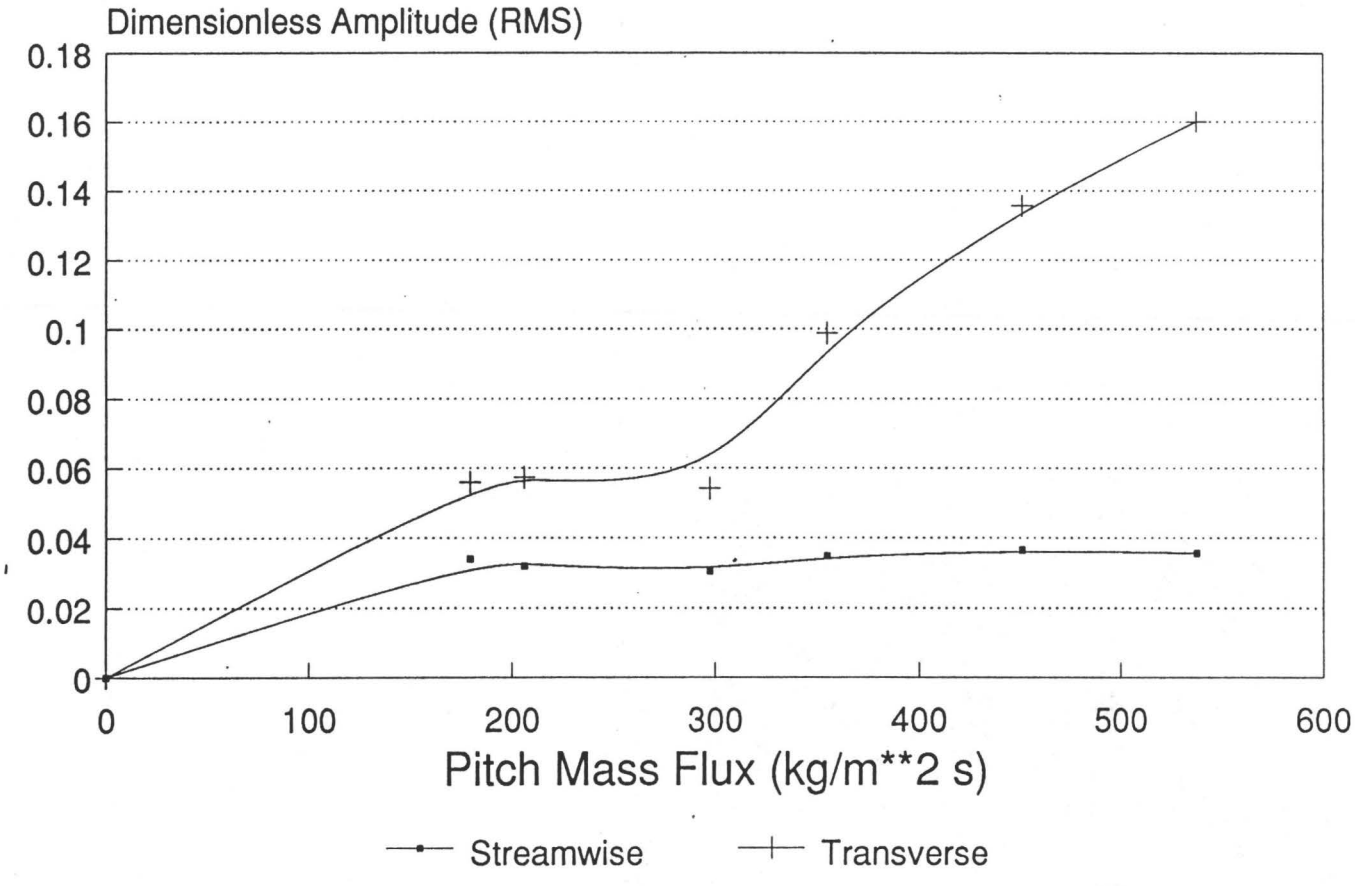

3.5% quality

Figure 6.11

Amplitude Response for 3.5% Quality

d=tube diameter (m)

G= mass flux of upstream flow (kg/(m^2.s))

The critical pitch mass flux 'G_r' is 293, although this point is somewhat obscured. The homogeneous assumption places the void fraction at approximately 80%. Combining this with the natural frequency in air, a reduced velocity of 3.70 can be calculated using the equations described in this chapter. The mass damping parameter is calculated to be 0.149 using the damping value measured in air. Comparison of the reduced velocity with comparable data shown in figure 2.4, shows this value to be at the upper end of the range seen in this plot. Using the measured response frequency of 39.125 hz and scaling the damping value in air using equation 6.21, a mass damping value of 2.926 is calculated, and the critical reduced velocity becomes 3.9. For this mass damping Pettigrew et al (1985) predict a reduced velocity of approximately 7.0 for a normal triangular bundle. This value is considerably higher than 3.9, but this is expected. Weaver and Fitzpatrick (1987) observed that a normal triangular array is expected to go unstable at a reduced velocity roughly twice that of a parallel triangular array.

There still lies some uncertainty associated with the response level at the onset of fluidelastic instability. The RMS response is found to be approximately 6% of the tube diameter, which is considered high. This points to the

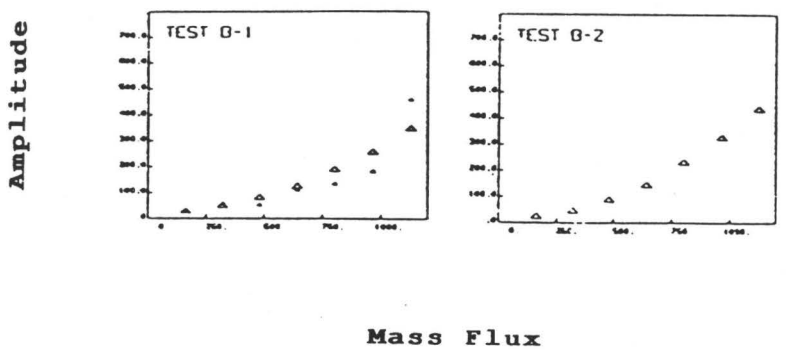

Figure 6.12
50% Void Results of
Pettigrew et al. (1985)

possibility of increased turbulence levels being present in the test section. This measurement may be reduced somewhat by limiting the RMS integration to the peak response, although this presents difficulties when a dominant peak is not evident as seen at lower flowrates in two phase flow.

The higher response at instability is seen in Pettigrew's data (1985) presented in figure 6.12. For a normal triangular bundle at 50% void in air and water, it is seen that for different tests the point of instability does show significantly higher amplitudes. The test section in this case was composed of 13mm tubes, resulting in an amplitude of approximately 4% of tube diameter. This indicates that response at intermediate void fractions can be expected to show higher amplitudes as the tube approaches instability than

seen in single phase flow.

The comparison between two phase experimental results from various studies leads to some questions. As seen in the discussion above, the characteristics of the flow are important in determining what results to compare. The problem lies in the chaotic nature of the two phase flow itself. The difficulties outlined in this section with the determination of the void fraction are not confined to this project. The large standard deviation noted on some of the better slip models illustrates the difficulty associated with comparing one 50% void experiment with another. It would appear that the particular geometries associated with each experiment may contribute to the inconsistencies observed.

In the two phase analysis presented in this chapter the void fraction was determined based upon the homogeneous model, for comparison purposes. This does not guarantee a meaningful comparison since slip is not expressly accounted for. If slip is accounted for, then the appropriate fluid density could be better identified and the added mass to the tube more accurately calculated. However, the resulting reduced velocity is a nondimensional representation of the fluid velocity as it passes around the tube. Slip between the phases means that one phase is moving faster than the other. In the two phase test discussed above, the slip is upwards of 3.0 which is a significant ratio. Is it correct to describe the tube response based on an averaged flow velocity. For low levels of slip,

the answer is yes, but as slip increases the answer is not so clear.

Measuring the void fraction does lend meaning to the plotting of particular void fraction cases, but the measurement techniques available today are limited in accuracy. The errors associated with the use of void fraction can be reduced by ensuring that several measurements are carried out at each specific set of conditions. Additionally, the presentation of the results could focus on forms such as used here, where basic results are provided without nondimensional scaling of the flow conditions. This may lend itself more readily to the determination of whether conditions of particular experiments are actually comparable. Moreover, slip levels should be measured and documented as a parameter describing the flow. Further consideration of the effects of slip in the future will determine how best to reduce all data to a common set of descriptors.

6.3.10 Summary of Two Phase Response

In contrast to the single phase response, the frequency spectrum showed no surprises, whereas the RMS amplitude response showed increased amplitudes at instability. The increased amplitudes have been seen before at intermediate void fractions. This phenomenon is a departure from the characteristics of single phase responses. Furthermore, the critical reduced velocity (which requires some assumptions) is

reasonable when compared to past experiments.

The underlying problem left to be solved is the determination of the void fraction. Four void fraction results are provided ranging from 45 to 75% for one set of conditions. There is no doubt that there must be some degree of slip between the phases, the question is how much. The slip models and the natural frequency of the tube indicate similar levels of void. However, every means of determining the void has an associated uncertainty. No conclusions can be made until the bundle is tuned and the gamma densitometer is reliable.

The presentation and analysis of the data posed an interesting problem. The slip levels in the test section make the usual methods of nondimensional comparison less meaningful. It is suggested that slip become a measured parameter when describing any two phase flow experiment. Future two phase experiments should address this problem.

6.4 Loop Operating Characteristics

6.4.1 Experimental Operation

Two phase flow experiments in flow induced vibrations are inherently difficult for two reasons. First, the control of a two phase flow loop can be difficult, even for two component air-water loops commonly used in this area of research. Therefore, it is the goal of the present work to provide the greatest degree of control possible.

The second concern relates entirely to the analysis of

the data. It is expected that the higher turbulence level characteristic of two phase flow will tend to make the determination of the critical flow velocity more difficult. Moreover, the calculation of these velocities are now subject to greater error, since velocity is a function of the void fraction being generated as mentioned in the previous section.

Consequently, the second difficulty can be partially alleviated by ensuring the greatest degree of control of the two phase flow loop. The desire to have the greatest degree of control resulted in the reconfiguration of the loop, which was mentioned in chapter 3 and is expanded upon in the appendices. The original design lacked control on the cooling side of the loop. The new design uses the heat exchangers to cool liquid as opposed to cooling vapour. Although, this may appear less efficient, the increased control more than compensates for the reduced flowrate capabilities. However, the question still remained, does the loop provide adequate control to permit experiments to be carried out with relative ease. Moreover, does the loop provide the capability to duplicate a given set of conditions from one day to the next.

To answer these questions, a two phase flow experiment was conducted at a constant void fraction. Since, it was also desirable to provide further verification of the loop instrumentation, a void was chosen that resulted in a significant number of bubbles flowing past the tube ends. Having met the second condition, the quality was calculated to

be 0.7%.

The procedure outlined previously was designed and implemented at this stage. Movement between points was found to be a simple exercise. As experience was gained the determination of the control settings to create given conditions also became a simple task. This initial experiment exposed the need to monitor loop conditions "on line", since slight variations in temperature or flowrate can greatly affect the quality of the flow.

Having achieved results showing that the loop operation is relatively simple during an experiment, the next point to be addressed was the repeatability of an experiment. The typical approach to such an experiment is to obtain a number of points covering the region of interest. After analyzing the results, additional test points are obtained in critical areas to give more complete information. Following this procedure, several more test point conditions were determined. Scaling the flowrates and heat input from the first experiment for the new test point, the loop achieved identical conditions to those of the previous day. Repeating the analysis dictated the need for two more test points. This time however, the scaling did not result in the immediate arrival at conditions comparable to the original experiment. However, patient adjustment of the controls finally resulted in the appropriate conditions.

The last two test points were taken at a slightly

increased quality. It is felt that this could have been avoided with a little more time, and a computer program that allowed the instantaneous determination of void fraction during the experiment. Ambient condition changes, such as a 3 degrees Celsius rise in cooling water inlet temperature, and a 4 degrees Celsius rise in room temperature, were noted during this last experiment, which is suspected as being the primary cause of the inconsistency. However, this last experiment also served to indicate that although attaining a specific set of conditions on a given day may require a greater amount of time in the establishment of the initial test point, alteration of conditions to obtain subsequent test points is again a simple task. Therefore, it can be safely stated that loop operation is acceptable and that the loop can now be used for experimental purposes.

6.4.2 Range Limitations

The preceding section describes a two phase flow loop with good behaviourial characteristics, but this does not address the scope of the loop's capabilities. The design of the loop was based upon physical modelling of the U-bend region of a CANDU steam generator, and the thermodynamic considerations necessary to generate these conditions. However, the design process concentrated on the ability to attain the specific conditions obtained from the modelling process, assuming that if these extreme conditions could be

met, more moderate conditions could be easily attained. This assumption, although it appears reasonable, is not strictly applicable.

The difficulty lies in the determination of velocity at which fluidelastic instability occurs. When calculating the velocity of the flow through the tube bundle, a trade-off becomes evident. With increased void fraction, a given mass flux results in a higher velocity, which tends to reduce the required mass flowrate to attain the same reduced velocity. However, past experiments by Pettigrew et al.(1985) show that for air-water experiments, the required mass flux to attain instability is significantly greater for voids up to 50%. The reason for this can be found by looking at Conner's equation:

$$V_r = K m_d^{.5}$$

The mass damping parameter 'm_d', as defined in equation 6.20, will increase as a result of the reduced density of the fluid at higher void fractions. Consequently, the velocity necessary to obtain the instability is also increased. Therefore, as the void fraction is increased, the velocity necessary to obtain instability increases. However, since the density decreases, the mass flux for a given velocity decreases. Therefore, these two effects have opposing actions upon the required mass flux as the void fraction is increased. The dominant effect will determine the change in mass flux

required to achieve instability for a change in void fraction. At lower void fractions the higher velocity requirement dominates, while the effects of lower density compensates for this effect at higher void fractions.

Although the loop was designed for the one specific set of conditions, the estimation of the instability velocity in the loop design was purposely overestimated. Moreover, the parallel triangular bundle configuration has been found to become unstable at a lower reduced velocity than other commonly used array formats (Weaver and Fitzpatrick (1987)). The combination of these facts indicates that there is still a possibility for the loop to be able to generate conditions for instability at 25-50% void fraction.

The 3.5% quality experiment discussed earlier showed a definite transition to instability. The mass flowrate levels were lower for this experiment than for the single phase experiment. This indicates that the conditions had already exceeded the maximum required mass flowrate conditions. Since the void fraction is potentially within the range of 50% void, the void at which the maximum mass flowrate is expected may be below 50%.

A second experiment at a lower homogeneous void fraction is shown in figure 6.13. The transition to instability is not clear due to the high amplitude levels, and more points are required to give detailed trends. At a pitch mass flux of approximately 550 $kg/m^2.s$ a change of slope occurs indicating

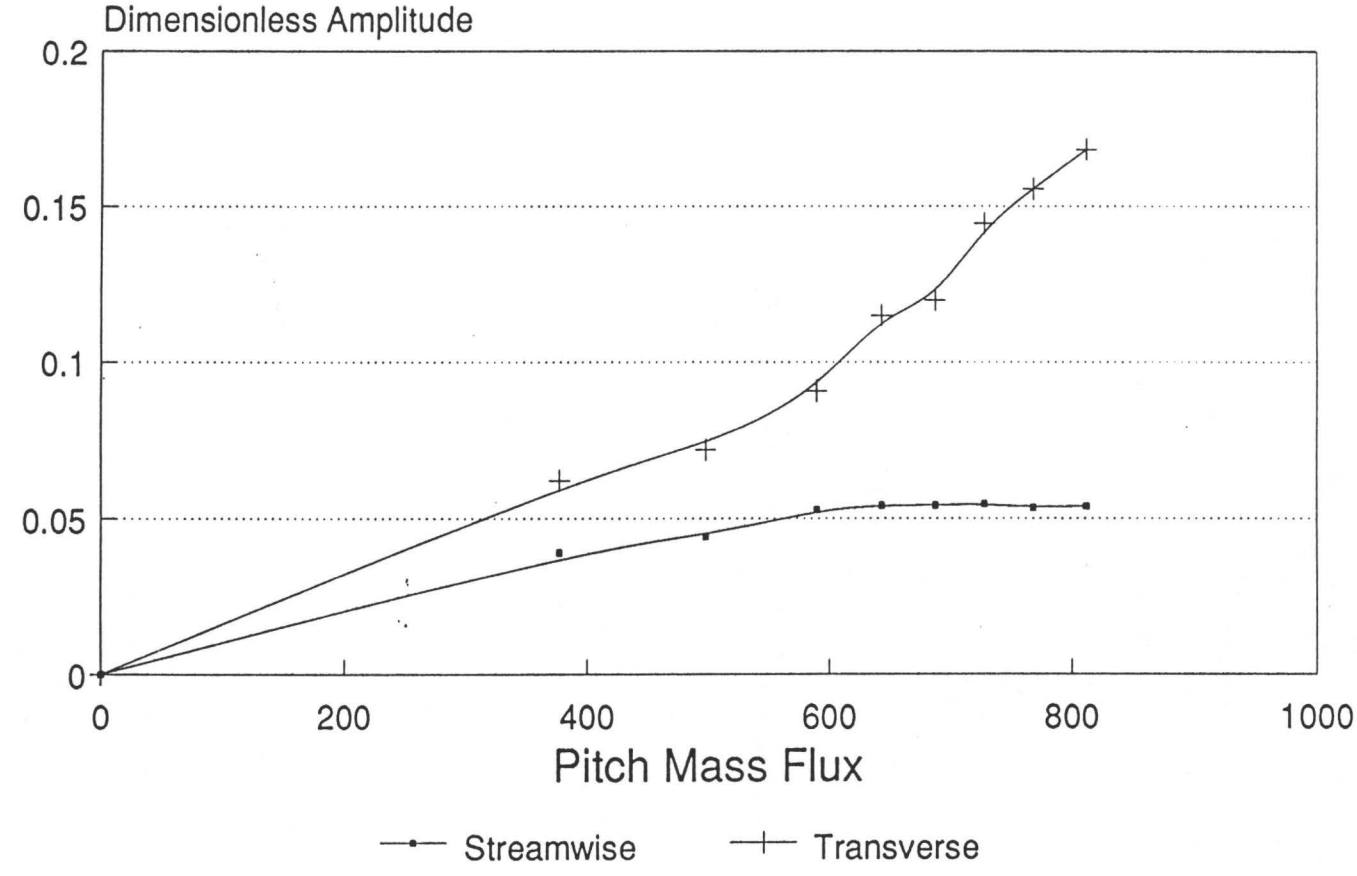

Freon 11 at 49 C

Figure 6.13
Amplitude Response at 0.7% Quality

the critical mass flux. The mass flowrates were higher than the single phase experiment for this case. Although this does not completely demonstrate that the loop can achieve instability flows for all void fractions, the loop could generate higher flows than that required for this experiment.

The power capabilities of the heater are presently 19.2 kW as opposed to the 48 KW the heater is designed to output. This reduces the void fraction capability of the loop. The mass flowrate is limited through the main subloop by the limits of the pump and the requirements of the cooling subloop. Experimental conditions are affected by these limitations, yet the design quality can be achieved at instability. This is possible since the required flowrate to achieve instability is lower than that purposely overestimated by Westermann (1987).

Moreover, the original design called for regulators to cause a pressure drop just prior to the heaters that would create saturation conditions. The higher pressure before the regulators would allow the input of heat before the regulators by the preheater to ensure saturation conditions. This is necessary only if the flowrate is approximately 2.25 kg/s, which according to Westermann's calculations would require 18.85 kW from the heater to achieve 85% void or a quality of 5.0%. Therefore, the heater would be near its capacity and saturated conditions would be required at the entrance.

To achieve these conditions and generate fluidelastic

instability, only 1.6 kg/s are actually needed, which requires only 13.4 kW from the heater. Since 19.2 kW is potentially available, the flow entering the heater can be subcooled. This makes it possible to lower the temperature before the heater, and allows the use of a lower pressure after the pump without fear of cavitation. Therefore, the regulator by-pass mentioned in chapter 3, is used to control the pressure drop across the regulators. The control of the overall pressure drop through the loop provides a means for generating the optimal loop operating conditions for a given flowrate and void fraction combination. Moreover, the additional energy available allows the desired quality to be generated at various pressures and temperatures, and with a variable degree of subcooling. To ascertain the true capability of the loop, a study is needed to explore all the possibilities.

In his thesis, Westermann (1987) discusses the possibility for flow instabilities. These are not as great a concern since the characteristics of a gear pump reduce the probability of this occurrence. Instabilities can also occur as a result of the transmission of vibrations from the pump to the remainder of the loop, resulting in an unstable flow condition. Here also, steps have been taken to reduce the possibility of this occurrence. However, heavy vibrations can result if the loop is pushed too quickly to achieve higher voids and future operators should be patient in generating the

desired conditions. This will ensure the continued smooth operation of the loop.

Although flows that are badly unstable are easily avoided, the sensitivity of the Differential Pressure Cells creates flowrate readings that have some degree of variability. Experiments have shown that flows below 1 kg/s possess a noticeably higher degree of variability if the control valves of the loop are not properly manipulated. Additionally, the temperature and void fraction conditions affect the variability of the higher flowrates. Where a flowrate of 3.3 kg/s is possible for 0 void at room temperature, only 2.3 kg/s is possible at 3.5% quality and 49 °C, when avoiding large variability. Although, higher flowrates can be achieved, the associated error with the flowrate grows as well, which is an undesirable situation.

6.4.3 Flow Observations

The present state of the art in two phase flow induced vibrations is in the early stages of development, as described in chapter 2. Consequently, there is interest in the flow pattern generated by the experimental apparatus. As noted previously, the windows on the test section are particularly well suited for this area of interest.

The two phase flow provides excellent flow visualization since the bubbles simulate a seeded flow, making flow patterns easily visible. During the experiments described in this

thesis, the flow was seen to develop some periodic phenomena. Moreover, observations through the end window indicate the existence of vortices immediately downstream of the tube bundle.

When passing through the test section, the fluid first sees two homogenizing bundles before interacting with the instrumented bundle. Supports used to hold the second homogenizing bundle in place act as flow splitters. It was assumed that the splitting of the flow would have little effect on the final response. The question can be posed as to whether or not the splitter plates cause the periodic horizontal shifting observed as the flow leaves the test section.

A liquid boundary layer on the splitter plates is visible for medium level void fractions. With the increase in void fraction and velocity, the higher turbulence level tends to reduce the thickness of this layer. However, it is during the relatively less turbulent conditions that the phenomenon is observed most frequently. Nonetheless, the effects of the plates cannot be directly linked by observation to cause the flow pattern. Moreover, the instrumented tube bundle itself seems to have a significant effect on the flow.

During the same conditions noted above, bubbles flow into sight while passing between the homogenizing bundles. At this time the bubbles follow essentially straight trajectories. Similarly, the bubbles flowing in the small space between the

second homogenizing bundle and the instrumented bundle also appear to be following a straight trajectory. However, upon emergence from the instrumented bundle, the flow is extremely turbulent. This observation indicates that the effect of the vibrating bundle is significant on the flow pattern. It is possible, then, that the cantilever orientation of the bundle can cause uneven flow effects as a result of the uneven magnitude of tube motion across the section. A diagram of these flow observations is provided in figure 6.14.

Furthermore, the splitter plates do separate the flow prior to the first homogenizing bundle. If the void is significantly different across the test section when the flow enters, the flow will have little chance of being distributed evenly when encountering the vibrating tube bundle. Power and temperature monitoring have lead to the conclusion that not all the heater elements are performing equally. Surface temperature measurements indicate a slight temperature gradient of 0.2 °C across the test section for low void flows. Therefore, the assumption of an equally distributed force seen by the vibrating tube is questioned.

Although the flow can become extremely turbulent, vortices form on either side of the test section immediately after the last half tubes for all two phase flows. From the large side windows, an area of liquid can be seen along the entire length of the top half tubes. From the perspective of the end window, (see figure 6.15) this liquid layer can be

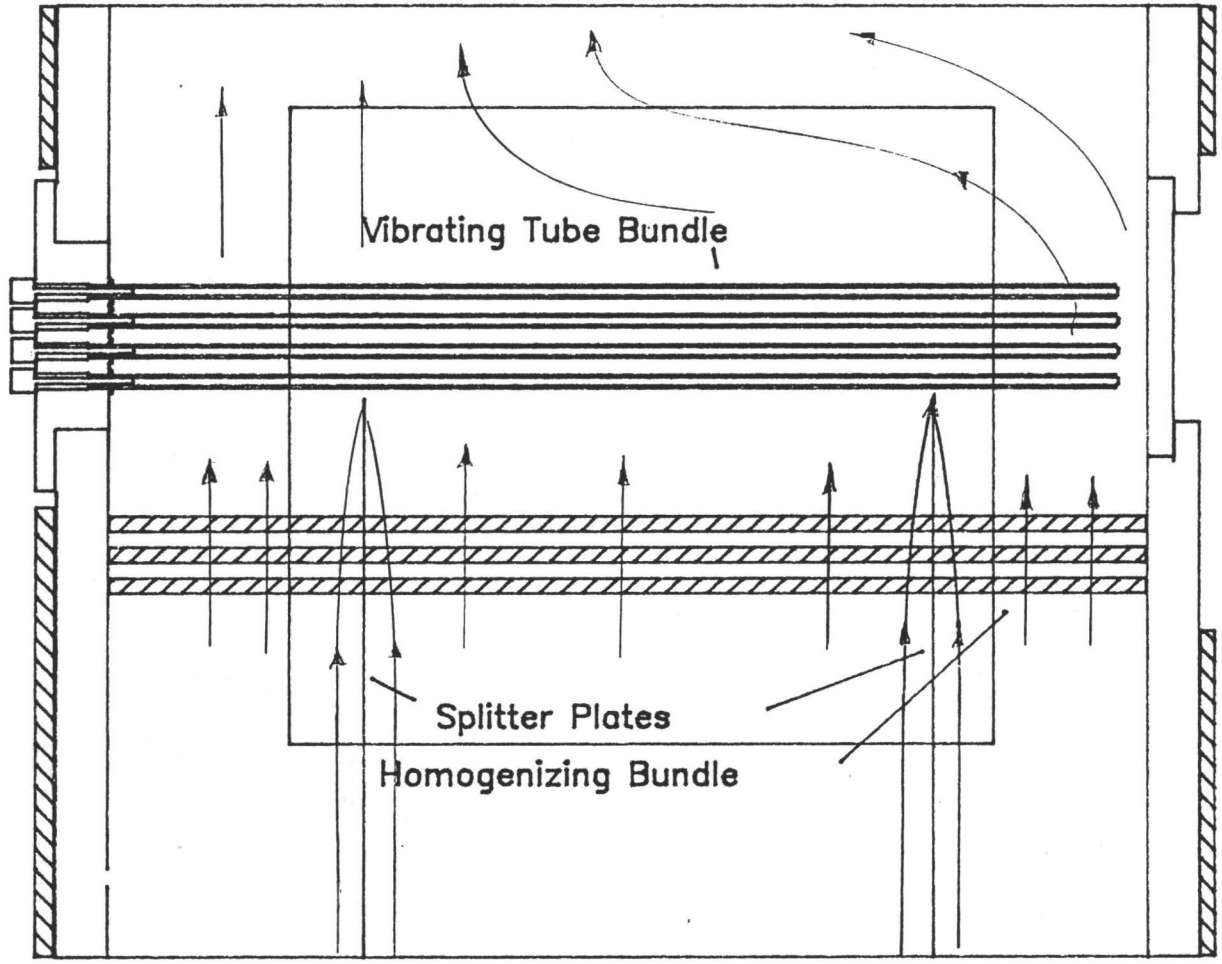

Figure 6.14
Diagram of Flow Pattern
as Seen from Large Windows

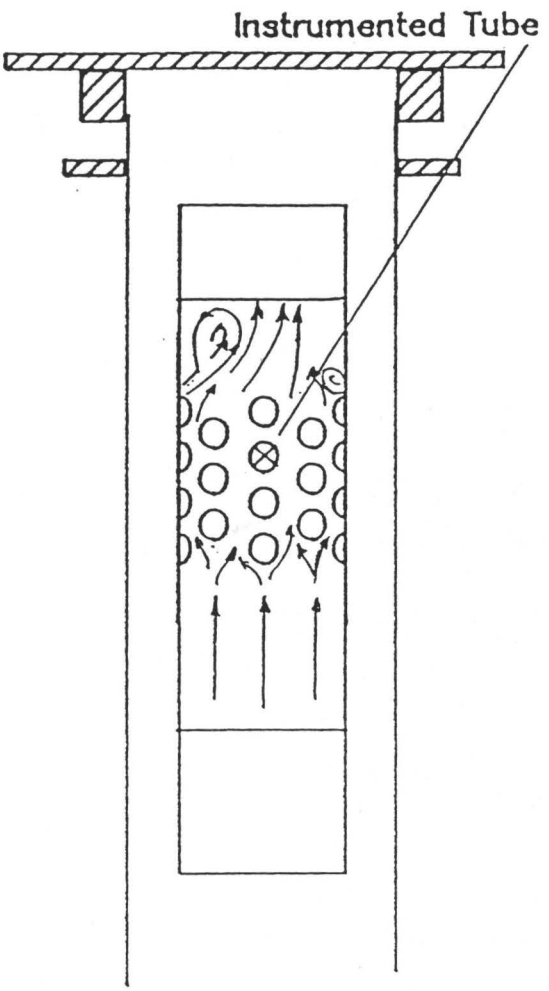

Figure 6.15
Diagram of Vortices After Tube Bundle
as Seen from End Window

seen as a vortex. The effect of this flow pattern is expected to be insignificant unless the vortices grow to influence the main flow. However, the observance of the pattern shows the interesting effects that can be seen with this test section.

The third observation of interest relates back to the influence of the vibrating tube bundle on the flow. The effect, however, deals with the addition of heat by the bundle. Low quality flows can be attained at temperatures close to room temperature, which does not translate into higher temperatures in the loop components. Alternatively, operating the loop at conditions where the temperature approaches 50 °C results in significant temperature increases in loop components. Particularly, the instrumented bundle, being composed of brass, acts as a path for the heat to escape to the outside.

As a result of the high conductivity of the brass, the bundle achieves temperatures near that of the fluid. When the fluid is nolonger heated directly by the main heater, the two phase flow disappears under most conditions. However, if the bundle is still hot, significant two phase flow is still generated as the fluid passes through the test section. During an experiment where steady state has been achieved, this should not pose a problem. The difficulty lies in the movement between points, where the test section temperature is used to monitor the condition changes in the loop. The hot tubes will tend to create the illusion of a constant temperature, even

though the loop temperature has dropped slightly. Therefore, when operating at high temperatures, extra time is required to ascertain that steady state has been reached for certain.

6.4.3 Loop Characteristics Summary

The experiments conducted to date have demonstrated that the loop is easily controlled and repeatability of flow conditions is good. The range of possible conditions relative to the flows necessary for fluidelastic instability has not been affected by the design changes described in chapter 3. This is possible since the original design purposely overestimated the flows required to achieve instability.

Several flow patterns were observed. The formation of vortices after the instrumented tube bundle and an apparent periodic flow pattern indicate interesting effects to be studied. These observations indicate that the intended purpose of the loop, to better understand the effects of two phase flow in cross flow induced vibrations, has been realized.

Chapter 7

Summary

Understanding of the phenomena involved in two phase flow induced vibrations is still in its preliminary stages. Although work in single phase flow induced vibrations provides an excellent background, researchers still have some questions about the modelling of the problem. The nature of two phase flow makes the vibrations problem much more difficult to model. Presently, there is some concern over the validity of air-water experiments where phase state changes cannot occur. Previous comparisons do indicate that this method of simulating two phase flow is conservative in its approximation.

Additionally, there is some concern of the different observations made by individual researchers. It would seem useful to study the two phase flow more closely to look for answers. Consequently, a project was undertaken at McMaster University to construct a two phase facility that uses a single component two phase flow and has a test section which provides the means of observing the flow as it passes through the section.

Loop construction involved many iterations on the original design. The final configuration provides simple control, and capabilities to repeat experiments within

reasonable error. Qualities in the range of 0.0 to 5.0% have been achieved and instability has also been present for select cases in this range. The corresponding level of void fraction is yet to be determined as significant slip between the phases is suspected to exist. Future work is required to address this concern.

As expected, early observations have shown that the two phase flow is extremely turbulent. Moreover, obvious periodic phenomena have been seen, although they are not present at all times. These notations serve to point to further work in determining the effects of the two phase flow characteristics on the tube response levels.

The second aspect of this thesis dealt with the redesign of the test section for strength and sealing purposes. The resulting design has addressed both concerns. Finite element analysis gives a factor of safety of approximately 20 for the maximum operating pressure of the test section. In addition, testing and further use have shown no signs of leakage or failure.

The third objective of the project resulted in the development of new instrumentation for measuring the magnitude and frequency of tube vibrations. The new approach uses light from a flash light, which is carried by an optic fibre to the end of the tube. The emerging light impinges on an array of light sensitive devices, which are used to monitor the position of the light. Results using a battery operated

circuit are very good. The output signal has a higher signal to noise ratio than strain gauges, and provides a higher sensitivity without the use of amplifiers. In addition, the instrumentation allows for the monitoring of several tubes without the duplication of circuitry. The one precaution still being observed is the constant calibration of the system, although this is a relatively simple task.

Having successfully built and tested the facility, the final step was to study its operating characteristics. These results were intended to demonstrate that for extreme flow conditions the loop provided comparable results to those obtained by other researchers. The single phase results are favourable and indicate classical tube responses with the exception of the discontinuous jump in the dominant tube frequency as instability is approached. It is expected that this phenomenon results from the instrumented tube being detuned in relation to the rest of the bundle. Correcting this situation will eliminate the problem.

The two phase results show a slightly higher response level conditions prior to instability in comparison to single phase, which has been seen in a previous study as well. Nevertheless, the onset of fluidelastic instability occurs at a mass flux, which is acceptable. A stated difficulty with presenting and analyzing two phase results is the uncertainty associated with determination of the void fraction. Consequently, it is suggested that slip be recorded to

facilitate better analysis of results.

In conclusion, it can be stated that the result of the work presented here is a working two phase flow facility. Moreover, the new instrumentation provides a new means of monitoring vibrations effectively. This in conjunction with the redesigned test section, provides the capability of gaining much insight into the problem of two phase flow induced vibrations in tube bundles.

Chapter 8

Recommendations

The description of the work of the author has been presented in the best light possible, while maintaining objectivity, as expected. However, there are several points to made concerning the safe operation of the loop. Moreover, there are many experiments to be conducted in light of the information given in the previous chapters.

8.1 Safety

It is suggested that future operators of the loop spend time learning to operate the loop at lower void fractions. This area of concern is further addressed in the accompanying operating manual. Additionally, some procedures should be incorporated into the maintenance of the loop for the sake of safety. Whenever a pressure vessel is constructed, it is important that the proper measures be taken to ensure that all safety features are periodically inspected to ensure proper operation. Such features include the various circuits used to cut heater power for given situations, and the pressure relief valves found in the pump and near the ceiling.

Moreover, the design of the test section involved a great deal of effort and time. The design appears to be more than adequate for the intended purpose. However, there may be

concern over the deterioration of the glass over time. Therefore, after a couple of years have past, the test section should be pressure tested again in order to ensure the its integrity. Also, since glass is a brittle material, any scratches that may cause concern should also result in pressure testing.

The final area of concern lies in the maintenance of good seals at mating surfaces of the loop components. Again, a great deal of time and effort went into ensuring a good seal throughout the loop. However, Freon 11 does affect most materials to some degree. Over time, the sealing materials may show signs of deteriation. This problem is difficult to predetermine for long periods of time. As with the test section, the problem is only pertinent in the long run.

8.2 Experiments

Prior to conducting experiments to look at the other phenomenon mentioned in the results chapter, the preliminary experiments must be repeated after tuning the instrumented bundle. Both the two phase and the single phase experiments must be repeated since the effects of the detuned tube are unknown in two phase. It is recommended that the tubes be modified to allow the tubes to be more easily tuned to a selected frequency. This would allow the effects of detuned tubes to be studied in a dense liquid in future studies.

Once the preliminary experiments have been completed, the

void fraction problem must be addressed. The void fraction should be determined by the use of the gamma densitometer. After satisfactory results have been obtained, an appropriate slip model could be used to simplify the experimental process.

Once benchmark results have been firmly established, and the actual loop capabilities confirmed, then the task of studying two phase flow induced vibrations can begin. The observations noted in the results chapter will provide indications as to where to look in gaining better understanding of this problem.

Appendix I

Error Calculation for Mean Path Deviation of Light for Light Instrumentation

This is the calculation performed to estimate the error associated with the light varying in angle of contact between the light beam and the end window as a result of tube movement. Castigliano's energy method is used to:

1) Calulate the necessary force to create the maximum possible tube deflection.
2) Use the information from 1 to calculate the slope of the tube at its end.

The following assumptions are made:

1) Ignore the effects of direct shear.
2) Ignore the mass of the tube.
3) Ignore mass of materials found inside and at the end of the tube.
4) Assume acting force is uniformly distributed along the tube.

Since the form of the deflection is the main concern for the calculation, then these assumptions will all be acceptable.

$$U=\int_0^L (M^2/(2*E*I))dx \qquad (A.1)$$

Note: 1) The integration is performed from the tube free end toward the tube fixed end. This eliminates the support force and moment from the calculation.

2) The results will be negative for upward displacements. See figure A.1 for the force system used in the calculation.

$$M=w*x^2/2+Q*x \qquad (A.2)$$

$$U=\int_0^L ((w*x^2/2+Q*x)^2/(2*E*I))dx \qquad (A.3)$$

$$=\int_0^L ((w^2*x^4/4-Q*w*x^3+Q^2*x^2)/(2*E*I))dx$$

$$=(w^2*x^5/20-Q*w*x^4/4+Q^2*x^3/3)/(2*E*I)\Big|_0^L$$

$$=(w^2*L^5/20-Q*w*L^4/4+Q^2*L^3/3)/(2*E*I)$$

$$y=\delta U/\delta Q=(-w*L^4/4+Q*L^3*2/3)/(2*E*I) \qquad (A.4)$$

$$=(-w*L^4)/(8*E*I)+Q*L^3/(3*E*I)$$

But Q=0 Therefore:

$$y=-w*L^4/(8*E*I) \qquad (A.5)$$

From this result, we are able to calculate the value of the distributed force constant w.

To determine the slope of the end of the tube, the following calculation is performed.

$$M=w*x^2/2-P \qquad (A.6)$$

Substitute M into equation (A.1)

$$U=\int_0^L ((w^2*x^4/4-w*x^2*P+P^2)/(2*E*I))dx \qquad (A.7)$$

$$=((w^2*x^5/20-w*x^3*P/3+P^2*x)/(2*E*I)\Big|_0^L$$

$$=((w^2*L^5/20-w*L^3*P/3+P^2*L)/(2*E*I)$$

$$\Theta=\delta U/\delta P=(-w*L^3/3+2*P*L)/(2*E*I)$$

But P=0 Therefore:

$$\Theta=-w*L^3/(6*E*I)$$

Substitution:

E=106 GPa for Brass

$I=\pi/64*(d_o^4-d_i^4)$

$d_o=0.00635$ m
$d_i=0.00385$ m

$I=6.90266*10^{-11}$ m^4

L=0.304 m

Therefore: $y=-w*L^4/(8*E*I)=-w*1.4591*10^{-4}$

The maximum deflection is expected to be less than .070 inches, therefore a value for w at this deflection value will provide conservative results.

Let y= -.070 inches = -0.001778 m

This gives the result w=12.18 N/m

For Θ then:

$$\theta = -12*(0.304)^3/(6*E*I) = -.007798 \text{ rad.}$$

Next, the error in the light spot position as seen by the probe is proportional to the distance between the probe and the end of the tube, as seen in figure I.1.

Therefore:

$$\epsilon_{abs} = \theta * \delta L \qquad \text{where } \delta L = 0.5 \text{ inches} = .0127 \text{ m}$$

$$= 9.9038*10^{-5} \text{ m}$$

$$\epsilon_{rel} = 9.9038*10^{-5}/1.778*10^{-3}*100 = 5.6\%$$

This result shows that the error is small. Moreover, it can be argued that this result is conservative. Considering figure I.3, the relative indices of refraction, as the light passes through the two intermediary interfaces, cause the light to follow a line with a mean slope lower than that calculated above. If, the remaining assumptions are reasonable, as it is suggested they are, then this result will be conservative in nature.

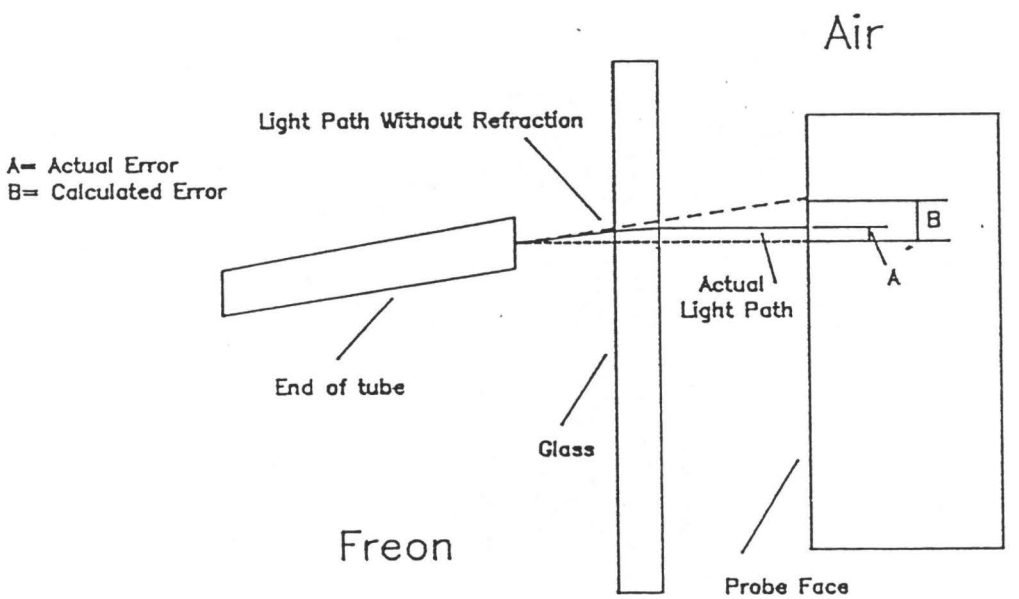

Figure I.1
Light Path Diagram

Appendix II

Proof for the Use of Two Wattmeters to Measure the Total Three Phase Power in a Delta Connected Load.

Based on figure II.1, the following proof is presented for the use of two wattmeters to measure the total three phase power in a delta connected load.

$$\text{Power= } P = v_{12}i_{12}+v_{23}i_{23}+v_{31}i_{31}$$

$$= v_{12}i_{12}+v_{23}i_{23}-i_{31}(v_{12}+v_{23})$$

since

$$v_{31}=-v_{13}=-(v_{12}+v_{23})$$

Thus

$$P=v_{12}(i_{12}-i_{31})+v_{23}(i_{23}-i_{31})$$

$$=v_{12}i_1+v_{23}i_3$$

$$=\text{reading on } W_1 + \text{ reading on } W_2$$

Note: v_{xy}, i_k, and i_{lm} are instantaneous, which makes the result true since the wattmeters give the average value of the instantaneous power.

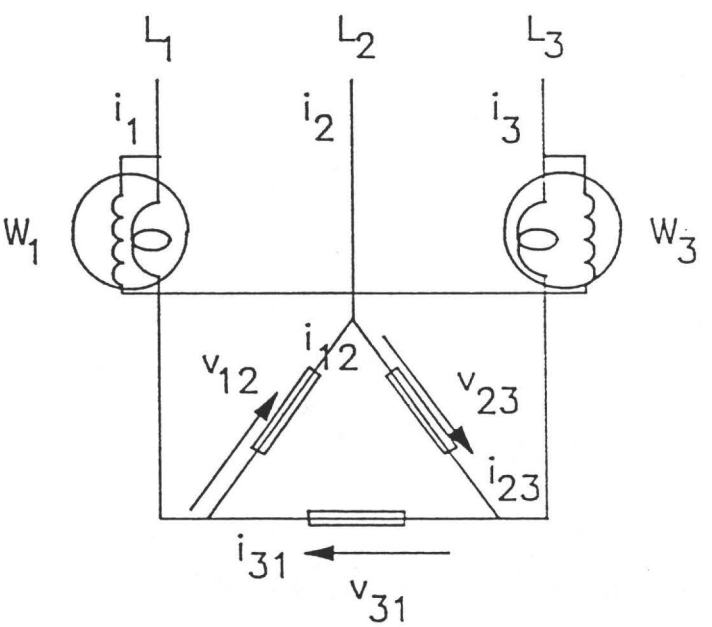

Figure II.1
Schematic of Three Phase Measurement Circuit
(Gregory 1981)

Appendix III

Two Phase Flow Loop Operating Manual

by
R.F. Dam

OPERATING MANUAL

FOR

THE TWO PHASE

FLOW LOOP

IN JHE-206

Index

Figures

Operating Instructions for Two Phase Flow Loop
Constructed for the Purpose of Simulating Flow Induced Vibrations In Steam Generators

The first part of this manual describes the instrumentation, control mechanisms, and procedures pertinent to the operation of the two phase flow loop located in JHE 206, including a description of the fundamental basis of the loop operation. The latter is provided both to correct the description in the thesis by G. Westermann, and to provide the understanding needed to follow the motivation behind the procedures described in the second part of this manual. The description will be accomplished by a discussion of the various loop components, their intended use, and the way in which they are used at present.

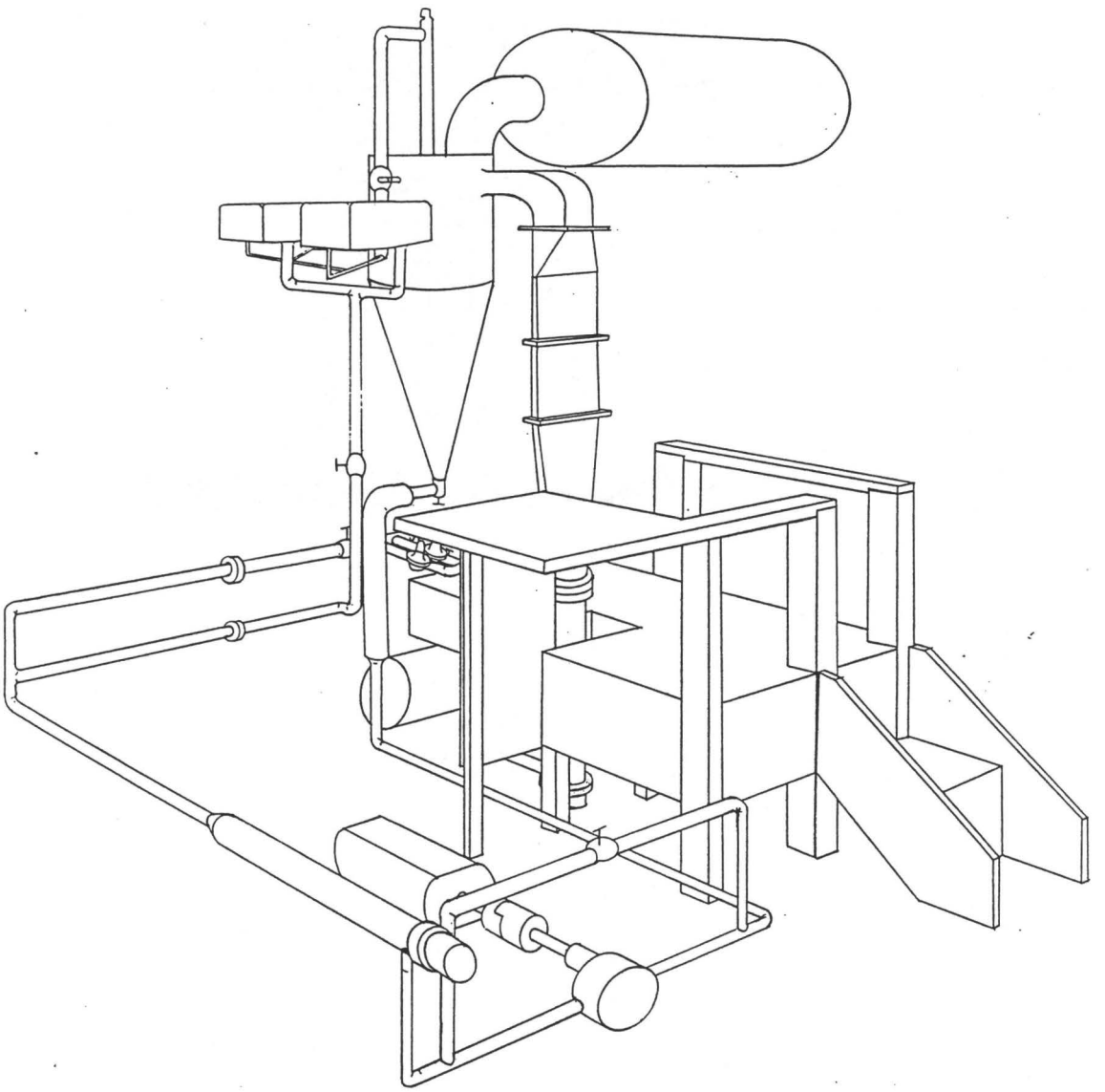

Fig 1

Complete Two Phase Flow Loop Diagram

The Loop

The loop, as depicted in Figure 1, consists of two parallel flow subloops, which are both supplied by a 2 HP gear pump. In addition, there are also two more subloops referred to as the service loop and the water line. The former is used in charging and discharging the Freon 11 from the main loop; the latter provides the cooling water for the condensers. The first two subloops interact to provide the necessary conditions to generate and regulate the two phase flow.

Main Flow Subloop

The first of the two parallel loops is the main flow loop. The fluid that is to pass through the test section flows in this portion of the loop. The path consists of eight components, some of which are common with the second flow loop. In the discussion of the components which follows, location refers to the numbering scheme shown in Fig. 2 .

1. Pump (Location 1) The driving force for the entire loop's flow, the Worthington Gear Pump is powered by a variable speed, 2 HP 3 phase induction motor.
2. Preheater (Location 2) It is now known that there is no necessity for the preheater. The original design with the pressure regulators would have made it useful had that design been practical. However, as described in a subsequent section, this is not the case.
3. Orifice Plate (Location 3) This is the larger of the two orifice plates which is situated in the part of the loop where the larger flowrate is encountered. A differential pressure cell, which monitors the pressure drop across the plate, is calibrated to indicate the flowrate. The output read on channel 1 corresponds to one inch of mercury per unit on the readout. The actual conversions to be used will be provided later. (see DP Cell Readout)
4. Control Valve (Location 4) This is a globe valve situated such that the entire flow is affected. This valve has

become redundant to loop operation since the loop was originally constructed. However, it does have value for component isolation if repairs are necessary.

5. Pressure Regulators and By-pass Valve (Location 5) Initially, the regulators were intended to provide a constant inlet pressure to the heater. However, the basic operation of the regulators requires a constant back pressure in order to provide constant pressure to the heater inlet. Investigation into the operation of these devices showed that the regulators simply provide a frictional pressure drop directly proportional to the square of the flowrate. The inadequacy of the regulators does not obviate their use use since it is possible that they could provide some flow conditioning. However, this is highly unlikely since signs of cavitation were noted as the fluid temperature approached the design conditions when the regulators were in use.

The net effect of the regulators was to reduce the attainable flowrate at design temperatures and pressures. Therefore, the loop was modified by installing a by-pass around the regulators with a valve to control the relative flowrate distribution between the regulators and the by-pass line. Moreover, the diameter of the line leading to the inlet side of the pump was enlarged to promote a higher potential

flowrate. These efforts were successful in promoting the generation of reasonable flowrates. The limits of the flowrate are temperature and pressure dependent, as will be discussed later.

As a result, the by-pass valve has become a major control mechanism for the loop.

6. Main Heater (Location 6) The fluid flows through the main heater that is designed to provide 48 KW of heat input over its length. Since the equipment required to control all of this power was not available, the heater was rewired to provide 19.2 KW, which is the maximum power output that can be obtained if a balance between the phases is maintained and the number of elements within each phase is equal. (See wiring diagram in Appendix F.)

This level of heat input still allows the generation of two phase flow, and through the use of a variable transformer, it is possible to vary heat input for other conditions as required. The original heating capacity was intended to match the heat removal capability of the loop, including heat loss to the room. However, experience has shown that the natural convection component of the heat loss was grossly over estimated. At present, the capacity of the cooling units about equals the capacity of the main heater as it is currently configured. Consequently, any increase

in heat input desired for future stages of the project will also require additional cooling capacity to be installed.

7. Separation Tank (Combination Tank) (Location 7) The separation tank was originally intended to promote the separation of the liquid from the vapor phase in order that the vapor might flow through the condensers. However, as a result of the unsteadiness of the vapor flowrate, the energy in the vapor phase could not be removed continually in this way and as a consequence, control of the loop conditions was erratic. The principle of loop operation is to maintain a constant pressure in the expansion and separation tanks while the heat input is increased, resulting in the generation of two phase flow. It was intended that the vapor be removed from the tanks directly, but since this method proved unreliable, the loop was modified to remove energy from the liquid phase instead. Consequently, cold liquid is introduced into the separation tank to combine with the main fluid flow. The result is that some vapor is removed by the cooled liquid spray, some is condensed before it leaves the fluid and some is condensed by contact with the cooled liquid mixture. In this manner, the vapor is removed indirectly.

Since the separation tank now promotes the

combination of the two fluids, it is proposed that the separation tank be renamed the combination tank. For the remainder of this paper, this will be the identification for the tank at location 7.

8. Angle Valve (Location 8) This valve restricts the flow between the combination tank and the pump. It originally allowed the operator to restrict the liquid flow which tended to increase the vapor pressure in the tanks. It was thought that this would control the liquid level in the condensate line and help develop the vapor flow through the condensers. The modifications described previously have rendered this valve redundant as a control mechanism. However, it still has value as a shut off valve for isolating portions of the loop from one another.

MAIN FLOW SUBLOOP

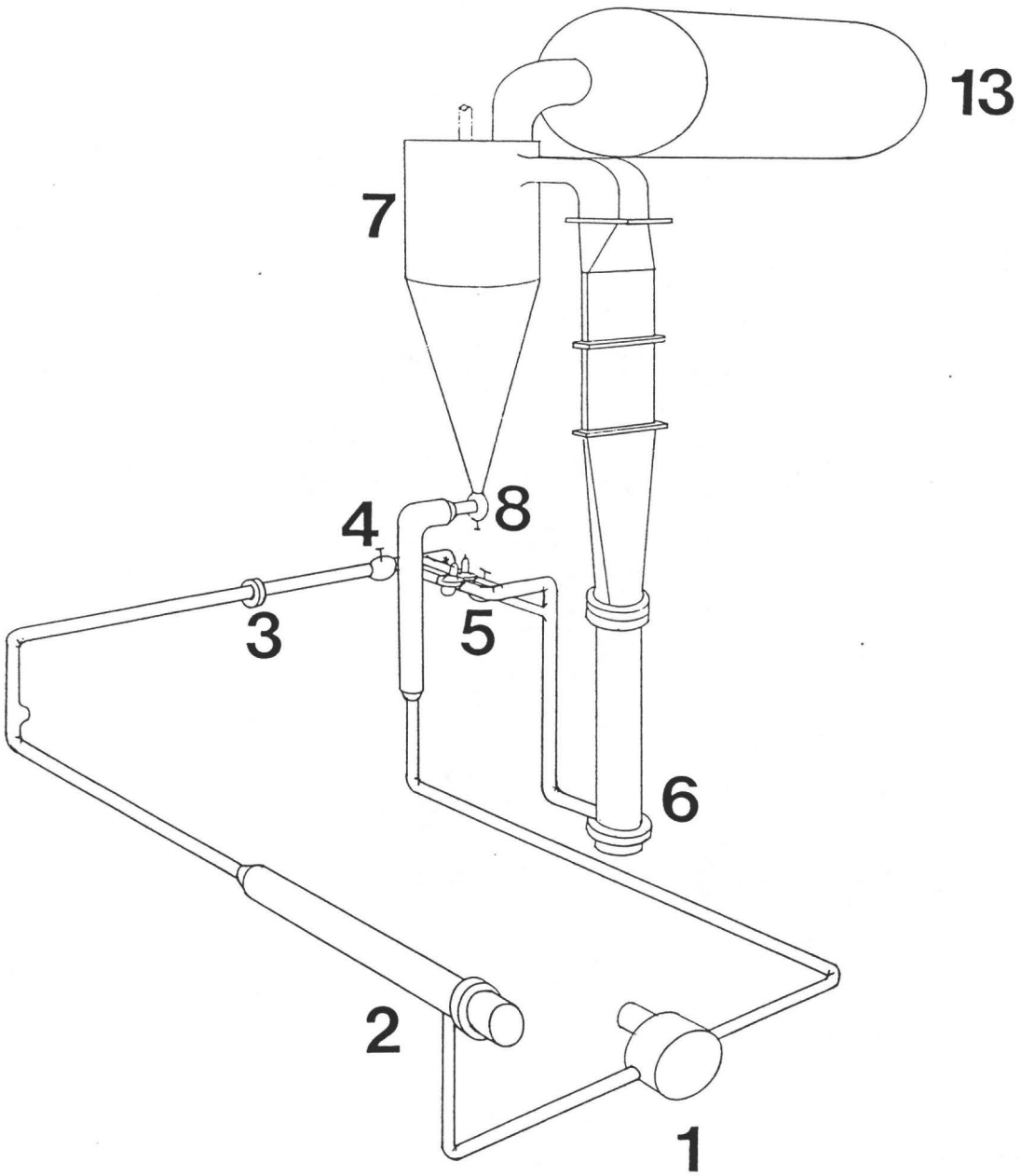

Heat Removal Subloop

The heat removal subloop takes a portion of the fluid flowing in the main loop and passes it through heat exchangers to remove the excess energy from the system. This loop is comprised of eight components, many of which are included in the main subloop and will be listed for completeness. In the discussion of the components which follows, location refers to the numbering scheme shown in Fig. 3 .

1. Pump (Location 1) -as above-
2. Preheater (Location 2) -as above-
3. Orifice Plate (Location 9) This orifice plate is mounted in the 1 inch copper pipe, and as before, a DP cell is used to measure pressure variations. The output read on channel 2 corresponds to one half inch mercury per unit on the readout. The actual conversions will be provided later.
4. Control Valve (Location 10) This is a gate valve used to control the flowrate through the heat removal subloop. This valve acts against or in conjunction with the by-pass control valve at location 4. It is a simple task to balance the resistance between the two loops to attain the relative flow rates that are desired.
5. Condensers (Location 11) The condensers were originally intended to condense vapor, but the modifications have them now operating to cool liquid. Hereinafter, the condensers will be referred to as coolers. The

consequence of this change is that the Freon 11 flowrate required to remove the heat is increased considerably as a result of the less efficient process of removing heat from liquid. The liquid flowrate was calculated to be approximately 4.2 USGPM. However, the loop operation required a flowrate of approximately 10 USGPM at maximum conditions. This discrepancy is most likely do to the approximate flow of the calculations and the inefficiencies observed within the heat exchangers. Fortunately, the modifications made also improved the potential flowrate capability. Therefore the loop can still achieve the design conditions. Additionally, this flowrate is well within the design specifications of the two heat exchangers.

6. Pressure Relief Valve (Location 12) As required, a pressure relief valve is located at the highest point in the entire system. This valve is set to open at 30 psig, which is approximately 1.5 times the operating pressure of the loop. This is also the pressure for which the tanks have been tested.
7. Combination Tank (Location 7) -as above-
8. Angle Valve (Location 8) -as above-

Other Subloop Components and Controls

Expansion Tank (Location 13) This is the one component that both subloops use, which does not appear to directly affect the flow. The existence of the expansion tank accounts for the possibility of sudden vaporization of a large quantity of liquid. The resulting expansion in fluid volume would generate extreme pressures if there were not space for the vapor to expand into. The expansion tank provides the necessary volume to reduce the effects of such occurrences.

Shut Off Valves- Throughout the loop, several shut off valves are located. These are usually ball valves with the intended purpose of isolating one portion of the loop from another. There is the capability of removing many portions of the loop without discharging the loop entirely and without excessive loss of Freon 11. Moreover, many of the valves serve to isolate the service loop and/or to improve the functioning of the discharging process. The use of these valves and the methods employed in charging or discharging the loop will be discussed in a subsequent section.

HEAT REMOVAL SUBLOOP

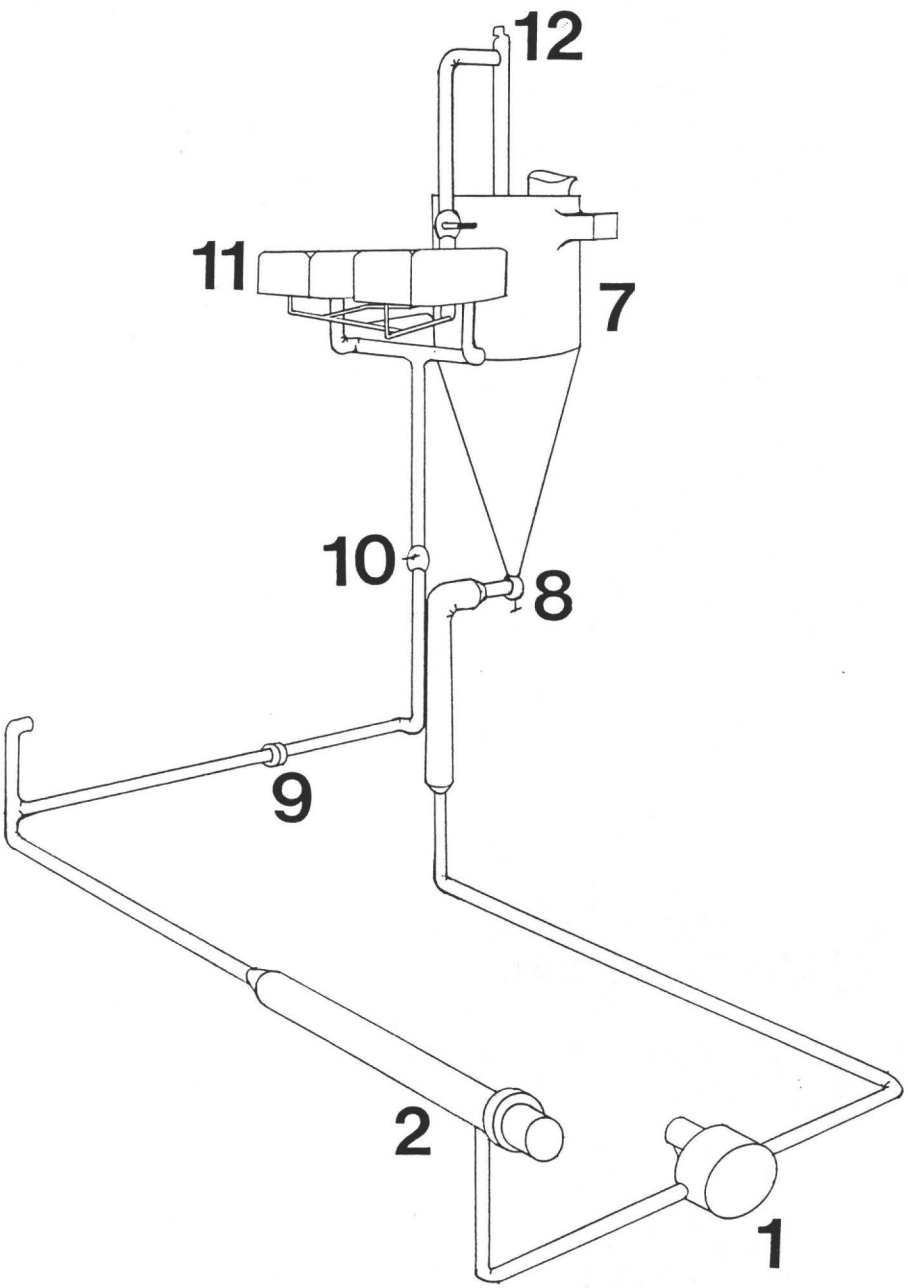

Water Line

The water for the coolers is supplied from the city water line. There are four components of interest for the purposes of flow control. Moreover, three more components are of interest for loop maintenance and water temperature control. The following discussion is of the four main components as depicted in Fig. 4.

1. Water Supply Shut Off Valve (Location 14) This valve is used to either open the water line or close it. The normal position is open, and it is usually left in this position unless the coolers must be drained for some reason. Furthermore, should it be desirable to create a condition in the condensers where the water side is only partially full, the shut off valve can used as a control valve. In conjunction with this, the usual water line control valve (see component 4) must be left fully open.
2. Coolers (Location 11) -see above-
3. Orifice Plate (Location 15) The pressure drop measured across the orifice plate can be used to determine the water flowrate through the use of the graph in Appendix A. However, the required water flowrate generates a pressure drop that exceeds the capacity of the mercury manometers presently installed and consequently they have been disconnected. Although they can be reconnected at any time, the restricted range would not allow the attainment of enough cooling for the higher

energy input operation of the loop.

4. Water Line Control Valve (Location 16) This valve, which is easily reached from the floor level, is used to control the water flowrate during normal operation.

The three remaining components are as follows:

1. Cooling Valve (Located outside of JHE-206 in JHE-207) The purpose of this valve is to bypass JHE-206 by allowing water to flow directly from the source to the drain. During the summer months, the water temperature can reach unacceptably high temperatures when not flowing in the pipelines. If this valve is opened for an hour or two, the temperature can be brought down to a lower, essentially more constant temperature.
2. Drain (Location 17) The water from the water line is allowed to flow into a drain in the floor. The water then passes into an open channel found on the floor of JHE-106. By the west wall of room 106, the water flows into a drain. This drain tends to accumulate dirt, and if high flowrates are to be used, the drain should be checked to avoid flooding of the first floor.
3. Discharge Valve (Location 18) This valve is intended to drain any remaining water found in the water line upstream of the condensers if repair is required. The piping has been installed in such a way as to make the location of this valve the lowest point in the water line, upstream of the coolers.

WATER LINE

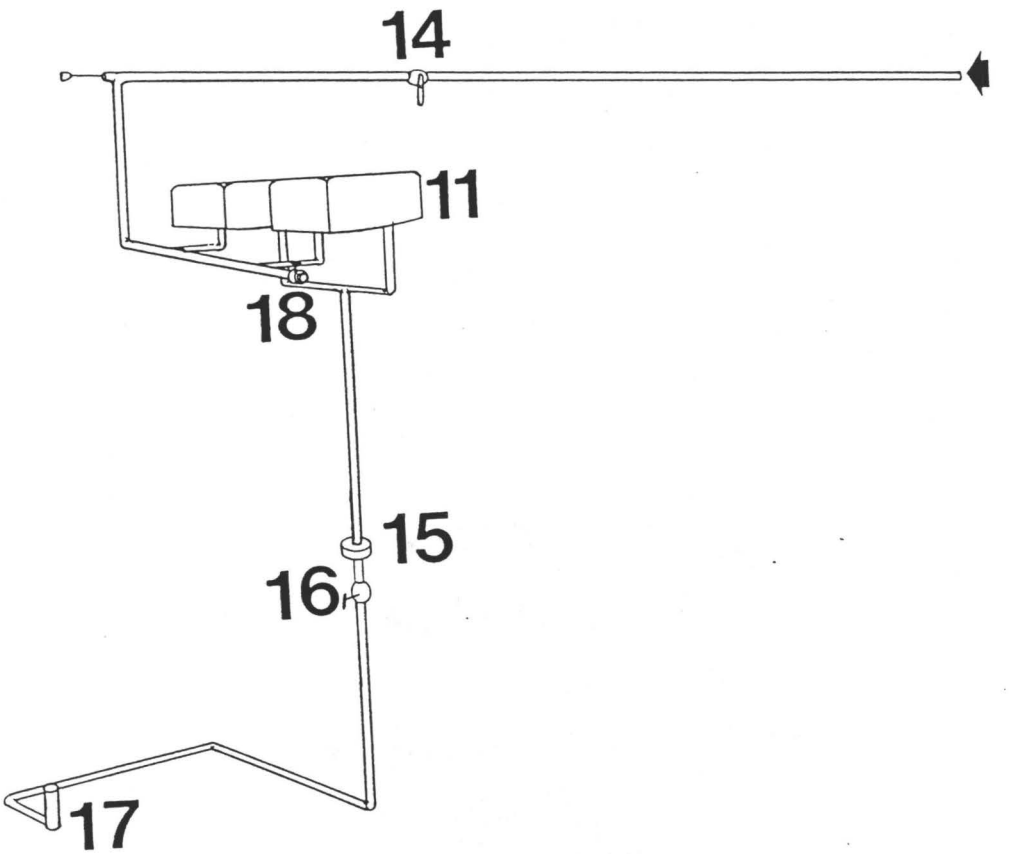

Service Loop

The service loop has the dual purpose of charging and discharging the Freon 11 from the flow loop. There are eight components used in either the charging or discharging operations. The following discussion will address both the nature of the components and the way in which they should be used. Reading the component descriptions should also provide the necessary information for performing the desired operations. The following is a discussion of the components as depicted in Fig. 5.

1. Holding Tank (Location 19) This tank, found at the back of the loop, is capable of holding 150 litres of Freon 11 which is needed for loop operation. The loop should be discharged into the tank if it is not to be used for a long period of time, as recommended by G. Westermann.

   When the loop is being discharged, the small valve on the tank should be opened to allow the air to escape. Moreover, this action reduces the pressure built up in the tank, which allows both a shorter discharging time, and as a consequence, a greater percentage of the fluid can be removed. The fluid is discharged using gravity as the driving force. Consequently, there is always some Freon 11 left in the lower regions of the loop. These regions can be easily isolated using various valves as described in the previous sections.

   Charging the loop also requires that the holding

tank valve be open. However, the valve should not be opened until the pressure in the tank has been reduced to the room pressure. The stored liquid will build up pressure as time passes, which can be used to help the pump generate a greater head during the charging process. Once at room pressure, the prevention of a vacuum in the tank is desirable. Therefore, the valve should be opened to maintain a constant pressure. The pressure in the tank can be determined by periodically opening the valve to see if the air is sucked in or the Freon 11 is blown out, corresponding to pressures below and above the room pressure.

The introduction of new Freon 11 to the system is accomplished by passing the liquid through the threaded metal plug found at the top of the tank. Once the operation has been completed, the plug must be adequately sealed to prevent loss of fluid during storage periods. The transfer of the new fluid can be accomplished by attaching the appropriate neoprene hoses to the drums in which the Freon is delivered. These hoses work well only for short exposure and they should not be left in contact with Freon 11 for long periods.

The drums can be emptied by using gravity to drain them from the deck built around the loop. To place the drums on the deck requires the removal of the stairs

and the use of the fork lift found in the Mechanical Engineering Department.

2. Tank Isolation Valve (Location 20) This valve allows the holding tank to be isolated from the remainder of the service loop. This valve must be fully open for both the charging and discharging procedures. Moreover, the valve should be closed at all other times.
3. Charging Line Bypass Valve (Location 21) The position of this valve determines the operation that will be performed. In the closed position (normally closed with handle vertical) the fluid can pass from the holding tank to the pump, and from there to the main loop. In the open position (handle in the horizontal position) the liquid in the loop has a direct path into the holding tank. Operation of the pump in this case will merely slow down the rate of discharge.
4. Lower Loop Service Valves (Location 22) Below and on either side of the main pump, two valves are located that isolate the service loop from the main loop. These valves are normally closed, but are opened for either mode of service loop operation.
5. Service Loop Pump (Location 23) A gear pump is used to send the fluid into the main loop. The activation of the pump requires that the motor that drives the pump be plugged in, since there is no on/off switch for this component. Before operating this pump, caution

should be used to ensure that all the necessary valves are open to allow the proper fluid flow.

While charging the loop, the pump operation should be closely monitored. There are two areas of concern:

1. The pump is not designed for long term operation for the conditions to which it is subjected. Consequently, the pump tends to become excessively hot at the rear bearing. Therefore, it is recommended that the charging be done in steps to allow the temperature of the pump to be controlled.

2. The completion of the charging procedure is determined by the liquid level as seen in the sight glass found on the combination tank. (The liquid can be any level visible in the sight glass.) Should loss of liquid occur, there may not be enough Freon 11 in the holding tank, resulting in the pump drying out. Close monitoring of pump performance will make this occurrence obvious.

6. Heater Service Valve (Location 24) This is a ball valve used to isolate the service loop from the heater service tap and the line leading to the lower loop service valves. The valve is normally closed, but is opened for both modes of service loop operation.

7. Heat Removal Subloop Service Valve (Location 25) This is another shut off valve for isolating the service loop. This valve controls the line that gives direct access

to the coolers. The valve is normally closed, but is open for either mode of service loop operation.

8. Cooler Drain Valves (Location 26) Two ball valves are located in the piping for the cooled Freon 11. The first is a tee valve that allows flow to pass from one cooler or the other into the drain line. The second valve acts as a shut off valve to close the drain line during normal loop operation. However, if the coolers are to be discharged, then the second valve is opened to allow the Freon 11 to flow directly into the sight glass. The first valve then allows the discharge from each cooler.

   The coolers should be discharged whenever Freon 11 is to be removed from the upper areas of the loop. Failure to do so could result in excessive loss of Freon 11.

Notes Concerning Service Loop Operation

There are four other items to be addressed to allow proper operation of the service loop. They are as follows:

1. For either mode of operation, the Nupro valve located on the expansion tank (mounted in conjunction with the pressure gauge on the back end of the tank) should be opened. In the case of charging, the cap and spring assembly should be totally removed.

This will prevent vaporization of the fluid during discharging, and prevent excessive build up of pressure on charging.

2. Upon the completion of charging, the Nupro valve should be left off while the loop is run for two to three minutes. This will help remove any trapped air.

3. Before charging, ensure that all the main loop valves are open. This will encourage quicker charging.

4. The DP cell shut off valves should be closed before charging or discharging. Concerns about the DP cells will be dealt with in a subsequent section. (See DP Cell Readout)

****

NOTE: Due to the hazardous effects of Freon 11 vapor, the room should be evacuated for 1/2 hour following either charging or discharging. Moreover, some windows should be opened to allow dispersion of the vapor.

The effects are not dangerous or long lasting should the quantities inhaled be moderate. If confusion occurs, get fresh air immediately

****

SERVICE LOOP

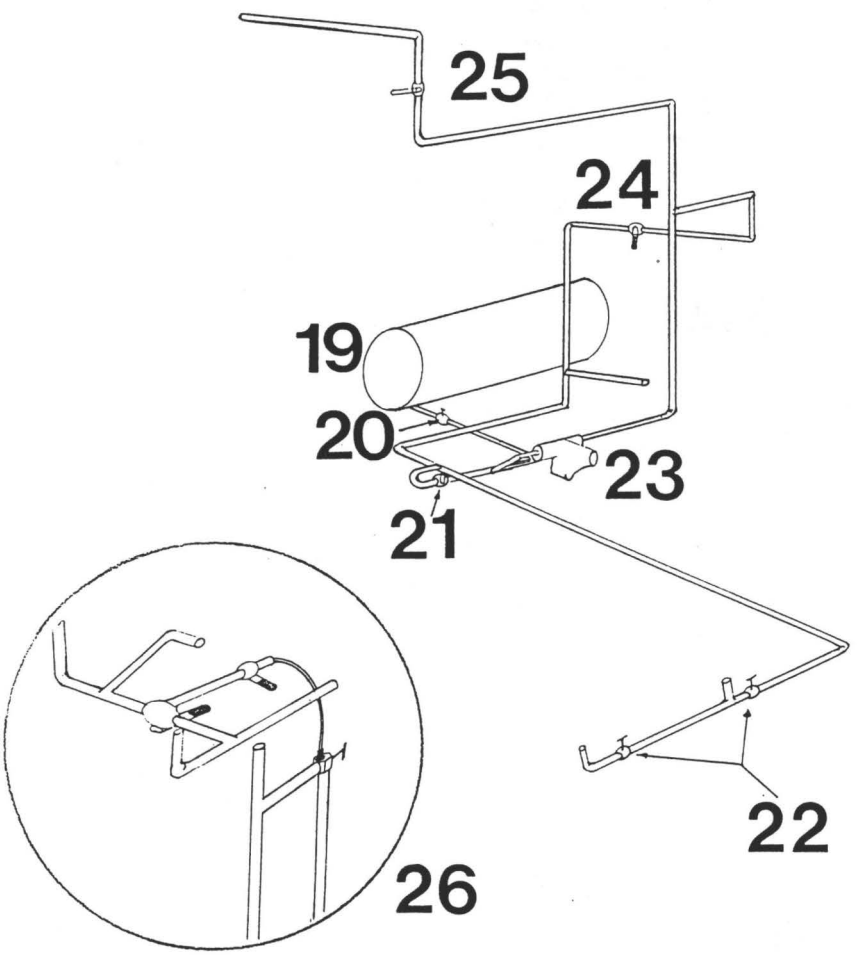

Instrumentation

Instruments were installed to provide information on pressure, temperature, flowrate, and current. This section considers only those instruments used for temperature reading, flowrate and pressure. The specific instrumentation for use with the pump and the heater will be discussed in a later section.

Thermocouples/Digital Recorder

Temperatures are measured in the loop through the use of 12 E type thermocouples. The output of these thermocouples cannot be directly input into the Phillips PM 8237 A, Multipoint Data Recorder since it does not have the capability to provide an electronic reference point for E type thermocouples. Therefore, it is necessary to use an ice bath as the reference temperature, and as a result the recorder provides output in millivolts. The ice bath is mounted on the left support of the stairway. Filling the thermos with ice and water allows temperature measurement for approximately two working days.

The thermocouples are connected by means of a 32 prong plug mounted above the ice bath. From here, the wires are fed into serial inputs at the back of the recorder. The recorder allows for the selective monitoring of preselected channels, and also provides several responses to preset alarm conditions. Furthermore, the scale of the output display can be altered to any desirable format. For details of the operation, see the operating manual for the recorder.

Presently, the recorder has the following 12 channels

dedicated to monitoring the following thermocouples:

Channel	Location	Figure 6 Locations
1.-	Test Section	1
2.-	Immediately Upstream of the Pump	2
3.-	Immediately Downstream of the Pump	3
4.-	Water Line - Post Coolers	6
5.-	Heat Removal Line- Pre Coolerers	6
6.-	Water Line - Pre Coolers	6
7,8,9.-	1/4 Power Heater Elements	5
10,11,12.-	Full Power Heater Elements	5

Thermocouples/Console

In addition to the digital recorder, there is a duplicate system using less advanced technology. This system is housed in the console that accompanies the loop. Originally intended to be the loop's control center, the console contains all the wiring and electronics necessary to monitor the twelve thermocouples and to duplicate the alarm capabilities of the Phillips recorder. The actual plotting of temperatures is accomplished through a Honeywell recorder found in JHE-206. The original input hardware for the console has been changed to serial plugs, therefore allowing the use of the existing connectors for input to the digital recorder to be easily plugged into the console if the need arises.

The knife switches, located on the console, provide the ability to select the channels that are to be recorded as well as allowing for the direct measurement of the signals using voltage meters. There is also a provision made for up to 6 more

thermocouples. The schematic for the console wiring is shown in Appendix E. Use of the start, stop, and reset buttons will be discussed in the section on heater operation.

Pressure Gauges

The loop uses seven pressure gauges to monitor the pressure at various locations around the loop depicted in Fig. 6. To suppress the occurrence of random fluctuations in the gauge readings, miniature control valves were installed between the gauges and the flow being measured. Consequently, the readings are the average pressures at the specific location. Should a particular gauge appear either to have a slow response or to have stopped responding altogether, the setting of these valves should be checked before the actual gauge is considered. Furthermore, should a particular gauge require removal, the valves can be shut off to allow easy removal without loss of fluid or necessitating the discharge of the loop. What follows are the locations and purposes of each.

1. Test Section (Location 1) This gauge provides measurement of the pressure in the test section. The pressure in the test section is one of the parameters that has to be controlled when operating the loop. Therefore, this gauge must be closely monitored while making adjustments in order to attain specified conditions, or determining the response of the loop as specified conditions are approached.

The importance of this gauge is such that it is the most accurate gauge in the loop. Should it need replacement, a gauge of

equal or better quality should be installed. There is no valve regulating the pressure fluctuation to dampen the pressure fluctuations at the gauge. The explanation of this apparent oversight in connection with such an important gauge is that the pressure tap hole is extremely small, and therefore it acts in a similar manner to the valves found with many of the other gauges.

2. Upstream of the Pump (Location 2) This gauge is found at the lowest point in the loop and also reads the lowest pressure in the loop. This reading should be monitored to determine the inlet pressure to the pump. If the angle valve, to which reference was made earlier, is manipulated, then this pressure will drop. A reduction of inlet pressure affects pump performance, and the valve can guide the operator as to the degree of pressure reduction obtained. However, as was noted earlier, this procedure has been ascertained as pointless for control purposes with the present loop configuration.

3. Downstream of the Pump (Location 3) This gauge allows two pieces of information to be obtained. First, in conjunction with the upstream gauge, changes in pump speed can be correlated to changes in pressure increase provided by the pump. Second, the increase in resistance that any particular control mechanism contributes can be seen as a direct pressure change in this reading. This result occurs since this gauge indicates the pressure necessary to generate the flowrate for the conditions present in the loop. During normal operation, this reading tends to rise as the loop approaches steady state.

4. Regulator Gauges (Location 4) Through the use of these two gauges, the pressure drop across the regulators can be determined. This was important in the past, but their use is now relegated to providing information on the pressure of the flow as it enters the heater section, and the pressure drop that the by-pass is creating. Although it is possible to adjust the pressure drop of the regulators, their present settings determine the maximum pressure drop in this section of the loop. When the by-pass is closed, the total flow passes through the regulators. When the by-pass is fully open, the flow passes almost entirely through the by-pass. Consequently, it is not possible to cut the flow off through the manipulation of the by-pass control valve. Furthermore, resetting the regulators would not have any significance.

5. Cooler Inlets (Location 6) Initially intended to measure condensate pressure, this gauge now provides the pressure of the flow in the heat removal subloop. This reading is of concern when adjusting the relative flowrates of the subloops. The change of either flowrate will affect the pressure seen at this point in the loop.

6. Expansion Tank (Location 7) This gauge measures the pressure of the vapor in the upper tanks. This pressure can also be considered the loop back pressure. It is through the control of this pressure that the fluid can be forced into two phase flow conditions. A gauge with a large and easily read face was chosen for this purpose.

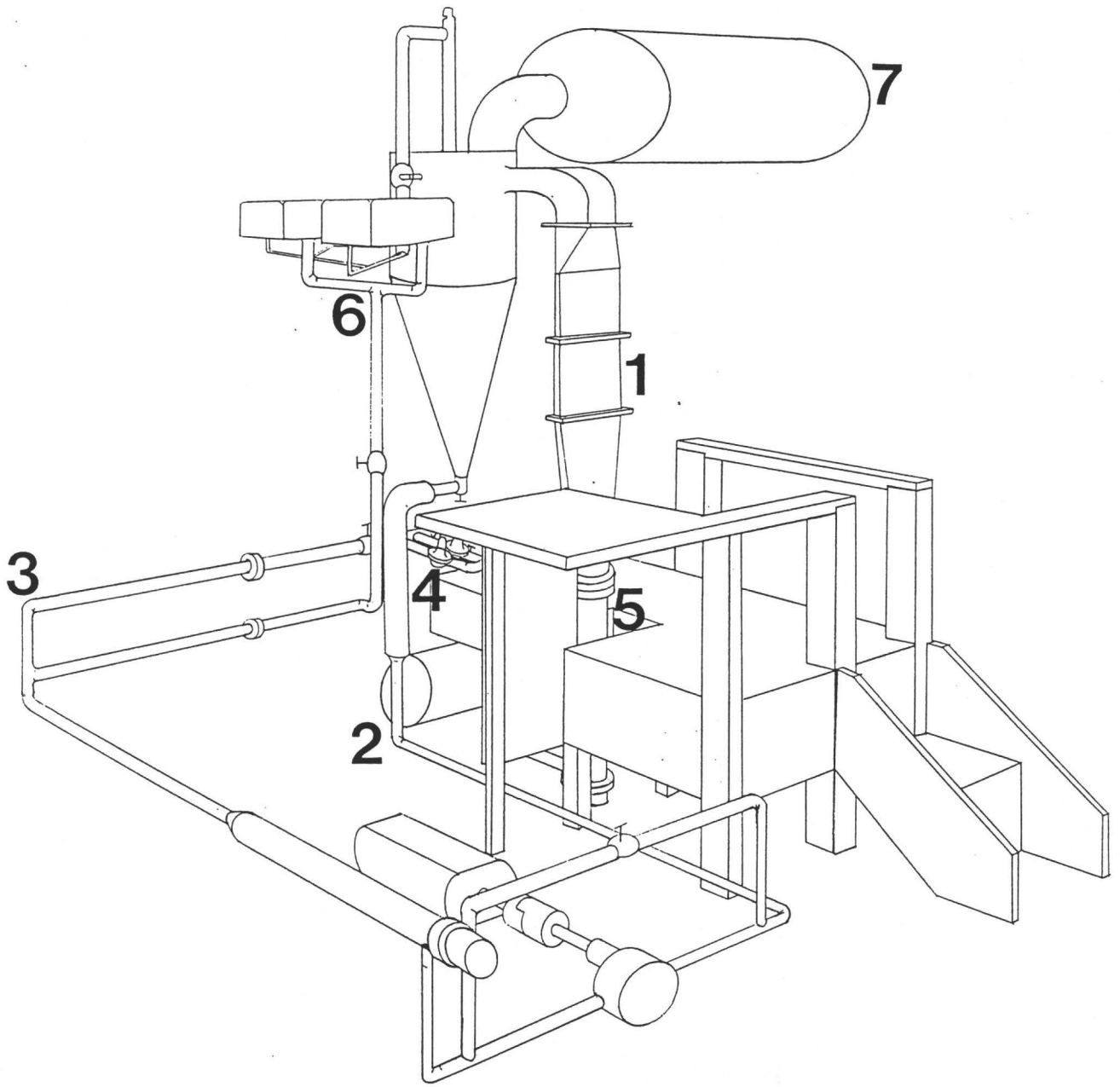

THERMOCOUPLES & PRESSURE GAUGES

DP Cell Readout (Flowrate)

Above and to the left of the orifice plates, a Validyne Digital DP cell readout device is found. There are two channels that can be read, and each channel corresponds to a different orifice plate. Channel 1 reads the pressure drop across the larger orifice plate, and channel 2 reads the pressure drop across the smaller orifice plate. Moreover, each channel can be read in two modes. The first provides readings to two decimal places, and the second reads to one decimal place, but allows readings of larger magnitude.

To convert the readings of each channel, one must incorporate the relationship between orifice plate pressure drop/ fluid flowrate/ and the DP cell readout in some common units of pressure measurement such as inches mercury.

For Channel 1

$$Q=A*(h)^{.5}$$

where: Q is flowrate corresponding to:

(kg/s) when A=1.018

(l/s) when A=.684

(USGPM) when A=10.864

h is in inches mercury

Channel 1 readout is in inches mercury per unit

For Channel 2

$$Q=B*(h)^{.5}$$

where: Q is flowrate corresponding to:

(kg/s) when B=.421

(l/s) when B=.283

(USGPM) when B=4.493

h is in inches mercury

Channel 2 readout is in .5 inches mercury per unit

A graph showing the resulting curve from each channel is provided in appendices B and C . These curves may be used in place of the relationships described above. However, it will become apparent with experience, that a basic understanding of approximately what the readouts represent will help when operating the loop. There is insufficient time to continually determine the exact flowrate that is being generated.

The DP cells are mounted in manifolds that allow the proper installation of the cells and also allow the easy removal of the cells. Miniature control valves, as seen in Fig. 7, can isolate the manifolds from the pressure taps. Once closed, the discharge valve can be opened to allow the removal of the fluid in the manifold. To remove the fluid from both branches, the centre valve must be open to allow liquid to flow from one side of the manifold to the other. Loosening the Swagelok connections will then allow the removal of the DP cells.

The process is reversed for the installation of the cells. However, the reintroduction of the fluid requires proper care to avoid damaging the diaphragms of the cells. Once the Swagelok connections have been tightened, the discharge valve must be closed and the center valve must be open to allow equal pressure on both

sides of the diaphragm. Then the valves at the pressure taps are opened slowly to allow fluid to enter the manifold.

To bleed the manifolds, there are two Allen screws in each DP cell. These should be loosened to allow the trapped air to escape, but they should not be removed or the Teflon seal will be lost, and this is not easily replaced. Moreover, the DP cells should be bled periodically to remove trapped air. Failure to do so may result in inaccurate readings, which can be seen as a failure to zero when the fluid is at rest.

The readout has been calibrated using the Heise mercury pressure gauges, which are considered very accurate. However, the scales selected for the DP cell readout were chosen such that the readout may not remain zeroed for even relatively short periods of time. The tradeoff is a more sensitive scale reading to allow greater accuracy in the flowrate determination. Moreover, this variance is small and can usually be corrected using the zero control screws on the readout device. This should be complemented by the bleeding procedure discussed above. Applying these procedures should not significantly affect the accuracy of the readings.

Note: 1. If the scale screws are tampered with, then the readouts must be recalibrated.

2. If recalibration is necessary, then note that the DP cells are different for each channel. Ensure that the cell with the correct identification number is replaced in the appropriate manifold.

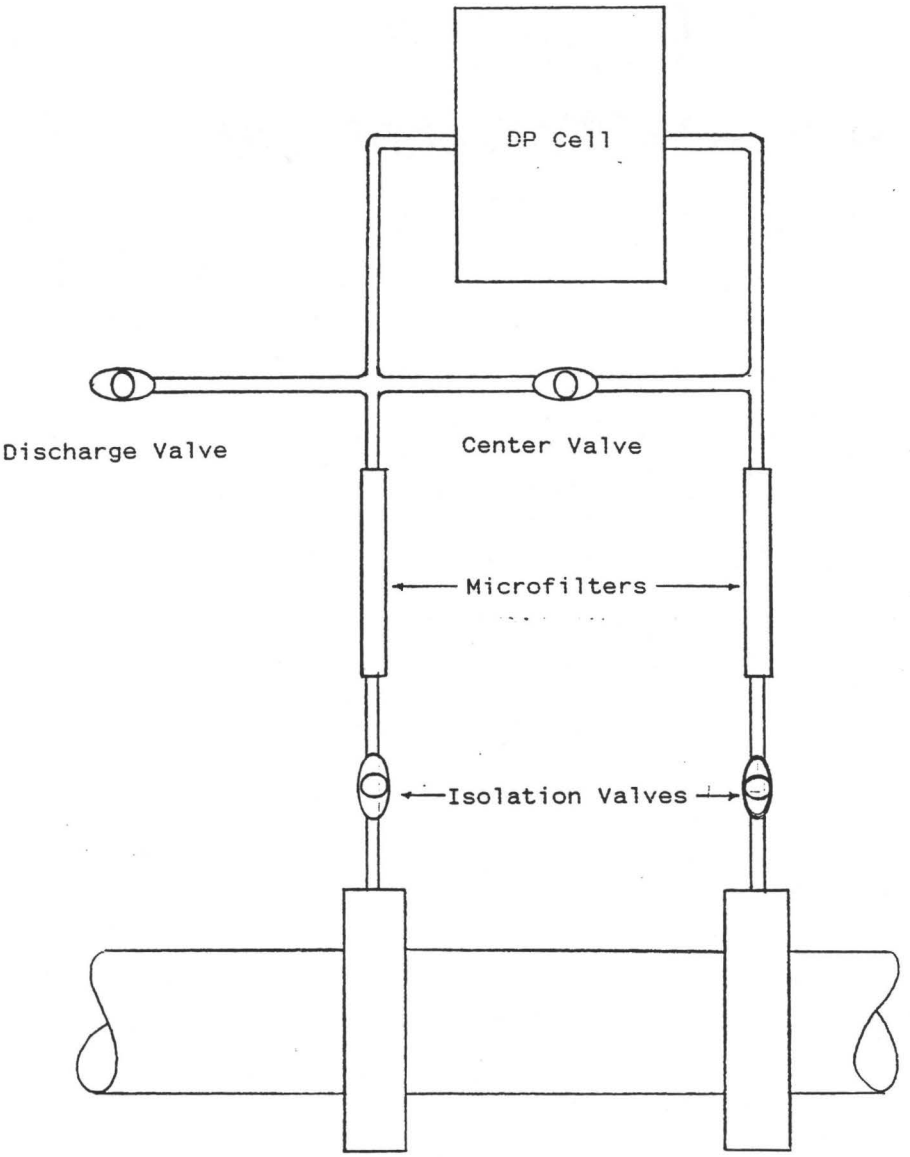

Fig. 7

DP Cell Manifold

Loop Operation

The remainder of the manual will deal with the actual operation of the loop. Primarily, this section is intended to provide the information necessary to start the various loop components. For added information, there is a description of the procedure to be followed in order to achieve a desired operating condition.

Pump Operation

Operation of the pump concerns the use of four pieces of instrumentation. First, to monitor the flowrate being generated, the DP cell readout must be activated. Second, to monitor the AC motor current, an ammeter has been installed below the DP cell readout. Third, the actual controller must be switched on using the large toggle switch found on the box with the word BOSTON written on it. (Upon activation, a light will come on showing that the controller is ready for use.) Fourth, the hand held speed control is needed to control pump speed.

At this point the DP cell readout should indicate 0.00 for the channel 1 readout. The current reading will be 0.0 , and the controller light should be on. Moreover, the selector with values of 0 to 100. on the hand held control should be set on 0. To start the pump, push the toggle switch marked start/stop in the start direction and release. This activates the controller, and now the speed control can be set. Slowly turn the dial until the motor begins to turn, then adjust the speed control until the readout on the DP cell is at the desired value. The speed may need to be

adjusted periodically depending on the flow conditions in the loop.

The rated current for the motor is 6.6 amps, and therefore the ammeter should be monitored periodically during long periods of use without adjustment to ensure that this value is not exceeded. Furthermore, the ammeter be must checked with every alteration of the loop controls, including any increase of heater power or cooling water flowrate. The conditions in the loop will change as steady state approaches, and may periodically make maintenance of a desired flowrate difficult. These conditions are always transitory in nature.

Additionally, the current monitoring is complemented by a breaker within the controller unit. If the speed of the pump requires approximately 7.5 amps, then the controller will cut the power to the pump. After resetting the controls to starting conditions, the pump can be reactivated. However, operation of the pump at current levels above 6.6 amps is not recommended since this would reduce the motor life. Therefore, the ammeter should be used to ensure the motor is operating within the safe region.

Heater Operation

-Preheater The preheater can be controlled by means of the small Variac located at the front left hand corner of the loop. The power switch for this heater is located on the back wall beside the AC motor controller. The activation of the heater requires two steps. The switch is placed in the on position, followed by the setting of the Variac for the desired percentage of voltage.

Note:1. The power input is proportional to the voltage

squared. Therefore, a large increase in power is experienced for small increases of voltage as the voltage approaches 100% of the rated voltage.

2. The preheater has no use in the present configuration of the loop.

-Main Heater/Digital Recorder The activation of the main heater is somewhat more complicated since it involves several switches and a breaker circuit designed to cut power should burnout be imminent in the heater section. There are a total of four switches mounted on the wall, located to the right of the loop and behind the welder. The first is a simple on/off type switch, which also contains fuses for each of the three phases. The second is a splitter switch that allows the power to be diverted to either of two projects. The down position provides power to the heater, and the center position is the neutral or off position.

The third switch is the 100 amp power box located at the back of the loop. As with the first switch, this one is a simple on/off type, that also has a breaker mounted in series for cutting off the power. From this last switch, the power is then fed to the three phase Variac found at the back right hand corner of the loop. The power level is a variable to be measured, so a fourth switch, found beside the third, was introduced to provide fusing for a higher power level in the future, and to provide easily accessable connections for voltmeters and ammeters.

Once the switches are on and the Variac set for the first power level, the heater must be controlled from a more convenient

location. The digital recorder is located to the left of a cast metal box mounted on a supporting post with start, stop, and on/off controls. To activate the heater, the on/off switch is activated, which will result in the light indicator coming on. Only when this light is on can the heater be turned on. With the light on, pushing the start button will close the power circuit and the heater will be activated. Similarly, deactivation is accomplished by pushing the stop button.

If the temperature read from the six heater thermocouples should rise above the preset alarm levels programmed in the recorder, then three different responses are programmed to occur. First, a signal is sent that will turn the heater off, by-passing the start button on the control box. The recorder chart speed will also increase by 30 times and combinations of dots for each channel will begin printing as opposed to a single dot.

NOTE If the digital recorder program is changed, it is important that at least the remote signal be reprogrammed into the recorder for all of the heater thermocouples.

Note:1. The switches should be returned to their off positions once the experiment is completed, and the light on the control box should be off.

Note:2. Pushing of the start button will momentarily reactivate the heater if the alarm has been tripped. Once in the alarm mode, the recorder must be cleared of the condition, which appears to require the

restarting of the recorder.

-Main Heater/Console The activation of the heater, in this case, is similar to the method outlined above, with the exception that the control box is duplicated on the console. Moreover, there is also a reset switch found on the console that is used to reset the comparator. The comparator determines whether any of the six heater thermocouples have exceeded the alarm level of 5.7 mV. Once tripped, the breaker will be turned off, resulting in the heater being deactivated. This is the equivalent of the alarm circuit for the digital recorder. However, the comparator will not allow the reactivation of the heater until alarm conditions are no longer exceeded. Pushing the reset button will allow reactivation if the conditions are favorable. Moreover, anytime the start button is inoperative, the reset button should be tried.

In addition to the heater control, the comparator also identifies the thermocouple that causes the problem. There are a set of six LED, which correspond to each of the six heater thermocouples. If any of these LEDs are on, the reset button must be used before the start button will be operable.

Note:1. As with the preheater, it should be noted that the power applied is proportional to the square of the voltage.

Suggested Method of Operation

The first decision to be made concerns the flowrate desired. Using the controller for the pump motor, the flowrate can be set to within approximately +/-2% of the determined DP cell readout on channel 1 . The setting of channel 2 should be set at between 3.0 and 4.0 . This will establish the heat removal flowrate and the loop flowrate. Prior to this, the recorder should have been activated and should have been operating long enough to obtain constant thermocouple readings. Moreover, the motor controller and DP cell readout should have been activated. This will allow the proper warm up of the equipment.

To increase the temperature and pressure of the loop, there are two basic approaches. First, the heater power can be kept low and the heat removal subloop flow can be reduced. Over a period of two to three hours, the temperature and pressure will rise. The higher temperatures and pressures may require a greater heat input in order to achieve them. Once the desired conditions have been achieved, their maintenance is accomplished by increasing the cooling capacity through either heat removal flowrate or water flowrate manipulation.

In addition, the movement into two phase flow requires that when the setting of the heater power to be increased, either the water flowrate is increased or the heat removal subloop flowrate is increased simultaneously. Manipulation of the latter will require greater pump input in order to maintain the main subloop flowrate. Moreover, the changes in fluid properties inherent in two phase

flow generation, result in pressure drop changes and instabilities that require manipulation of control valves to control. The most influential of these is the regulator bypass control valve. There is a trade off between efficiency and flowrate within the loop. As the loop conditions rise and two phase flow is obtained, the bypass control can be opened further to allow greater flowrates. However, at the lower temperatures and pressures, it has been observed that the performance of the pump is more efficient if a higher operating pressure is used. That is, the pump can provide the flowrate required more smoothly as evidenced by its quieter operation. Without the higher pressure, there is an inability to achieve higher flowrate with higher motor speeds once a certain flowrate has been achieved. It is suspected that some cavitation may be taking place in the pump. Therefore increasing the loop operating pressure can suppress this phenomenon. The higher operating pressure is obtained by adjusting the bypass valve.

The manipulation of any control that affects flowrate will result in both subloop flowrates changing. Immediately following any manipulation, both flowrates should be checked. In most cases, the heat removal flowrate is not as critical, and consequently the loop control is not as difficult as it might appear at first. Furthermore, the cooling rate can also be affected by the water flowrate, although this method is not as effective.

The second method of loop operation takes advantage of the heater power and the ability of the operator to know how to obtain the desired conditions. With experience, the operator can use

increments of heater power of between 10 and 20% to achieve the desired conditions more quickly. Starting with 10 % power, then possibly incrementing the power to 20% after 20 minutes, the loop can be brought to the desired pressure and temperature conditions in less than an hour. Once achieved, the cooling level can be increased to create steady state. At these power levels, the loop can generate all the pressure and temperature conditions at which it is capable of attaining stable conditions. The only constraint is that pressures above 21 psig must be avoided since these are above the design conditions.

The control of the heater was described earlier and should be adhered to strictly. The shut down of the loop, upon completion of experiments, requires fifteen minutes in the worst case. As described earlier, the heater can be shut off with the stop button on the control box. After deactivation, the switches are returned to the off or neutral position and the Variac returned to the zero position. However, prior to this action the flowrate of the loop must be adjusted. The flowrate will decrease significantly, requiring the manipulation of two valves and the reduction of pump power. First the bypass valve can be opened, and second the heat removal subloop control valve should be closed slightly. This will force more fluid through the main subloop, but there will still be a considerable degree of cooling. Within fifteen minutes the loop can be shut down completely at a temperature below that of the room.

Recommendations

The suggested method of operation just discussed is intended to be representative of loop operation. It is recommended that the reader learn by trying to operate the loop. If this manual is read and understood, then all the controls should be known. Moreover, the intended use of these controls should also be understood, as well as the basic fundamentals of operation underlying the loop design. If the operator understands what is happening within the loop, learning how to manipulate the controls in an effective manner should be relatively simple. However, the value of experience cannot be underestimated. Therefore, some time should be spent learning the controls before any attempts are made to control the higher power levels. In addition, effects such as warm outside temperatures have not been addressed. The ambient conditions are important to the loop operation. Therefore, care is required to accommodate these effects each time the loop is used. The same settings from one day to the next will not guarantee the same results. However, the instrumentation is more than adequate and will provide all the necessary information.

Appendix A

Water Orifice Plate Flowrate Graph

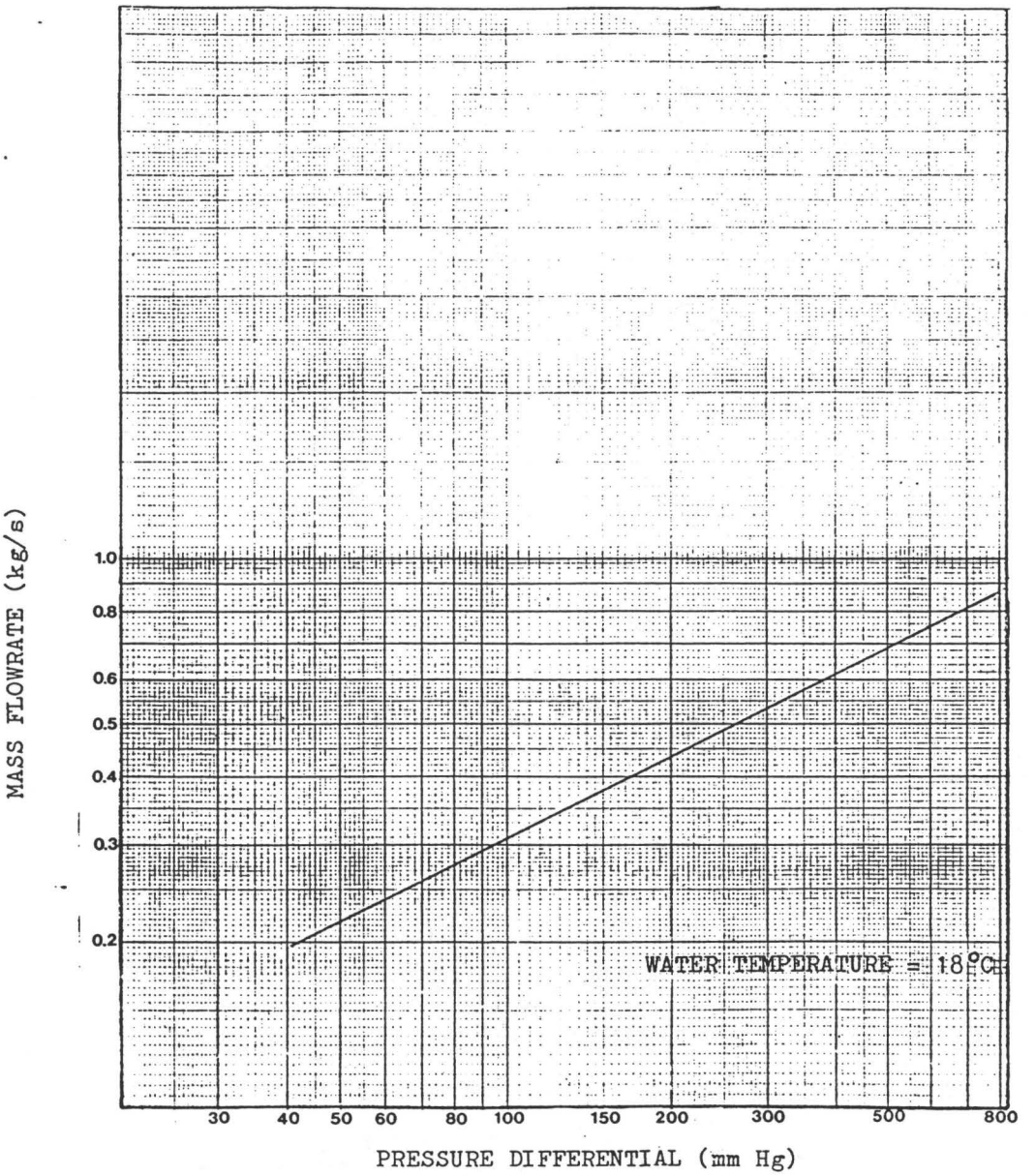

Cooling Water Orifice Plate
Mass Flowrate vs. Pressure Differential

Appendix B

Main Subloop Orifice Plate Flowrate Graph

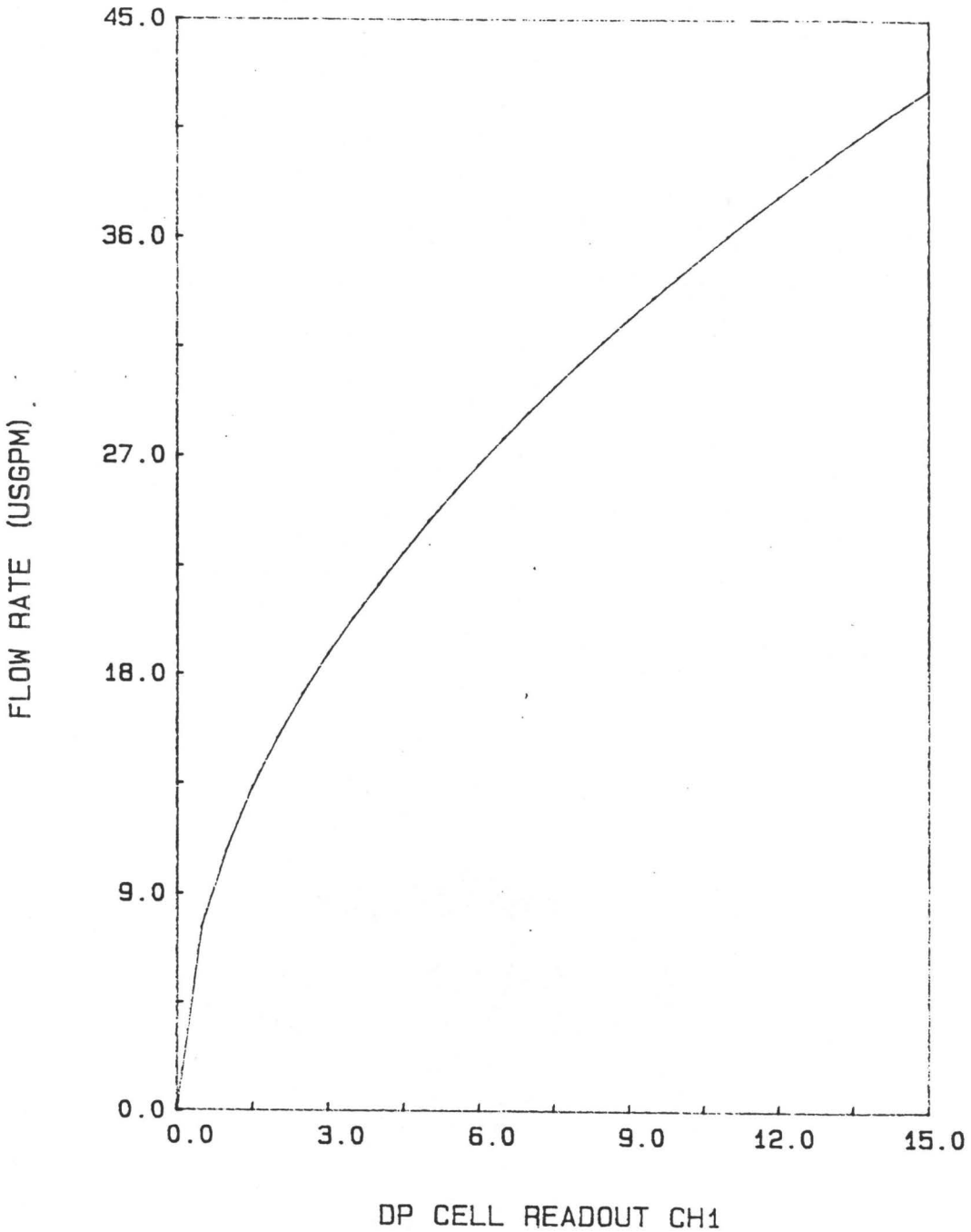
45.0
36.0
27.0
18.0
9.0
0.0
FLOW RATE (USGPM)
0.0
3.0
6.0
9.0
12.0
15.0
DP CELL READOUT CH1

Appendix C

Heat Removal Subloop Orifice Plate Flowrate Graph

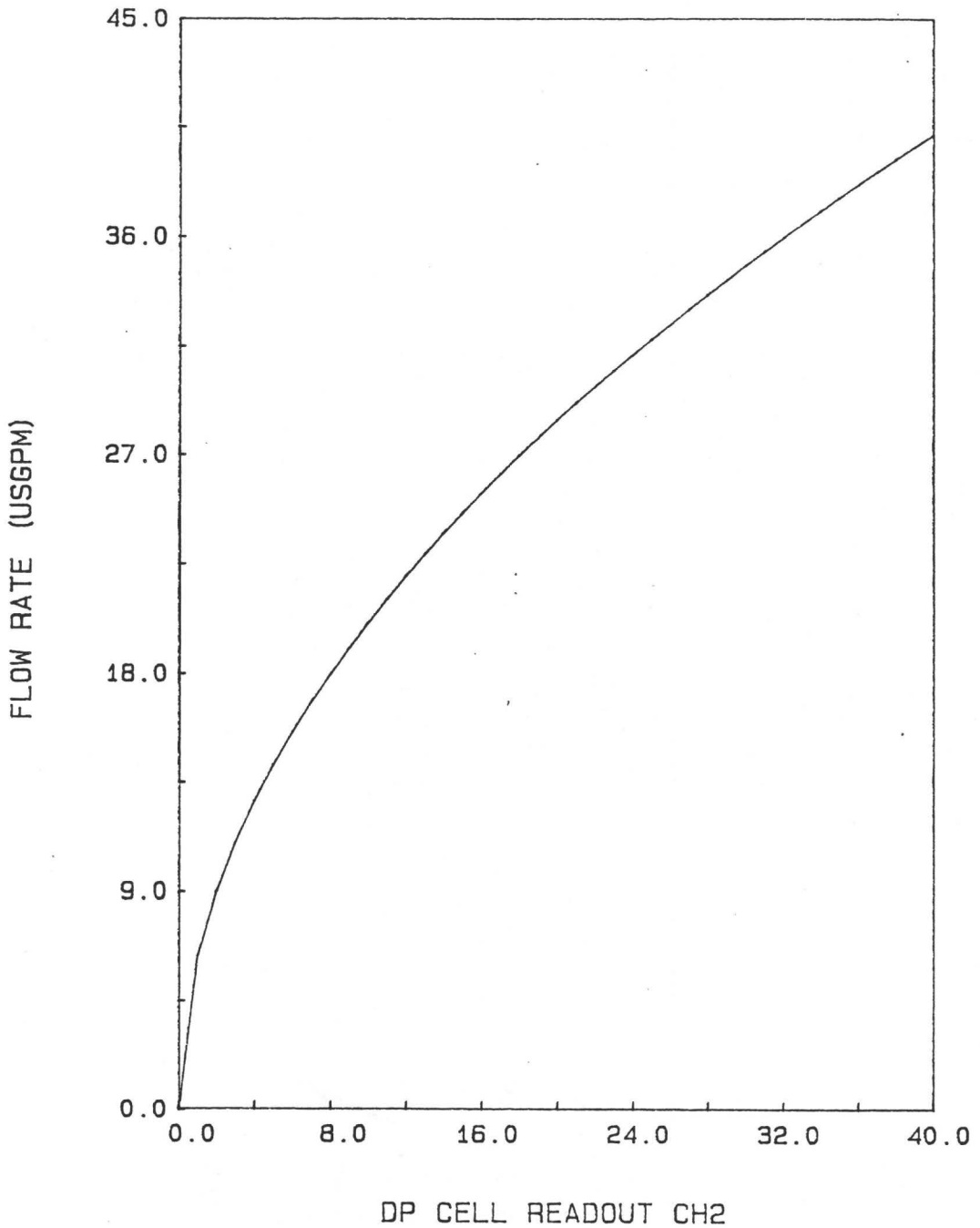
45.0
36.0
27.0
18.0
9.0
0.0
FLOW RATE (USGPM)
0.0
8.0
16.0
24.0
32.0
40.0
DP CELL READOUT CH2

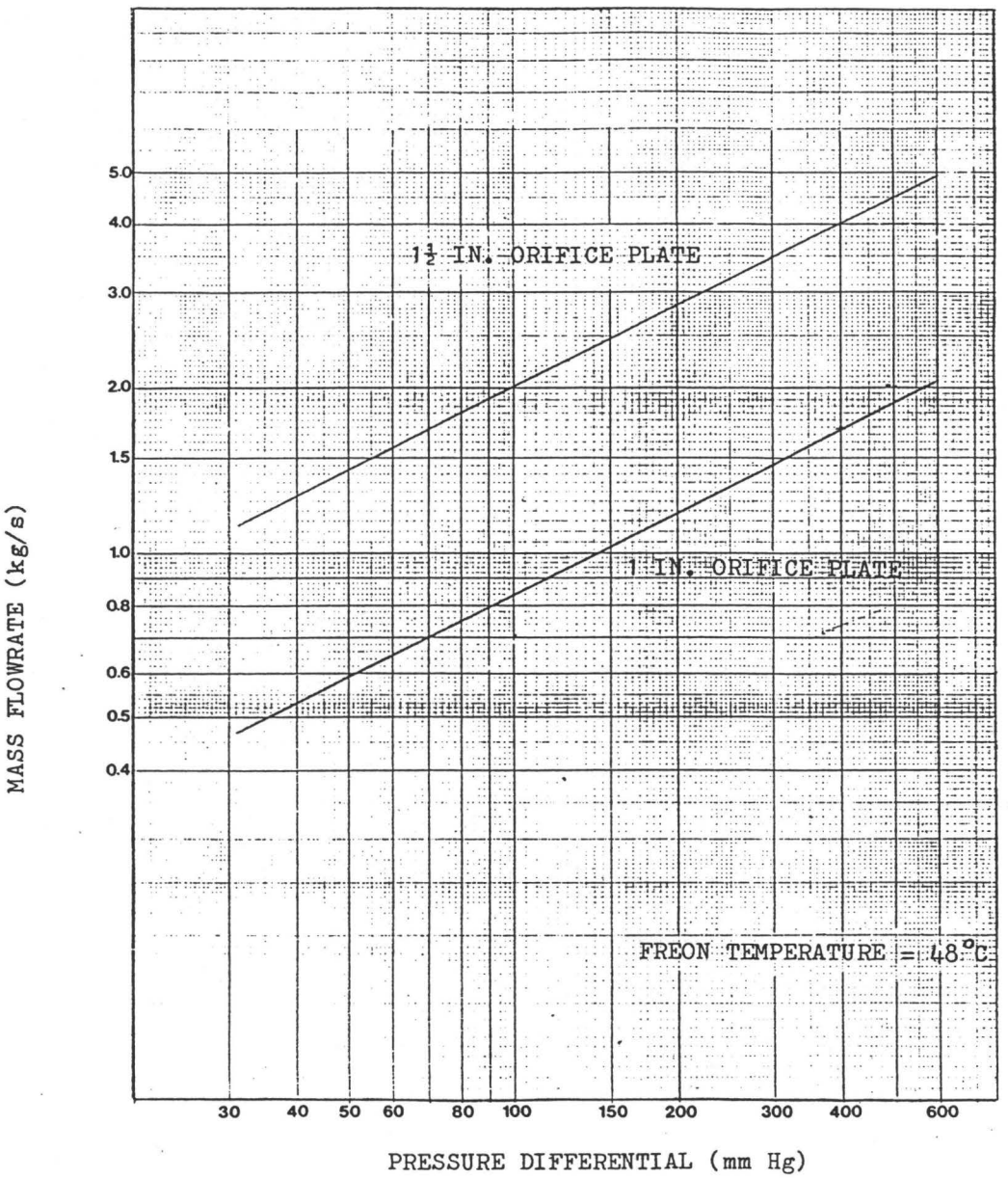

Freon 11 Orifice Plates
Mass Flowrate vs. Pressure Differential

Appendix D

Program For Digital Recorder

PROGRAMMING CARD PM8237A

CHANNEL NUMBER	odd	1	3	5	7	9	11	13	15	17	19	21	23	25	27	29
	even	2	4	6	8	10	12	14	16	18	20	22	24	26	28	30
CHANNEL MODE	odd	211	211	211	211	211	211	200	200	200	200	200	200	200	200	200
	even	211	211	211	211	211	211	200	200	200	200	200	200	200	200	200
RESPONSE TO ALARM	odd	000	000	000	111	111	111	000	000	000	000	000	000	000	000	000
	even	000	000	000	111	111	111	000	000	000	000	000	000	000	000	000
MEASURING FUNCTION		1000	1000	1000	1000	1000	1000									
ZERO-SCALE VALUE		0.0	0.0	0.0	0.0	0.0	0.0									
FULL-SCALE VALUE		10.0	10.0	10.0	10.0	10.0	10.0									
Span																
MAXIMUM ALARM LEVEL		5.7	5.7	5.7	5.7	5.7	5.7									
MINIMUM ALARM LEVEL		-0.4	-0.4	-0.4	-0.4	-0.4	-0.4									

CHANNEL MODE

DATA : Q R S
- 4 : 4-INPUT TERMINAL CONFIGURATION
- 2 : 2-INPUT TERMINAL CONFIGURATION
- 1 : CHANNEL IS MEASURED
- 0 : CHANNEL IS SKIPPED
  - 0 : NO RECORDING IN DOT MODE (ZERO DOTS)
  - 1 : RECORDING WITH SINGLE DOT
  - 2 : RECORDING WITH A SPECIAL MARKING

RESPONSE TO ALARM

DATA : Q R S
- 0 : NO RESPONSE TO EXT. CONTROL CONNECTOR
- 1 : RESPONSE TO EXT. CONTROL CONNECTOR
  - 0 : NO INCREASE OF CHART SPEED AFTER ALARM
  - 1 : INCREASED CHART SPEED AFTER ALARM (X10)
    - 0 : NORMAL RECORDING AFTER ALARM
    - 1 : RECORDING WITH A SPECIAL MARKING AFTER ALARM

MEASURING FUNCTION

DATA : P Q R S
- 0 0 N N : DIFFERENTIAL MEASUREMENT WITH CHANNEL NN
- 1 0 0 0 : MILLIVOLT
- 1 5 0 0 : VOLT
- 2 0 0 0 : PT 100

THERMOCOUPLES
- 3 Q R S : SPECIAL TYPE
- 4 Q R S : TYPE J
- 5 Q R S : TYPE L
- 6 Q R S : TYPE K
- 7 Q R S : TYPE S
- 8 Q R S : TYPE T
- 9 Q R S : TYPE U

COLD-JUNCTION COMPENSATION
Q R S
- 0 0 0 : FOR 0°C
- 2 0 0 : FOR 20°C
- 5 0 0 : FOR 50°C
- 8 N N : FOR TEMPERATURE OF CHANNEL NN
- 9 0 0 : AUTOMATIC (TEMPERATURE OF INPUT BLOCK)

FULL-SCALE/ZERO-SCALE VALUE

DATA : SIGNED 4-DIGIT NUMBER WITH OR WITHOUT DECIMAL POINT

MAXIMUM/MINIMUM ALARM LEVEL

DATA : SIGNED 4-DIGIT NUMBER WITH OR WITHOUT DECIMAL POINT

CHART DRIVE

DOT MODE	
NUMERAL MODE	
EXT.CONTROL	

DATA : SPEED BETWEEN 00 AND 60
+ MM/MIN - MM/HOUR
DATA : PRINT INTERVAL TIME BETWEEN 0 AND 99
DATA : DIVIDE FACTOR FOR EXT. CLOCK PULSES

CHART SPEED RULE-OF-THUMB METHOD FOR SMOOTH LINES

CHART SPEED : $< \frac{25}{n}$ mm/min

$< \frac{1500}{n}$ mm/hr

n is the number of measured channels

DATE :	

Appendix E

Console Wiring Schematic

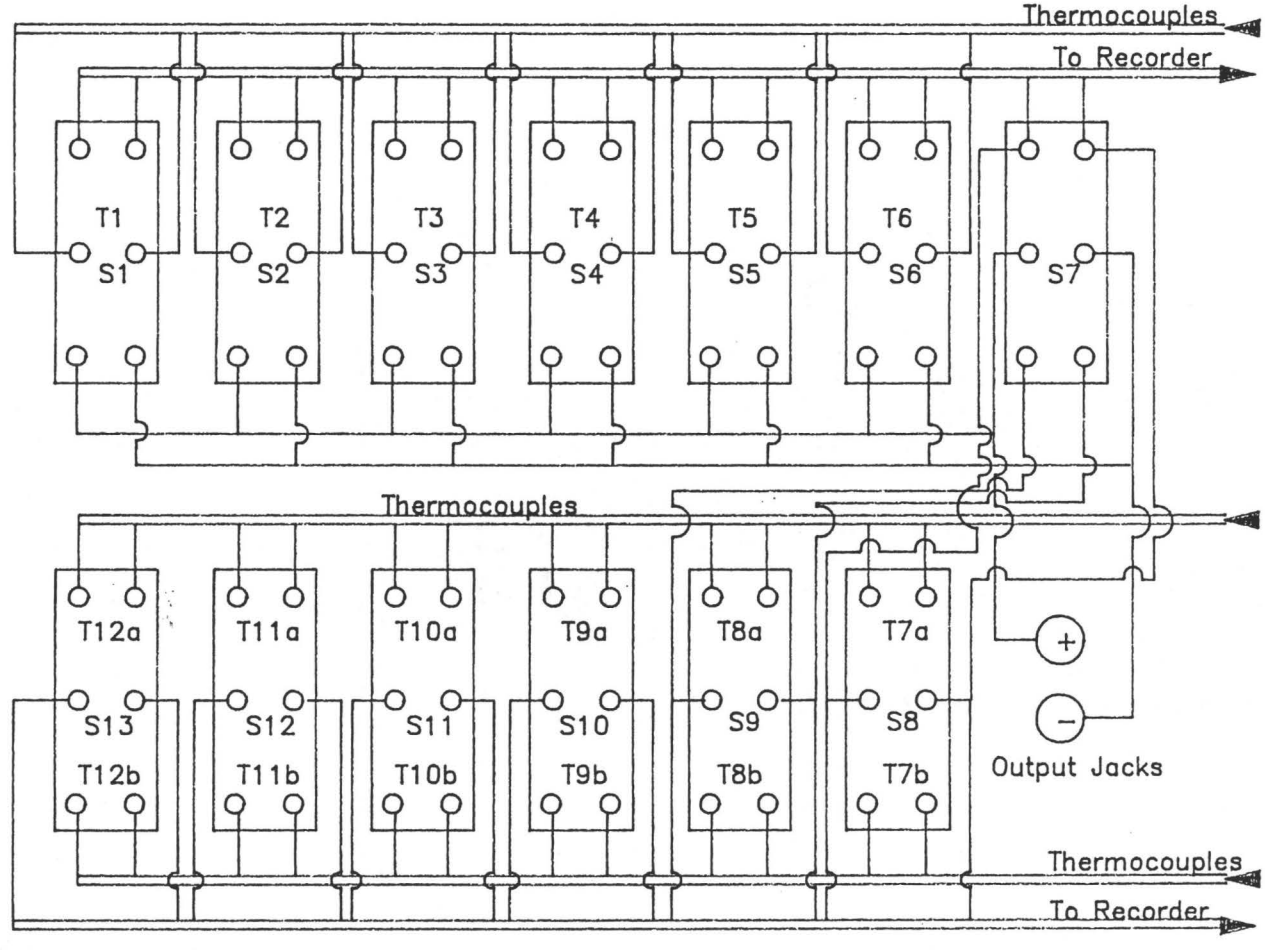

T=Thermocouple
S=Switch

Figure E1 Schematic of Thermocouple Switch Board

Appendix F

Main Heater Wiring Schematics

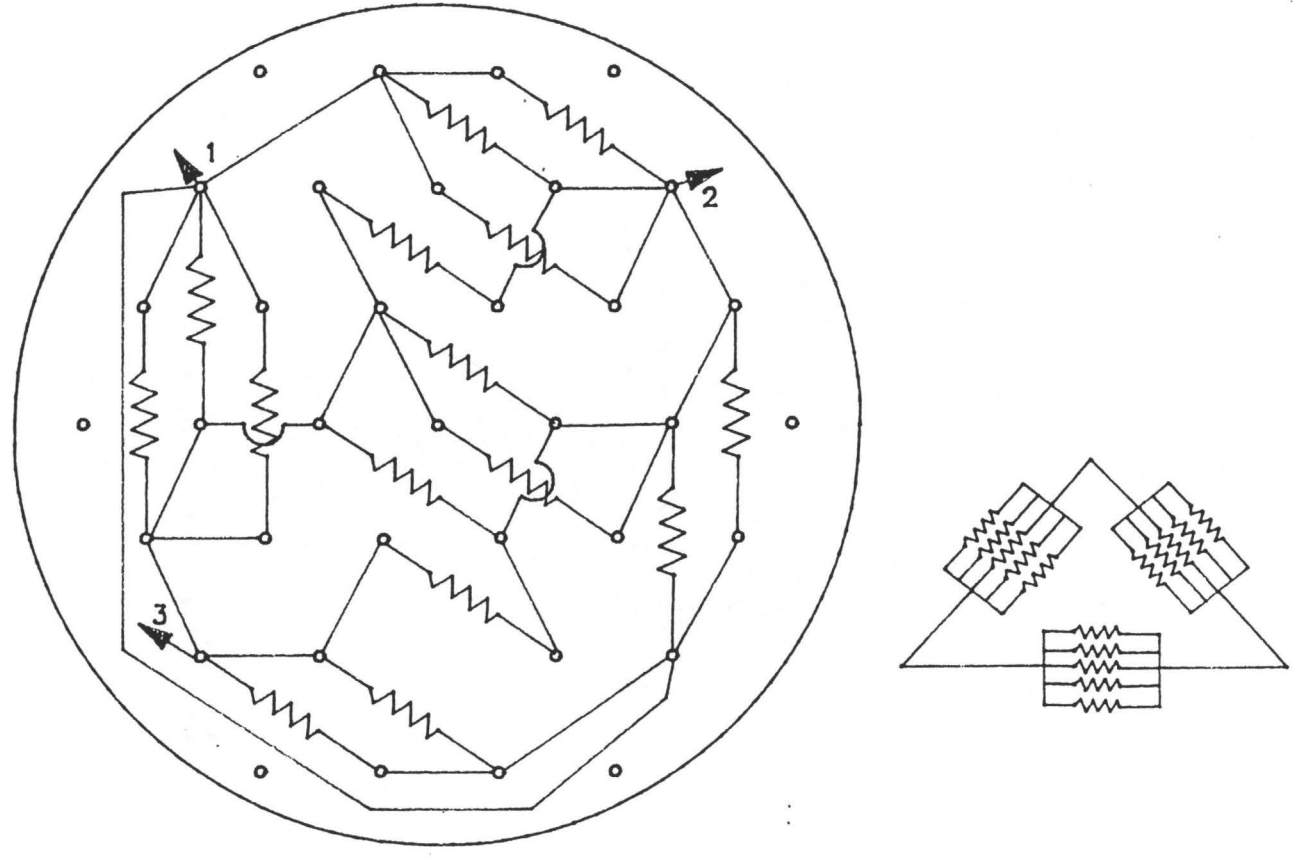

Heater Wiring Diagram :48 KW

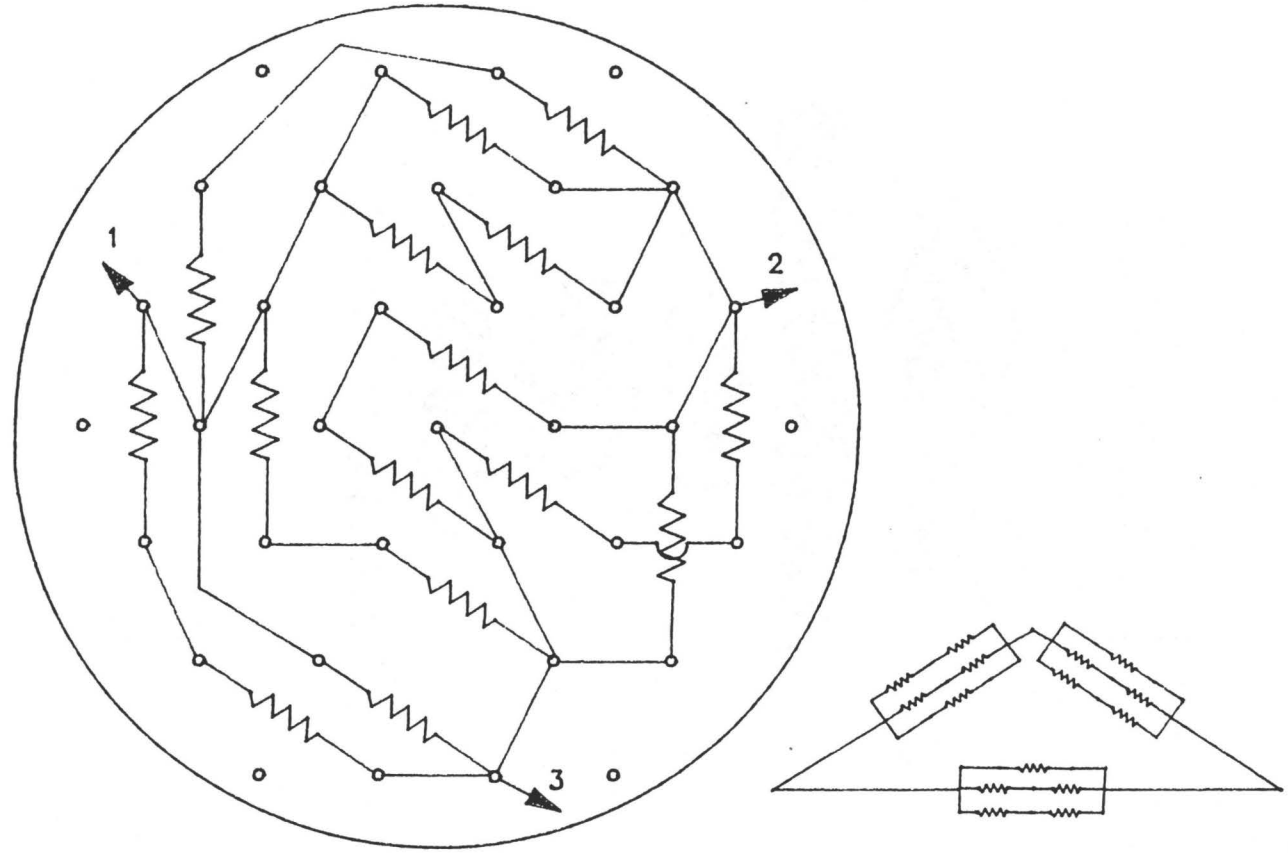

Heater Wiring Diagram: 19.2 KW

Appendix G

MSDS Hazardous Material Information on Freon 11

HEALTH HAZARD DATA

TLV'S: TLV - "CEILING" IS 1000 PPM (ACGIH 1983-84)

ROUTES OF EXPOSURE: VAPOUR TOXICITY IS LOW. IRRITATES THE RESPIRATORY PASSAGES AT HIGH CONCENTRATIONS, AND HAS NARCOTIC EFFECTS AT VERY HIGH CONCENTRATIONS. THE LCLO (INHALATION, RAT) >100000 PPM. LIQUID CONTACT MAY CAUSE FROST-BITE DUE TO RAPID EVAPORATION, AND REPEATED, PROLONGED SKIN CONTACT CAN CAUSE DERMATITIS. CONTACT WITH EYES IS MILDLY IRRITATING AND MAY CAUSE FROST-BITE. ORAL TOXICITY IS LOW, WITH SOME CENTRAL NERVOUS SYSTEM (CNS) EFFECTS.

EFFECTS OF OVEREXPOSURE - ACUTE: MILD IRRITATION OF UPPER RESPIRATORY TRACT. LIGHT-HEADEDNESS, GIDDINESS, SHORTNESS OF BREATH; AT VERY HIGH CONCENTRATIONS, NARCOSIS AND CARDIAC ARRHYTHMIA. LIQUID CONTACT WITH SKIN OR EYES CAN CAUSE FROST-BITE. EFFECTS OF OVEREXPOSURE - CHRONIC: DERMATITIS.

EMERGENCY AND FIRST AID PROCEDURES

INHALATION: GET TO FRESH AIR; IF NOT BREATHING, GIVE ARTIFICIAL RESPIRATION. GET MEDICAL ATTENTION.

INGESTION: IF CONSCIOUS, GIVE TWO GLASSES OF WATER TO DRINK AND INDUCE VOMITING. CALL A PHYSICIAN.

SKIN OR EYES: IN CASE OF CONTACT WITH LIQUID, IMMEDIATELY FLUSH THE AFFECTED AREA WITH LARGE AMOUNTS OF TEPID WATER. LOOSEN ANY CLOTHING WHICH MIGHT RESTRICT CIRCULATION. DO NOT APPLY HEAT. COVER AFFECTED AREA WITH A STERILE DRESSING (USE CLEAN SHEET IF THE AREA IS LARGE). CALL A PHYSICIAN AT ONCE.

NOTE TO PHYSICIAN: 1) TREAT FROZEN TISSUE BY IMMEDIATE IMMERSION IN 40-45 DEG C WATER. AVOID THE USE OF DRY HEAT. POTENT ANALGESICS MAY BE INDICATED DURING THAWING. RAPID REWARMING OF TISSUES IS NOT RECOMMENDED IF TRANSFER TO HOSPITAL IS DELAYED. SHOCK AND CARDIAC DYSRHYTHMIA MAY ACCOMPANY HYPOTHERMIA. 2) EPINEPHRINE AND SIMILAR DRUGS ARE CONTRAINDICATED.

REACTIVITY DATA

PRODUCT STABILITY: VERY STABLE. WILL DECOMPOSE IN FLAME OR IF HEATED ABOVE 260 - 320 DEG C.

HAZARDOUS POLYMERIZATION: DOES NOT OCCUR

INCOMPATIBILITY: (MATERIALS TO AVOID): CHEMICALLY ACTIVE METALS, SUCH AS SODIUM, POTASSIUM, POWDERED ALUMINUM, ETC. CAN REACT VIOLENTLY

HAZARDOUS COMBUSTION OR DECOMPOSITION PRODUCTS: TOXIC CHLORIDE AND FLUORIDE COMPOUNDS - PRINCIPALLY HYDROGEN CHLORIDE AND HYDROGEN FLUORIDE, WITH SMALL AMOUNTS OF CHLORINE AND CARBONYL HALIDES POSSIBLE

SPILL OR LEAK PROCEDURES

CLEANUP: NEUTRALIZING CHEMICALS: NONE. RESTRICT ACCESS. VENTILATE AREA, ESPECIALLY LOW PLACES WHERE VAPOUR MIGHT COLLECT. ABSORB ON SAND OR EARTH AND SHOVEL OR SCOOP INTO DRUMS. MOVE TO REMOTE AREA AND SPREAD OUTDOORS TO EVAPORATE.

DISPOSAL: EVAPORATE IN REMOTE AREA OUTDOORS AWAY FROM HEAT OR OPEN FLAME. AQUATIC TOXICITY: NOT KNOWN.

EYE PROTECTION: FACE SHIELD AND COVERALL GOGGLES WHERE CONTACT WITH THE LIQUID IS POSSIBLE

SKIN PROTECTION: NEOPRENE OR BUTYL RUBBER GLOVES WHERE CONTACT WITH THE LIQUID IS LIKELY

RESPIRATORY PROTECTION: ATMOSPHERE-SUPPLYING RESPIRATOR WHERE OVER-EXPOSURE IS LIKELY

VENTILATION REQUIREMENTS: USE LOCAL EXHAUST WITH MECHANICAL VENTILATION AT SOURCES (KEEP <1000 PPM).

OTHER CLOTHING AND EQUIPMENT: ACID SUIT (JACKET AND PANTS), WHERE LIQUID CONTACT IS LIKELY

STORAGE AND HANDLING

STORAGE AND HANDLING: OTHER HANDLING AND STORAGE REQUIREMENTS: STORE IN A CLEAN, DRY AREA, AWAY FROM ACTIVE METALS. DO NOT HEAT CONTAINERS ABOVE 50 DEG C. PRECAUTIONARY STATEMENTS: CAUTION. CONTACT WITH LIQUID OR INHALATION OF VAPOUR MAY BE HARMFUL. RELEASES TOXIC GASES WHEN HEATED TO DECOMPOSITION. KEEP AWAY FROM HEAT OR OPEN FLAME. AVOID CONTACT WITH SKIN OR EYES, AND DO NOT BREATHE VAPOUR.

ADDITIONAL INFORMATION

TRANSPORT CANADA CLASSIFICATION: NON-REGULATED

D.O.T. HAZARD CLASSIFICATION: NON-REGULATED

TRADE NAMES

Canadian Centre for Occupational Health and Safety

*** IDENTIFICATION ***

RECORD NUMBER	9785
LANGUAGE	ENGLISH
TRADE NAME(S)	FREON (R) 11
PRODUCT IDENTIFICATION DATA	DU PONT CODE: TOR. (#373)1

*** MANUFACTURER INFORMATION ***

MANUFACTURER	DU PONT CANADA INC
ADDRESS	26 TORONTO DOMINION CENTRE TORONTO ONTARIO CANADA M5K 1B6 Telephone: 416-362-5621
EMERGENCY TELEPHONE NO.(S)	613-348-3616
DISCLAIMER	NOTE FROM DU PONT: THE INFORMATION ON THIS MATERIAL SAFETY DATA SHEET IS PROVIDED BY DU PONT FREE OF CHARGE. WHILE BELIEVED TO BE RELIABLE IT IS INTENDED FOR USE BY SKILLED PERSONS AT THEIR OWN RISK. DU PONT ASSUMES NO RESPONSIBILITY FOR EVENTS RESULTING OR DAMAGES INCURRED FROM ITS USE. THE INFORMATION ON THIS MATERIAL SAFETY DATA SHEET RELATES ONLY TO THE SPECIFIC MATERIAL DESIGNATED HEREIN AND DOES NOT RELATE TO USE IN COMBINATION WITH ANY OTHER MATERIAL OR IN ANY PROCESS.

*** MATERIAL SAFETY DATA ***

PRODUCT TRADE NAME(S): FREON (R) 11

PRODUCT DESCRIPTION: COLOURLESS LIQUID WITH SLIGHT ETHER-LIKE ODOUR
DOCUMENT REFERENCE FOR DATA SHEET: DU PONT CODE: TOR. (#373)1

INGREDIENTS

TRICHLOROFLUOROMETHANE; F-11 (CAS NO.: 75-69-4)

PHYSICAL PROPERTIES OF PRODUCT

SOLUBILITY (%): 0.11% @ 25 DEG C
BOILING POINT OF PRODUCT: 23.8 DEG C
MELTING POINT OF PRODUCT: -111 DEG C
VAPOUR PRESSURE OF PRODUCT: 106 KPA @ 25 DEG C
VAPOUR DENSITY OF PRODUCT: 4.9 @ 25 DEG C (AIR = 1)
SPECIFIC GRAVITY OF PRODUCT: 1.48 @ 25 DEG C
PERCENT VOLATILE (%): 100
EVAPORATION RATE: APPROX. 0.3 (BUTYL ACETATE = 1)

FIRE AND EXPLOSION HAZARD DATA

UNUSUAL FIRE/EXPLOS HAZARDS: WILL NOT BURN BUT THERMAL DECOMPOSITION CAN PRODUCE TOXIC CHLORIDE AND FLUORIDE COMPOUNDS IN A FIRE AND HEATING CYLINDERS CAN GENERATE EXPLOSIVE PRESSURES. WEAR SCBA RESPIRATOR TO FIGHT FIRE. MOVE CYLINDERS FROM VICINITY, IF POSSIBLE, OR COOL THEM WITH WATER

Appendix H

Reference Diagram of Loop Component Locations

Diagram #	Description	References in Manual
T	Test Section	29,30
1	Main Pump	7,12,13,16
2	Preheater	7,12,13,16
3	Main Flow Subloop Orifice Plate	7,12,App. B
4	Main Flow Subloop Control Valve	7,12
5	Regulators And Bypass Valve	8,12,13,31
6	Main Heater	9,12,39,40, App. F
7	Combination Tank (Separation Tank)	11,12,14,16
8	Angle Valve	7,11,14,16
9	Heat Removal Subloop Orifice Plate	13,16,App. C
10	Heat Removal Subloop Control Valve	13,16
11	Condensers	13,16,17,19
12	Pressure Relief Valve	14,16
13	Expansion Tank	12,15
* 14	Water Line Shut Off Valve	17,19
* 15	Water Line Orifice Plate	17,19,App. A
* 16	Water Line Control Valve	18,19
* 17	Drain	18,19
* 18	Discharge Valve	18,19
19	Holding Tank	20,26
@ 20	Isolation Valve	22,26
@ 21	Charging Line Bypass	22,26
@ 22	Lower Loop Service Valves	22,26
@ 23	Service Loop Pump	22,26
@ 24	Heater Service Valve	23,26
@ 25	Heat removal Subloop Service Valve	23,26
@ 26	Condenser Drain Valves	24,26

* See fig. 4 for locations of these components.

@ See fig. 5 for locations of these components.

See figure 6 for locations of thermocouples and pressure guages.

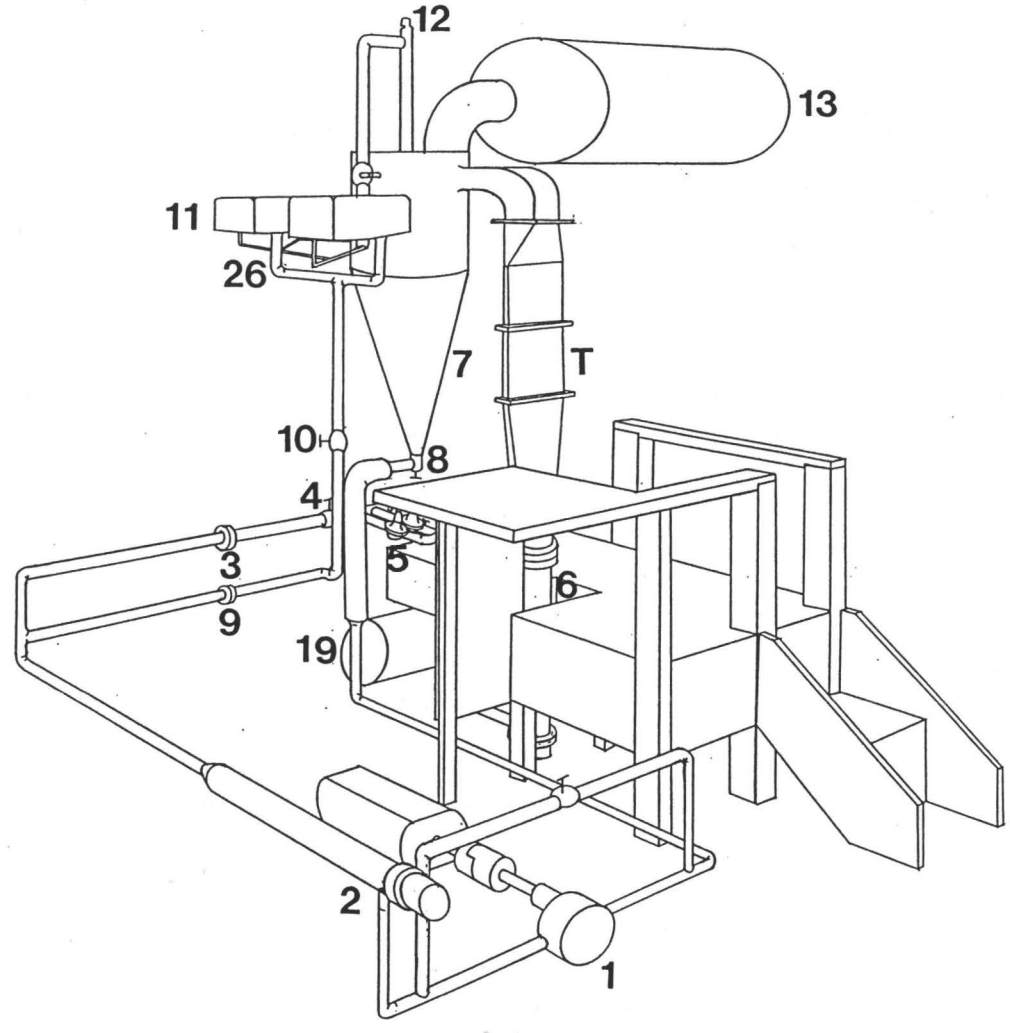

References

1. Axisa, F., B. Villard, R.J. Gilbert, G. Hetsroni, P. Sundheimer, "Vibration of Tube Bundles Subjected to Air -Water and Steam-Water Cross Flow: Preliminary Results in Fluidelastic Instability", 1983 International Symposium on Flow-Induced Vibration pp 269-284.

2. Axisa, F., J. Antunes, B. Villard, "Overview of Numerical Methods for Predicting Flow-Induced Vibration", Journal of Pressure Vessel Technology, vol. 110, Feb. 1988, pp 6-14.

3. Axisa, F., J. Antunes, B. Villard, M. Wullshieger, "Random Excitation of Heat Exchanger Tubes By Cross-Flow", 1988 International Symposium on Flow-Induced Vibration and Noise, Vol. 2, pp 79-103.

4. Bergles, A.E., J.G. Collier, J.M. Delhaye, G.F. Hewitt, F. Mayinger, "Two-Phase Flow and Heat Transfer in the Power and Process Industries", Hemisphere Publishing Corp., New York, 1981.

5. Blevins, Robert D.,"Formulas for Natural Frequency and Mode Shape", Van Nostrand Reinhold Company, Toronto, 1988.

6. Chen, Shoei-Sheng, "Flow Induced Vibration of Circular Cylindrical Structures", Hemisphere Publishing Corp., New York, 1987.

7. Chen, S.S., " Some Issues Concerning Fluidelastic Instability of a Group of Circular Cylinders In Crossflow", 1988 International Symposium on Flow-Induced Vibration and Noise, Vol. 3, pp 1-24.

8. Conners, H.J., "Flow Induced Vibration and Wear of Steam Generator Tubes", Nuclear Technology, Vol. 55, Nov. 1981, pp 311-331.

9. Gay, N., P. Decembre, J. Launay, "Comparison of Air-Water to Freon-Water Two Phase Cross Flow Effects on the Vibratory Behaviour of a Tube Bundle", 1988 International Symposium on Flow-Induced Vibration and Noise, Vol. 3, pp 139-158.

10. Goyder, H.G.D., "Fluidelastic Instability and Buffeting of Heat Exchanger Tube Bundles Due to Single and Two-Phase Flows", 1988 International Symposium on Flow-Induced Vibration and Noise, Vol. 2, pp 151-168.

11. Gregory, B. A., "An Introduction to Electrical Instrumentation and Measurement Systems", Halsted Press, John Wiley & Sons, New York, 1981.

12. Hara, F., "A Flow Visualization Study of a Single Row of

Circular Cylinders Vibrating in Water and Two-Phase Cross Flows", 1988 International Symposium on Flow-Induced Vibration and Noise, Vol. 1, pp 75-89.

13. Lever, J.H., D.S. Weaver, "A Theoretical Model for Fluidelastic Instability in Heat Exchanger Tube Bundles", Journal of Pressure Vessel Technology, Aug. 1982, Vol. 104, pp 147-158.

14. Lever, J.H., D.S. Weaver, "On the Stability of Heat Exchanger Tube Bundles: Part 1- Modified Theoretical Model", 1984 International Symposium on Flow-Induced Vibration, Vol. 2, pp 83-97.

15. Lever, J.H., D.S. Weaver, "On the Stability of Heat Exchanger Tube Bundles: Part II- Numerical Results and Comparison With Experiments", 1984 International Symposium on Flow-Induced Vibration, Vol. 2, pp 99-116.

16. Lever, J., and D.S. Weaver, "Tube Frequency Effects on Cross Flow Induced Vibrations in Tube Arrays", Proceedings of the Fifth Biennial Symposium on Turbulence, University of Missouri -Rolla, October 1977, pp 323-331.

17. Moretti, P.M., R.L. Lowery, "Hydrodynamic Inertia Coefficients of a Tube Surrounded by Rigid Tubes", J. Pressure Vessel Technology,1976, 98, pp 190-193.

18. Nakamura, T., K. Fujita, "Large Amplitude Vibration of a Tube Array By a Two-Phase Flow"' Journal of Wind Engineering, No. 37 Oct 1988, pp 599-608.

19. Paidoussis, M.P., "Fluidelastic Vibration of Cylinder Arrays in Axial and Cross Flow: State of the Art", Journal of Sound and Vibration, 76 (1981), pp 329-360.

20. Paidoussis, M.P., "A Review of Flow-Induced Vibrations in Reactors and Reactor Components", Nuclear Engineering and Design, 74 (1982), pp 31-60.

21. Paidoussis, M.P., S.J. Price, "The Mechanics Underlying Flow-Induced Instabilities of Cylinder Arrays in Cross Flow", Journal of Fluid Mechanics, Vol. 187, 1988, pp 45- 59.

22. Paidoussis, M.P., D. Mavriplis, S.J. Price, "A Potential Flow Theory for the Dynamics of Cylinder Arrays in Cross-Flow", Journal of Fluid Mechanics, Vol. 146, 1984, pp 227-252.

23. Paidoussis, M.P., S.J. Price, D. Mavriplis, " A Semi-Potential Flow Theory for the Dynamics of Cylinder Arrays in Cross Flows", Journal of Fluids Engineering, Vol. 107, 1985, pp 500-506.

24. Pettigrew, M.J., D.J. Gorman, "Vibration of Heat Exchanger

Tube Bundles in Liquid and Two-Phase Cross-Flow", 1984 International Symposium on Flow-Induced Vibration, Vol 3, pp 89-98.

25. Pettigrew, M.J., Y. Sylvestre, A.O. Campagna, "Vibration Analysis of Heat Exchanger and Steam Generator Designs", Nuclear Engineering and Design, Vol. 48, 1978, pp 97-115.

26. Pettigrew, M.J., J.H. Tromp, J. Mastorakos, "Vibration of Tube Bundles Subjected to Two-Phase Cross-Flow", Journal of Pressure Vessel Technology, Nov. 1985, Vol. 107, pp 335-343.

27. Pettigrew, M.J., C.E. Taylor, B.S. Kim, "Vibration of Tube Bundles in Two-Phase Cross-Flow: Part 1- Hydrodynamic Mass and Damping", 1988 International Symposium on Flow-Induced Vibration and Noise, Vol. 2, pp 79-103.

28. Pettigrew, M.J., J.H. Tromp, C.E. Taylor, B.S. Kim, "Vibration of Tube Bundles in Two-Phase Cross-Flow: Part 2- Fluidelastic Instability", 1988 International Symposium on Flow -Induced Vibration and Noise, Vol.3, pp 159-179.

29. Rao, M.S.M., D.A. Steininger, F.L. Eisinger, "Numerical Simulation of Fluidelastic Vibration and Wear of Multispan Tubes With Clearances at Supports", 1988 International Symposium on Flow-Induced Vibration and Noise, Vol. 5, pp 235-250.

30. Taylor, C.E., M.J. Pettigrew, F. Axisa, B. Villard, "Experimental Determination of Single and Two-Phase Cross Flow-Induced Forces on Tube Rows", Journal of Pressure Vessel Technology, Feb. 1988, Vol. 110, pp 22-28.

31. Taylor, C.E., I.G. Currie, M.J. Pettigrew, B.S. Kim, "Vibration of Tube Bundles in Two-Phase Cross-Flow: Part 3- Turbulence-Induced Excitation", 1988 International Symposium on Flow-Induced Vibration and Noise, Vol. 2, pp 105-129.

32. Weaver, D.S., M. El-Kashlan, "On the Number of Tube Rows Required to Study Cross-Flow Induced Vibrations in Tube Banks", Journal of Sound and Vibration, Vol. 75, 1981, pp 265-273.

33. Weaver, D.S., D. Koroyannakis, "Flow-Induced Vibrations of Heat Exchanger U-Tubes: A Simulation to Study the Effects of Asymmetric Stiffness", Journal of Vibrations, Acoustics, Stress and Reliability in Design, Jan. 1983, Vol. 105, pp 67-75.

34. Weaver, D.S., J.A. Fitzpatrick, "A Review of Cross-Flow Induced Vibrations in Heat Exchanger Tube Arrays", Journal of Fluids and Structures, Vol. 2, 1988, pp 73-93.

35. Westermann, Gerold D., "The Design and Construction of a Flow Loop for the Study of Two Phase Crossflow-Induced Vibrations of Heat Exchanger Tubes", Masters Thesis, McMaster University, April 1987.

36. Yetisir, M., D.S. Weaver, "On an Unsteady Theory for Fluidelastic Instability of Heat Exchanger Tube Arrays", 1988 International Symposium on Flow-Induced Vibration and Noise, Vol. 3, pp 181-195.

37. Yeung, H.C., D.S. Weaver, "The Effect of Approach Flow Direction on the Flow-Induced Vibrations of a Triangular Tube Array", Journal of Vibrations, Acoustics, Stress and Reliability in Design, Jan. 1983, Vol. 105, pp 77-81.